Integrative bioinformatics pipeline for genome-wide association studies in neuropsychiatry and the subsequent application in Autism Spectrum Disorder cohorts

Dissertation

zur Erlangung des Doktorgrades

der Naturwissenschaften

im Fach Bioinformatik

vorgelegt beim Fachbereich Mathematik und Informatik

der Johann Wolfgang Goethe-Universität

in Frankfurt am Main

von

Afsheen Yousaf

aus Peshawar, Pakistan

Frankfurt (2019)

(D30)

vom Fachbereich Mathematik und Informatik der

Johann Wolfgang Goethe-Universität als Dissertation angenommen.

Dekan: Prof. Dr.-Ing. Lars Hedrich

1. Gutachter: Prof. Dr. Ina Koch

2. Gutachter: Prof. Dr. Christine M. Freitag

Datum der Disputation:

Table of contents

I. List of figures I

II. List of tables I

III. List of abbreviations II

IV. List of genes IV

V. Preface VII

VI. Zusammenfassung IX

VII. Abstract XVII

1. Introduction 1

1.1. Motivation and structure of the thesis 1
1.2. Genetic concepts 2
1.3. Types of data in genetic studies 4
1.4. ASD 8
1.5. Genetic studies designs 10
1.6. ASD data 18
1.7. Data analysis 20
1.8. Aims of the study 26

2. Materials and methods 29

2.1. ASD quantitative data 29
2.2. SNP genotype data 30

I. Preliminary data analysis of phenotype data 30

2.3. Quality assurance of ADI-R data 30
2.4. Phenotype imputation of missing ADI-R data 31
2.5. Identifying ADI-R subdomains 32

II. The MAGNET tool: Implemented methods 37

2.6. QC 37
2.7. Genotype imputation 44
2.8. GWAS 49
2.9. Gene-based analysis 51
2.10. Gene Ontology (GO) analysis 52
2.11. Brain enrichment analysis 54

III. Additional data analysis 55

2.12. Genetic correlation 55
2.13. SNP-based heritability analysis 56
2.14. Polygenic risk scores (PRS) 57

3. Results and Discussion 59

I. Preliminary analysis of phenotype data 59

3.1. Phenotype imputation 59

II. (a) The MAGNET tool: Methodological results 64

3.2. MAGNET implementation and architecture 64
3.3. MAGNET-lite 78
3.4. Discussion 78

II. (b) The MAGNET tool: Biological results

II. (b) The MAGNET tool: Biological results 81
3.5. Quality check of genotype data 81
3.6. Imputation of missing genotype data 82
3.7. GWAS 83
3.8. Gene and pathway analysis 86
3.9. GO-term analysis 88
3.10. KEGG pathway analysis 88
3.11. Brain enrichment analysis 89
III. Additional data analysis 96
3.12. Genetic heritability of ASD phenotypes 96
3.13. Correlation among ASD phenotypes 97
3.14. PRS for ASD phenotypes 97
3.15. SNPs and genes overlap among the subdomains 99
3.16. Discussion 101
4. Conclusion and outlook 111
5. Appendix 115
5.1. Genetic terminologies 115
5.2. Genotype file formats 117
5.3. Statistical terms 119
5.4. Supplementary figure 120
6. References 127
7. Curriculum vitae 141

I. List of figures

Figure 1 Allele frequency versus disease penetrance at different effect sizes.. 3
Figure 2 Genotype imputation.. 23
Figure 3 Minimac3 workflow using state-space reduction.. 49
Figure 4 Scree plot of the AGP cohort 60
Figure 5 PCA based subdomains of the 28 ADI-R items.. 61
Figure 6 MAGNET workflow.. 64
Figure 7 General architecture of MAGNET 66
Figure 8 Quality check plots of IQ trait in German cohort... 69
Figure 9 MDS plot of the first two dimensions 81
Figure 10 Manhattan plots of the six subdomains from comb. cohort and IQ from the German cohort85
Figure 11 Gene Ontology (GO) analysis 90
Figure 12 KEGG pathway analysis 92
Figure 13 Expression profiles of associated brain gene modules 94
Figure 14 Heritability estimates 96
Figure 15 Heatmaps illustrating the (a) phenotypic and (b) genetic corr. among ASD subdomains....... 97
Figure 16 Polygenic risk score analysis 98
Figure 17 Overlap of significant findings.. 100

II. List of tables

Table 1 Software used in MAGNET 37
Table 2 Sample adequacy tests.. 59
Table 3 Factor loadings in AGP data set.. 62
Table 4 Confirmatory factor analysis in the German cohort 63
Table 5 Descriptive statistics... 63
Table 6 Computational requirements for MAGNET.. 66
Table 7 Comparison with state-of-the-art Imputation frameworks. 77
Table 8 Genome-wide hits in combined, AGP and German cohort.. 84
Table 9 Significant genes in both cohorts from MAGMA analysis 87

III. List of abbreviations

ADHD	Attention deficit hyperactivity disorder
ADI-R	Autism Diagnostic Interview-Revised
ADOS	Autism Diagnostic Observation Schedule
AGP	Autism Genome Project
AGRE	Autism Genetic Resource Exchange
API	Application Program Interface
ASC	Autism Sequencing Consortium
ASD	Autism Spectrum Disorders
BD	Bipolar Disorder
cDNA	complementary Deoxyribonucleic Acid
CFI	Comparative Fit Index
CI	Confidence Interval
CNV	Copy number variant
DAVID	Database for Annotation, Visualization and Integrated Discovery
Df	Degree of freedom
DFC	Dorsolateral prefrontal cortex
DNA	Deoxyribonucleic acid
DSM-IV	Diagnostic and Statistical Manual of Mental Disorders, 4th Edition
DZ	Dizygotic twins
EFA	Exploratory Factor Analysis
eQTL	Expression quantitative trait loci
FDR	False Discovery Rate
GO	Gene Ontology
GRCh37	Genome Reference Consortium Human build 37
grm	genetic relationship matrix
GSEA	Gene set enrichment analysis
GWAS	Genome-wide association studies
GUI	Graphical User Interface
Hs	Homosapiens
ICD	International Statistical Classification of Diseases and Related Health Problems
IPA	Ingenuity Pathway Analysis
IPC	Inferior parietal cortex
IQ	Intelligence Quotient
JA	Joint attention
kb	kilobases
KEGG	Kyoto Encyclopedia of Genes and Genomes
KMO	Kaiser Maier Olkin
KO	Knockout
LD	Linkage Disequilibrium
LOD	Logarithm of odds
LTD	Long Term Depression
LTP	Long Term Potentiation
MAGMA	Multi-marker Analysis of GenoMic Annotation
MAGNET	MApping the Genetics of Neuropsychological Traits to molecular NETworks of human brain
MAF	Minor Allele Frequency
MCQs	Multiple-choice questions
MI	Multiple imputation
MDS	Multidimensional Scaling
MZ	Monozygotic
NCBI	National Center for Biotechnology Information
OFC	orbito frontal cortex

ORA	Over-representation analysis
PCA	Principal components analysis
pcw	post-conceptional weeks
PDD-NOS	Pervasive developmental disorder-not otherwise specified
PGC	Psychiatric Genomics Consortium
pmm	predictive mean matching
PRS	Polygenic risk scores
QC	Quality Check
QQ	Quantile-quantile
qGWAS	quantitative genome-wide association study
RB	Repetitive sensory motor behavior
RMSEA	Root Mean Square Error Approximation
RNA	Ribonucleic acid
RNA-Seq	Ribonucleic acid- sequencing
SNP	Single Nucleotide Polymorphism
SNV	Single Nucleotide Variants
SRMR	Standardized Root Mean Square Residual
STC	Superior temporal cortex
SRS	Social Responsiveness Scale
SZ	Schizophrenia
TDT	Transmission-Disequilibrium Test
TLI	Tucker Lewis Index
VCF	Variant calling file
VEGAS2	Versatile Gene-based Association Study 2

IV. List of genes

ADCY2	Adenylate Cyclase 2
ADCY5	Adenylate Cyclase 5
ASTN2	Astrotactin 2
BIN1	Bridging Integrator 1
C8ORFK32	Family With Sequence Similarity 135 Member B
CALCOCO2	Calcium Binding And Coiled-Coil Domain 2
CLIP2	CAP-Gly Domain Containing Linker Protein 2
CDH9	Cadherin 9
CDH10	Cadherin 10
CECR2	Cat Eye Syndrome Chromosome Region, Candidate 2
CMIP	C-Maf Inducing Protein
CNTNAP2	Contactin-associated protein-like 2
CNTN4	Contactin 4
CNTN5	Contactin 5
COBLL1	Cordon-Bleu WH2 Repeat Protein Like 1
CX3CR1	C-X3-C Motif Chemokine Receptor 1
DAGLA	Diacylglycerol Lipase Alpha
DDX53	DEAD-Box Helicase 53
DLGAP2	DLG Associated Protein 2
DLX3	Distal-Less Homeobox 3
ENPP3	Ectonucleotide Pyrophosphatase
ERBB4	Erb-B2 Receptor Tyrosine Kinase 4
FER	FER Tyrosine Kinase
FTL	Ferritin Light Chain
GABRB3	Gamma-aminobutyric acid type A receptor beta3 subunit
GNAO1	G Protein Subunit Alpha O1
GNAS	Guanine Nucleotide Binding Protein (G Protein)
GNG2	G Protein Subunit Gamma 2
GYS1	Glycogen Synthase 1
HTT	Huntingtin
ICA1	Islet Cell Autoantigen 1
IL20	Interleukin 20
KCND2	Potassium Voltage-Gated Channel Subfamily D Member 2
LHB	Luteinizing Hormone Beta Polypeptide
MACROD2	Mono-ADP Ribosylhydrolase 2
MCF2L	MCF2 Cell Line Derived Transforming Sequence Like
MNS1	Meiosis Specific Nuclear Structural 1
MPN2	Serine Protease 38
NELL1	Neural EGFL Like 1
NLGN1	Neuroligin 1
NLGN4	Neuroligin 4
NLRP3	NLR Family Pyrin Domain Containing 3
NOS2A	Nitric Oxide Synthase 2
NRXN1	Neurexin 1
NSUN5	NOP2/Sun RNA Methyltransferase 5
NTRK3	Neurotrophic Receptor Tyrosine Kinase 3
PANX1	Pannexin 1
PANX2	Pannexin 2
PARK2	Parkin RBR E3 Ubiquitin Protein Ligase
PATJ	PALS1-Associated Tight Junction Protein
PGLYRP2	Peptidoglycan Recognition Protein 2
PHB	Prohibitin
PLCB2	Phospholipase C Beta 2

PPM1N	Probable Protein Phosphatase 1N
PTCHD1	Patched Domain Containing 1
QPRT	Quinolinate Phosphoribosyltransferase
RGS10	Regulator Of G Protein Signaling 10
RNPS1	RNA Binding Protein With Serine Rich Domain 1
RORA	Retinoic acid-related orphan receptor alpha
S100A3	S100 calcium-binding protein A3
S100A4	S100 calcium-binding protein A4
S100A5	S100 calcium-binding protein A5
SCN5A	Sodium Voltage-Gated Channel Alpha Subunit 5
SCN8A	Sodium Voltage-Gated Channel Alpha Subunit 8
SDK1	Sidekick Cell Adhesion Molecule 1
SEMA5A	Semaphorin 5A
SHANK2	SH3 And Multiple Ankyrin Repeat Domains 2
SLC22A18AS	Solute Carrier Family 22 Member 18 Antisense
SLC25A12	Solute Carrier Family 25 Member 12
SLC26A5	Solute Carrier Family 26 Member 5
SLC35B1	Solute Carrier Family 35 Member B1
SYNGAP1	Synaptic Ras GTPase Activating Protein 1
TAS2R1	Taste 2 Receptor Member 1
THRA	Thyroid Hormone Receptor Alpha
TM4SF4	Transmembrane 4 L Six Family Member 4
TTC17	Tetratricopeptide Repeat Domain 17
TYROPB	TYRO Protein Tyrosine Kinase Binding Protein

V. Preface

The work presented in this thesis has been performed at two Departments of the Goethe University Frankfurt, which is the "Molecular Bioinformatics" (Prof. Dr. Ina Koch) and "Department of Child and Adolescent Psychiatry, Psychosomatics and Psychotherapy" (Prof. Dr. Christine M. Freitag). In addition, Dr. Andreas G. Chiocchetti supervised my thesis at the Molecular Genetics Lab of the Department of Child and Adolescent Psychiatry, Psychosomatics and Psychotherapy.

In this work, I present the development and implementation of an integrative bioinformatics pipeline designed for genetic analyses of neuropsychiatric traits. The aim is to identify the associated genetic variants, underlying biological pathways of the traits, and to map the genetic association to the developing human brain. The pipeline is called "MAGNET" (**MA**pping the **G**enetics of neuropsychiatric traits to molecular **NET**works of the human brain). MAGNET was developed adhering to the state-of-the-art guidelines for genome-wide single nucleotide polymorphism (SNP) imputation, quality control and genome-wide association studies (GWAS).

MAGNET has been already used successfully to analyse data in different studies that have already been published. This includes a meta-analysis study across five different European populations analysing variants associated with ASD candidate genes. This study entitled "Lack of replication of previous autism spectrum disorder GWAS hits in European populations" was published in Autism Research by Dr. Bàrbara Torrico and Dr. Claudio Toma where I and Dr. Andreas G. Chiocchetti helped to provide the respective variants by using MAGNET for imputation in large ASD datasets [1].

In another study, we investigated the genetic variants of the glutamatergic system in ASD with high and low intellectual abilities. This work was published in the Journal of Neurotransmission as "Common functional variants of the glutamatergic system in Autism spectrum disorder with high and low intellectual abilities". I performed the data analysis, mainly using the MAGNET pipeline along with other algorithms to identify genes associated with high and low Intelligence Quotient (IQ) cohorts. The concept and design of this work were developed by Dr. Andreas G. Chiocchetti and Prof. Christine M. Freitag [2].

Parts of MAGNET have also been implemented in the work by Dr. Denise Haslinger and Dr. Andreas G. Chiocchetti, i.e. "Loss of the Chr16p11.2 ASD candidate gene *QPRT* leads to aberrant neuronal differentiation in the SH-SY5Y neuronal cell model". There, we applied MAGNET on a transcriptome dataset to identify the gene networks of brain development within genes significantly differentially regulated upon knock out (KO) of the gene *QPRT* [3].

A paper regarding the detailed features and implementation of MAGNET on IQ trait in a cohort is available as a preprint at bioarXiv. This work helped to identify novel candidate genes associated with IQ and also identified the genes already known in association with IQ. Thus, the study provided a successful proof of concept for MAGNET. The design and analysis were supported by Dr. Andreas G. Chiocchetti and supervised by Prof. Ina Koch.

The main work related to MAGNET has been submitted to Translational Psychiatry. The publication focuses on the results generated using MAGNET and important novel findings gathered with respect to ASD quantitative phenotypes. I analysed two large ASD cohorts by using MAGNET and wrote the manuscript. The concept and design of the project were supported by Dr. Andreas G: Chiocchetti and Prof. Christine M. Freitag. Prof as well as both the co-authors supported in manuscript preparation. Ina Koch supported data analysis and manuscript revision.

In summary, the presented pipeline has been already implemented in three publications [1–3] (see Publication list). The pipeline is available as a preprint at bioarXiv and the work related to the implementation of the pipeline on ASD cohorts has been submitted to the journal of Translational Psychiatry. This thesis focuses on the work presented in the following two publications:

I. MApping the Genetics of neuropsychiatric traits to molecular NETworks of the human brain (preprint bioRxiv 10.1101/336776).

II. Quantitative genome-wide association study of six phenotypic subdomains identifies novel genome-wide significant variants in Autism Spectrum Disorder (In review).

VI. Zusammenfassung

Motivation

Neuropsychiatrische Erkrankungen sind komplexe Störungen mit hoher Heritabilität und weitestgehend unaufgeklärten Pathomechanismen. Die klinische und genetische Heterogenität dieser Erkrankungen stellt eine große Herausforderung für die Identifizierung von krankheitsbezogenen Biomarkern dar. Neben signifikanten Fortschritten bei der Aufklärung der genetischen Grundlagen dieser Erkrankungen bleiben die zugrunde liegenden Ursachen und biologischen Mechanismen verborgen. Mit der Weiterentwicklung der Array-, Sequenzierungs- und Big-Data-Technologien werden große Datenmengen von Einzelpersonen auf verschiedensten Plattformen und in verschiedensten Datenstrukturen erzeugt. Es gibt allerdings nur wenige Bioinformatik-Tools, die diese Fülle von Daten integrieren und verarbeiten können. Daher ist es notwendig, ein integratives bioinformatisches Datenanalysetool zu entwickeln, welches diese Daten im Sinne eines Big-Data Ansatzes kombiniert, um die zugrunde liegende Genetik besser zu verstehen und die Ergebnisse auf die humane Gehirnentwicklung zu übertragen, mit dem Ziel die mit den jeweiligen Störungen verbundenen Pathomechanismen aufzuklären.

Einleitung:

Diese Arbeit stellt eine Bioinformatik-Pipeline vor, welche Daten von verschiedenen Plattformen implementiert, um ein grundlegendes Verständnis der genetischen Ätiologie eines neuropsychiatrischen quantitativen/qualitativen Merkmals zu generieren. Innerhalb dieser Arbeit werden zwei Aspekte behandelt: Einer ist die Entwicklung und der Aufbau einer Bioinformatik-Pipeline namens *MApping the Genetics of neuropsychiatric traits to the molecular NETworks of the human brain* (MAGNET). Der andere Teil zeigt die Implementierung und den Nutzen von MAGNET bei der Analyse großer ASS-Kohorten (Autismus-Spektrum-Störungen).

Um biologische und klinische Daten verschiedener Plattformen zu integrieren, sind effiziente Bioinformatik-Werkzeuge erforderlich, von denen derzeit nur wenige verfügbar sind. In dieser Arbeit

präsentieren wir eine Bioinformatik-Pipeline, die Genotyp-, Verhaltensmerkmal- und Genexpressionsdaten kombiniert. Ziel ist hierbei die genetischen Assoziationen eines neuropsychiatrischen Merkmals mit der genetischen Regulation der Gehirnentwicklung in Relation zu setzen, um so ein umfassendes Verständnis zu erhalten, das über die Identifikation von genetischen Risikofaktoren hinausgeht. MAGNET ist ein frei verfügbares command-line Tool, das innerhalb eines Frameworks Datenintegrationsansätze auf der Grundlage modernster Algorithmen und Software implementiert, um schließlich die Gene und Pfade zu identifizieren, die genetisch mit einem spezifischen quantitativen aber auch qualitativen Merkmal verbunden sind. MAGNET bietet einen zentralen Vorteil gegenüber den bestehenden Tools, da es neben der umfassenden genetischen Analyse die Datenverarbeitung und die Daten-Parsing-Schritte automatisiert, die für die Kommunikation zwischen den verschiedenen APIs (Application Program Interface) notwendig sind. Dabei unterstützt MAGNET genau die Zwischenschritte der Datenverarbeitung, die von Forschern benötigt werden, um von einer Analyse zur nächsten zu gelangen. Darüber hinaus können Anwender je nach Größe des Datensatzes innerhalb weniger Tage essentielle Informationen über ihr gewünschtes Merkmal ableiten wie genetische Assoziationen oder die Kartierung der zugehörigen Gene auf die Entwicklung des menschlichen Gehirns mit Transkriptomdaten von 16 verschiedenen Gehirnregionen von der 5. postkonzeptionellen Woche bis zum Alter von über 40 Jahren.

MAGNET kann für jede neuropsychiatrische Störung, für die häufige Varianten ätiologisch relevant sind, verwendet werden. MAGNET verarbeitet SNP- (Single Nucleotide Polymorphism/Einzelnukleotidpolymorphismus) basierte Genotypdaten und setzt diese in Korrelation mit einem quantitativen bzw qualitativen Merkmal. Speziell neuropsychiatrische Erkrankungen sind komplexe und heterogene Störungen, welche zwar eine hohe Heritabilität aufweisen, aber deren Pathomechanismen trotz Fortschritten in der DNA-Analyse noch weitgehend unklar sind. Zu diesen Störungen gehören ASS (Autismus-Spektrum-Störung), ADHS (Aufmerksamkeitsdefizit-Hyperaktivitätsstörung), BS (Bipolare Störung) und SZ (Schizophrenie). Von betroffenen Personen stehen große Mengen an Genotyp- und Verhaltensdaten zur Verfügung. Basierend auf diesen Daten können wir signifikante genetische Varianten sowie Gene identifizieren, die mit den Verhaltensdaten oder klinischen Daten assoziiert sind. Darüber hinaus kann der Vergleich dieser assoziierten Gene mit Genexpressionsdaten des menschlichen Gehirns Schlüsselregionen und Zeitpunkte identifizieren, welche für verschiedene neuronale Entwicklungsphasen des menschlichen Gehirns eine Rolle spielen. Unser Ziel war es also, ein bioinformatisches Werkzeug zu entwickeln, das es Forschern erleichtert, die zugrundeliegenden genetischen Aspekte ihres gewünschten Merkmals in einer Pipeline zu sammeln, indem Daten aus verschiedenen Ebenen kombiniert werden. Auf diese Weise können die Pathomechanismen neuropsychiatrischer Störungen besser identifiziert werden.

Im zweiten Teil, dem Proof of Concept, haben wir MAGNET auf zwei ASD-Kohorten implementiert. Diese Arbeit konzentriert sich auf die Auswertung von Daten, welche in einer Stichprobe von Patienten mit ASS erhoben wurden. ASS ist eine Gruppe von psychiatrischen Erkrankungen, denen eine neuronale Entwicklungsstörung zugrunde liegt. Klinisch wird die Psychopathologie von ASS wie folgt charakterisiert: A) Einschränkungen in der sozialen Interaktion und Kommunikation sowie B) eingeschränktes, repetitives Verhalten. Die Ätiologie der Erkrankungen ist aufgrund ihrer heterogenen klinischen und genetischen Eigenschaften äußerst komplex. Daher wurden bisher keine zuverlässigen Biomarker identifiziert. Die Diagnose basiert aktuell ausschließlich auf der Beschreibung des Verhaltens durch die Eltern sowie auf der direkten Verhaltensbeobachtung des Kindes. Ziel dieses Teils der Studie war es, die genetische Architektur von ASS unter Berücksichtigung der beiden oben genannten ASS-Diagnostikgebiete zu charakterisieren. Außerdem wurde untersucht, ob diese Bereiche genetisch verknüpft oder unabhängig voneinander sind. Darüber hinaus haben wir uns mit der Frage beschäftigt, ob diese Merkmale das genetische Risiko (polygenic risk score/PRS) mit der kategorischen Diagnose von ASS teilen und wie viel von der phänotypischen Varianz dieser Merkmale durch die zugrunde liegende Genetik erklärt werden kann.

Methoden:

Im ersten Teil wurden vorbereitende Analysen zur Aufbereitung der Phänotpydaten durchgeführt. Es wurden folgende Datensätze eingeschlossen: Patienten mit ASS aus dem Autism-Genome-Project

(AGP, n=2 735) sowie eine deutsche Kohorte, bestehend aus Proben, welche in Frankfurt gesammelt wurden (n=705). Ziel der Studie war es, die genetische Architektur von ASS unter Berücksichtigung der beiden ASS-Diagnosebereiche Domäne A (soziale Interaktion und Kommunikation) und Domäne B (repetitives, stereotypes Verhalten, sensorische Auffälligkeiten und Sonderinteressen) zu charakterisieren.

Die verwendeten Phänotypdaten wurden mithilfe des Tools „Diagnostisches Interview für Autismus – Revidiert" (ADI-R) erhoben. Es beinhaltet 93 Items zur frühkindlichen Entwicklung, zu Spracherwerb und möglichem Verlust von sprachlichen Fertigkeiten, verbalen und nonverbalen kommunikativen Fähigkeiten, Spiel- und sozialem Interaktionsverhalten sowie stereotypen Interessen und Aktivitäten. Wir haben 28 Items ausgewählt, welche zum einen für die diagnostischen Algorithmen aus ADI-R notwendig sind, und zum anderen sowohl für verbale als auch für nonverbale Personen verfügbar waren. Darüber hinaus wurden demografische Daten wie Alter, Geschlecht und IQ der betroffenen Personen verwendet. Personen mit mehr als 10% fehlenden Phänotypinformationen nach Qualitätskontrolle wurden ausgeschlossen. Anschließend wurde die Phänotypdaten-Imputation für die 28 Algorithmenelemente durchgeführt. Die korrekte Kodierung des ADI-R wurde zusätzlich überprüft. Um die bekannte phänotypische Heterogenität zu reduzieren und die dimensionalen Eigenschaften als Zielgröße für die Analyse genetischer Risikofaktoren für einen unterschiedlichen ASS-Schweregrad zu definieren, wurde eine Hauptkomponentenanalyse für die einzelnen Items des ADI-R in der AGP-Kohorte durchgeführt, um mögliche Komponenten/Subdomänen zu beschreiben. Im Anschluss wurde in der deutschen Kohorte eine konfirmatorische Faktorenanalyse durchgeführt, um festzustellen, ob die in der AGP-Kohorte erhaltenen Subdomänen in einer unabhängigen Kohorte repliziert werden können.

Im zweiten Teil wurde MAGNET auf jede der ASS-Subdomänen als eine quantitative abhängige Variable angewendet. Die Analyse-Pipeline MAGNET ist in fünf Hauptabschnitte unterteilt. Der erste Abschnitt führt eine umfassende Qualitätsprüfung der Genotypdaten durch. Diese umfasst das Filtern fehlender Genotypdaten über einem bestimmten Schwellenwert, die Überprüfung auf Geschlechtsunterschiede,

Kontaminations- und Inzuchtfehler sowie die Visualisierung der Populationsstratifikation. Nach der Qualitätskontrolle der Genotypdaten werden im zweiten Abschnitt die fehlenden Genotypen anhand eines Referenzdatensatzes imputiert. Im dritten Abschnitt wird die Assoziationsanalyse von Genotyp- und einzelnen Merkmalsdaten mittels Regressionsanalyse durchgeführt, um assoziierte genetische Varianten zu finden. Im vierten Abschnitt wird eine genbasierte Analyse durchgeführt, die alle Varianten aus der Regressionsanalyse als Input übernimmt. Danach werden die genetischen Varianten den entsprechenden Genen zugeordnet und signifikante Gene werden weiteren Analysen unterzogen. Zusätzlich werden in diesem Abschnitt biologische Signalwege identifiziert, welche mit den signifikanten Genen assoziiert sind. Im letzten Abschnitt werden bereits vorhandene Genexpressionsdaten aus dem menschlichen Gehirn integriert (Kang et al.,2011). Diese Daten beschreiben 29 verschiedene genetische neuronale Module mit einem spezifischen Expressionsmuster zu verschiedenen Zeitpunkten (beginnend mit der 5. postkonzeptionellen Woche bis über 40 Jahre) in 16 verschiedenen Gehirnregionen. Die mit den unterschiedlichen Phänotypen assoziierten Gene werden bezüglich ihrer Überlappungen mit den 29 Genexpressionsmodulen getestet. Für die wichtigsten Gene werden Heatmaps der Expression aller Gene innerhalb des assoziierten Moduls erstellt, sodass eine ätiologische Interpretation möglich wird.

Im dritten Teil dieser Arbeit wurden zusätzliche Analysen durchgeführt, um den Anteil der phänotypischen Varianz zu bestimmen, der durch genetische Varianten (SNPs) für jede Subdomäne, d.h. die SNP-basierte Heritabilität erklärt wird. Darüber hinaus wurde eine genetische Korrelationsanalyse zwischen den Subdomänen durchgeführt, um festzustellen, ob Subdomänen, die sich auf Domäne A beziehen, und die Subdomänen, die sich auf Domäne B beziehen, genetisch verknüpft oder unabhängig voneinander sind. Am Ende wurde das polygenetische Risiko berücksichtigt, welches zwischen ASS und den einzelnen Subdomänen überlappt.

Ergebnisse:

Die Analyse aus dem ersten Teil der Arbeit (Aufbereitung der Phänotypdaten) identifizierte sechs aussagekräftige Komponenten in der AGP-Stichprobe, die jeweils ein quantitatives ASS-Merkmal oder

eine Subdomäne darstellen. Vier Subdomänen, nämlich "social interaction" (SI), "joint attention" (JA), "peer interaction" (PI) und "non-verbal communication" (NVC) sind Subdomänen des Bereichs A (soziale Interaktion und Kommunikation), die beiden weiteren Subdomänen "repetitive sensory-motor behavior" (RB) und "restricted interests" (RI) gehören zu Bereich B (repetitives, stereotypes Verhalten, sensorische Auffälligkeiten und Sonderinteressen). Die Subdomänen wurden in der zweiten, deutschen ASS-Kohorten bestätigt.

Die Qualitätskontrolle und Imputation der fehlenden SNP-Genotypdaten in einzelnen Kohorten im zweiten Teil (MAGNET Implmentierung) der Arbeit erfolgte automatisiert durch MAGNET. Im nächsten Schritt wurden assoziierte Varianten für jede Subdomäne im kombinierten AGP und deutschen Datensatz identifiziert und ihren jeweiligen Genen zugeordnet. Wir fanden acht genomweit signifikante SNPs, sowie 292 nominal signifikante bekannte und neue ASS-Risikogene. Diese Gene wurden im Anschluss über MAGNET biologischen Signalwegen und Gen-Ontologien zugeordnet. Die zugrundeliegenden biologischen Mechanismen konvergierten zu neuronalen Übertragungs- und Entwicklungsprozessen. Über einen erneuten Abgleich dieser Gene mit dem Transkriptom des sich entwickelnden humanen Gehirns konnte über MAGNET herausgefunden werden, dass die signifikanten, mit den Subdomänen assoziierten Gene zu bestimmten Zeitpunkten in Gehirnarealen wie dem Hippocampus, der Amygdala und kortikalen Regionen exprimiert werden.

In der zusätzlichen Analyse im dritten Teil haben wir festgestellt, dass die kollektive SNP-basierte Heritabilität, die durch einzelne Subdomänen erklärt wird, höher ist als die bekannte SNP-basierte Heritabilität von ASS. Wir konnten außerdem zeigen, dass die Subdomänen NVC, SI und PI das polygenetische Risiko teilen, während die Subdomänen von RB und RI genetisch unabhängig voneinander scheinen. Darüber hinaus spiegelt die genetische Korrelation zwischen den Subdomänen teilweise phänotypische Domänen von ASS wider.

Conclusio:

MAGNET ist ein frei verfügbares command line tool, das auf Github zugänglich ist (https://github.com/SheenYo/MAGNET). MAGNET bietet eine effiziente Datenintegration der Big-Data-

Analyse und bewältigt automatisches Datenparsing sowie parallele Berechnung und Datenqualitätsprüfungen . Es führt gründliche Analysen durch, die von der Qualitätskontrolle der Genotypdaten bis hin zur Visualisierung von Gennetzwerken und Genexpressionsmustern wichtiger Gene reichen. MAGNET implementiert state-of-the-art Software, um assoziierte häufige genetische Varianten und Gene sowie deren biologische Relevanz zu identifizieren, welche mit einem bestimmten Merkmal assoziiert sind. Darüber hinaus können die Gene in Beziehung zum Transkriptom des sich entwickelnden menschlichen Gehirns gesetzt werden. MAGNET wurde erfolgreich zur Optimierung genomweiter Assoziationsstudien eingesetzt und hat sich im Bereich der ASS-Forschung bewährt. Die vom ADI-R-Algorithmus abgeleiteten Subdomänen im Zusammenhang mit der sozialen Kommunikation zeigen eine gemeinsame genetische Ätiologie im Gegensatz zu eingeschränkten und repetitiven Verhaltensweisen. Die ASS-spezifischen PRS überschnitten sich nur teilweise, was auf eine zusätzliche Rolle der spezifischen gemeinsamen Variation bei der Gestaltung der phänotypischen Expression von ASS-Subdomänen hindeutet.

VII. Abstract

Motivation

Neuropsychiatric disorders are complex, highly heritable but incompletely understood disorders. The clinical and genetic heterogeneity of these disorders poses a significant challenge to the identification of disorder related biomarkers. Besides significant progress in unveiling the genetic basis of these disorders, the underlying causes and biological mechanisms remain obscure. With the advancement in the array, sequencing, and big data technologies, a huge amount of data is generated from individuals across different platforms and in various data structures. But there is a paucity of bioinformatics tools that can integrate this plethora of data. Therefore, there is a need to develop an integrative bioinformatics data analysis tool that combines biological and clinical data from different data types to better understand the underlying genetics. For example, identifying significant genetic variants as well as genes that are associated with the behavioral data of these disorders. Moreover, integrating gene expression data of the human brain can highlight these associated genes with respect to key regions and time points that are altered during different neurodevelopmental stages of a human brain.

Introduction

This thesis presents a bioinformatics pipeline implementing data from different platforms to provide a thorough understanding of the genetic etiology of a neuropsychiatric quantitative as well as a qualitative trait of interest. Throughout the thesis, we present two aspects: one is the development and architecture of the bioinformatics pipeline named ***MA**pping the **G**enetics of neuropsychiatric traits to the molecular **NET**works of the human brain (MAGNET)*. The other part demonstrates the implementation and usefulness of MAGNET analysing large Autism Spectrum Disorder (ASD) cohorts.

MAGNET is a freely available command-line tool available on GitHub (https://github.com/SheenYo/MAGNET). It is implemented within one framework using data integration approaches based on state-of-the-art algorithms and software to ultimately identify the genes and pathways genetically associated with a trait of interest. MAGNET provides an edge over the existing tools since it performs a comprehensive analysis taking care of the data handling and parsing steps necessary to communicate between the different APIs (Application Program Interface). Thus, this avoids the in-between data handling steps required by researchers to provide output from one analysis to the next. Moreover, depending on the size of the dataset users can deduce important information regarding their trait of interest within a time frame of a few days. Besides gaining insights into genetic associations, one of the central features is the mapping of the associated genes onto developing human brain implementing transcriptome data of 16 different brain regions starting from the 5th post-conceptional week to over 40 years of age.

In the second part as proof of concept, we implemented MAGNET on two ASD cohorts. ASD is a group of psychiatric disorders. Clinically, ASD is characterized by the following psychopathology: A) limitations in social interaction and communication, and B) restricted, repetitive behavior. The etiology of this disorder is extremely complex due to its heterogeneous clinical traits and genetics. Therefore, to date, no reliable biomarkers are identified. Here, the aim is to characterize the genetic architecture of ASD taking into account the two aforementioned ASD diagnostic domains. As well as to investigate if these domains are genetically linked or independent of each other. Moreover, we addressed the question if these traits share genetic risk with the categorical diagnosis of ASD and how much of the phenotypic variance of these traits can be explained by the underlying genetics.

Methods

In the first part, preliminary analyses were performed which incorporated statistical data analysis approaches. We included affected individuals from two ASD cohorts, i.e. the Autism Genome Project (AGP) and a German cohort consisting of 2,735 and 705 families respectively. We used phenotype data gathered from diagnostic interviews for Autism - Revised (ADI-R). Firstly, the quality of the phenotype data was ensured. In order to reduce the known phenotypic heterogeneity and to define the dimensional properties as a target for the analysis of genetic risk factors, a principal component analysis was performed on the ADI-R data in the AGP cohort. Subsequently, a confirmatory factor analysis was performed in the German cohort to determine whether the subdomains obtained in the AGP cohort could be replicated in an independent cohort.

In the second part, MAGNET was applied to each of the ASD subdomains as a quantitative dependent variable. MAGNET is divided into five main sections i.e. (1) quality check of the genotype data, (2) imputation of missing genotype data, (3) association analysis of genotype and trait data, (4) gene-based analysis, and (5) enrichment analysis using gene expression data from the human brain.

In the third part of this thesis, the proof of concept study was extended with additional analyses. These analyses included determination of the SNP-based heritability for each subdomain. In addition, a genetic correlation analysis between subdomains was performed to identify whether subdomains related to ASD domains A and B are genetically linked or independent of each other. Finally, the polygenic risk overlapping between ASD and each subdomain was considered.

Results

The preliminary analyses identified six meaningful components in the AGP sample, each representing a quantitative ASD subdomain. Four subdomains, namely "social interaction" (SI), "joint attention" (JA), "peer interaction" (PI) and "non-verbal communication" (NVC), are subdomains of domain A (social interaction and communication), the other two subdomains "repetitive sensory-motor behavior" (RB) and "restricted interests" (RI) belong to domain B (repetitive, stereotypical behavior, sensory abnormalities, and special interests). The subdomains were confirmed in the second German ASD cohort.

The quality control and imputation of the missing SNP genotype data in individual cohorts in the second part of the work were automated by MAGNET. In the next step, associated variants for each subdomain were identified in the combined AGP and German cohort and mapped to their respective genes. We found eight genome-wide significant SNPs, and 292 known and new ASD risk genes. These genes were subsequently assigned to biological signaling pathways and gene ontologies via MAGNET. The underlying biological mechanisms converged with respect to neuronal transmission and development processes. By reconciling these genes with the transcriptome of the developing human brain, MAGNET was able to identify that the significant genes associated with the subdomains are expressed at specific time points in brain areas such as the hippocampus, amygdala, and cortical regions.

In the additional analysis in the third part, we found that the collective SNP-based heritability explained by single subdomains is higher than the known SNP-based heritability of ASD. We have also shown that the subdomains NVC, SI and PI share polygenic risk factors, while the subdomains of RB and RI seem genetically independent. Furthermore, the genetic correlation between the subdomains reflects partially phenotypic domains of ASD.

Conclusion

MAGNET offers an advantage over existing tools as it performs efficient data integration and deals with the challenges faced during big data analysis by providing automatic data parsing, parallel computation, and data quality checks. It performs thorough analysis ranging from quality control of genotype data to visualization of gene networks and gene expression patterns of significant genes.

MAGNET has been successfully implemented on ASD cohorts optimizing quantitative genome-wide association studies and has proven to be valuable in the field of ASD-research. The ADI-R algorithm derived subdomains related to social communication show a shared genetic etiology in contrast to restricted and repetitive behaviors. The ASD specific PRS overlapped only partially, suggesting an additional role of specific common variation in shaping the phenotypic expression of ASD subdomains.

1. Introduction

1.1. Motivation and structure of the thesis

The complex mechanisms underlying neuropsychiatric conditions such as ASD (Autism spectrum disorders), BD (Bipolar disorder), ADHD (Attention deficit hyperactivity disorder) and SZ (Schizophrenia) [5–8] are a challenging area of research. These disorders are highly heritable and exhibit a broad variety of expression of the various clinical traits. The high heritability of the diagnoses and the related traits indicate that the underlying genetics need to be dismantled in order to understand the pathomechanisms of these disorders.

To determine the association between these genetic factors and the disorder, as well as to understand the biological and functional mechanisms behind the phenotypes, GWAS (Genome-wide association studies) are performed. GWAS requires efficient computational tools and their results are highly dependent on extensive QC (Quality check/control) procedures as well as an accurately performed imputation of missing genetic information.

At present, there are numerous bioinformatics genetics pipelines available such as SNPQC [9], which perform an extensive QC of the genotype data. Similarly, for imputing missing genotype data, there are state-of-the-art pipelines such as ENIGMA [10] and Molgenis-impute [11]. For genotype analyses GWAS applications are existing, e.g. GWASpi [12]. There are also pipelines published combining QC and imputation, such as the Ricopili pipeline [13]. All these available tools separately perform the individual steps needed for GWAS. However, in the area of neuropsychiatry, there currently is no framework, which besides performing association studies to identify the genes associated with a trait combines the different tools in an automated manner and translates the genetic findings at the brain and gene network level within a single framework. For example, integrating spatial and temporal properties of the available brain transcriptome (gene readouts present within a cell) data can contribute important insight to other neurodevelopmental disorders for understanding disease biology. Gene expression patterns in the developing human brain are highly dynamic and can reflect the underlying biological processes. Thus, this information can assist researchers not only to find the genes associated with a specific trait but can also highlight the regions and time points when those specific genes are expressed in the brain.

In the first chapter, a detailed overview of the state-of-the-art methods and an introduction to the key concepts in the field of ASD is provided. The second chapter of this thesis firstly highlights the methods used in the preliminary analyses performed on ASD phenotype data that will be used by MAGNET, then, the algorithms implemented in MAGNET. The third part of this chapter consists of the additional analysis performed to further answer the biological questions related to the two ASD cohorts. Chapter three shows MAGNET's structure in detail, as well as its implementation on two large ASD cohorts in the same order as in the previous chapter. Chapter four elaborates on the methodological as well as biological results. Firstly, the results from the preliminary analyses are shown followed by methodological results which detail the structure of MAGNET and its use. Further, the chapter focuses on the biological results related to MAGNET's implementation on the two ASD cohorts. Chapter four concludes the thesis in terms of its major outcomes and limitations.

1.2. Genetic concepts

Complex genetic disorders result from a combination of distinctive characteristics. These disorders result from a combination of allele frequencies and disease penetrance in a population. Figure 1 shows the effect of allele frequency with respect to disease penetrance. Genetic studies in the past have shown that genetic variants with a very rare allele frequency and low disease penetrance are hard to identify. However, for Mendelian diseases like Huntington's, one rare mutation of the single gene *HTT* (Huntingtin) is responsible for the disease (high penetrance). To identify genetic variants with modest effect sizes genome-wide association studies (GWAS) are performed, though these studies can not completely account for the phenotype risk. For variants with very low allele frequency, it is difficult to find enough cases and get significant associations. Though rare variants have a small effect size but are found to increase genetic liability and clinical presentation of neurodevelopmental disorders such as

ASD. Variants with a common allele frequency contribute significantly to the genetics of ASD, although the identification of individual risk polymorphisms is still not clear due to their small effect sizes and limited sample sizes available for association studies [1]. More details about the genetic terminologies can be found in the Appendix.

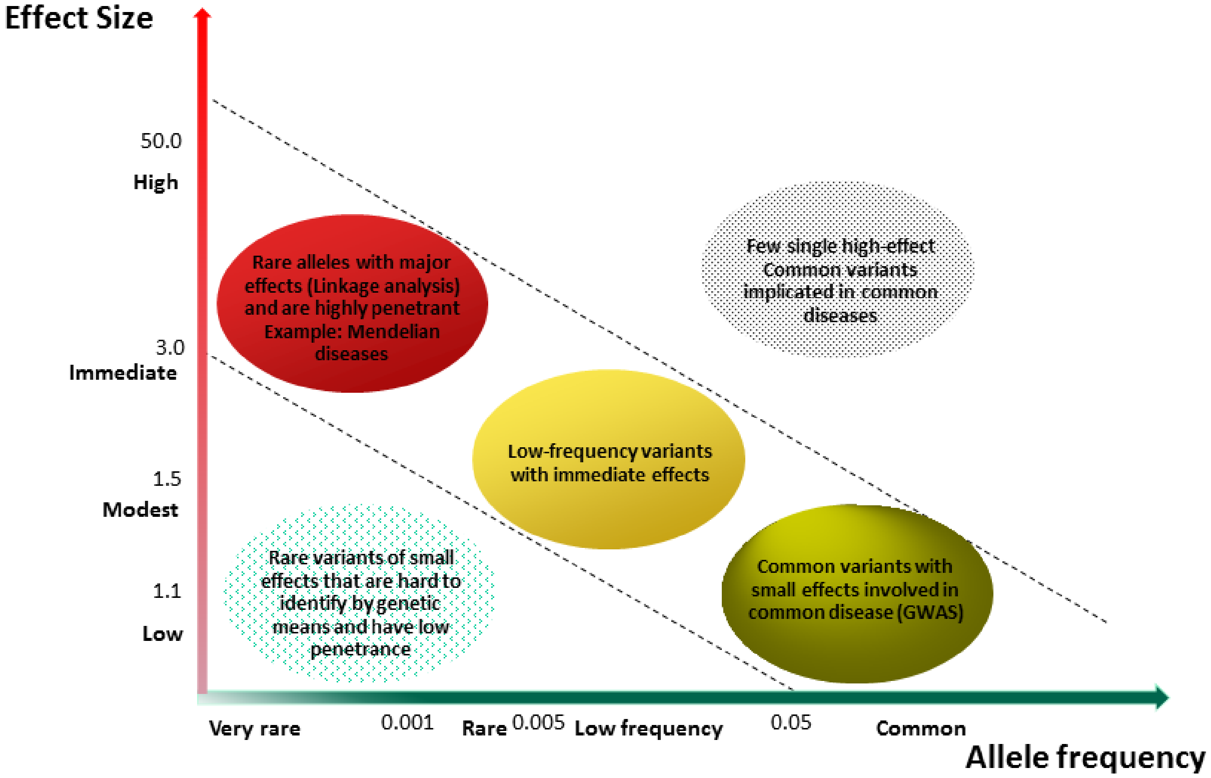
Effect Size
50.0
High
3.0
Immediate
1.5
Modest
1.1
Low
Rare alleles with major effects (Linkage analysis) and are highly penetrant Example: Mendelian diseases
Few single high-effect Common variants implicated in common diseases
Low-frequency variants with immediate effects
Rare variants of small effects that are hard to identify by genetic means and have low penetrance
Common variants with small effects involved in common disease (GWAS)
Very rare
0.001
Rare
0.005
Low frequency
0.05
Common
Allele frequency

Figure 1 Allele frequency versus disease penetrance at different effect sizes

This figure shows on the x-axis the allele frequency and the y-axis shows the effect size. The effect sizes of genetic variants change with allele frequency. On the lower left, we see that the rare variants with low effect sizes are hard to identify compared to variants with low frequency and intermediate effects. On the other side, common variants with small effects can be detected using genome-wide association analysis in common disease. On the top right, we see that only a few single high effect common variants are implicated in common diseases. This figure is adapted from McCarthy et al., 2009.

1.3. Types of data in genetic studies

1.3.1. Phenotype data

Neuropsychiatric disorders generally come with a discrete diagnosis. For example, although the ASD phenotype is discussed to be at the far right end of a normally distributed behavioral phenotype in the general populations, the most frequent kind of available data is as categorical diagnosis. Interestingly, the categorical diagnosis of ASD is usually based on quantitative phenotypic data, as generated during the clinical assessments [83]. These can include physical examinations, a series of interviews, cognitive and personality tests. The diagnostic instruments are clinical interviews conducted by expert clinicians from the (1) parent, primary caretaker or teacher, e.g. the ADI-R (Autism diagnostic interview-Revised) [13]or (2) directly from the individual, e.g., the ADOS (Autism diagnostic observation schedule) [34].

The challenges faced for generating and retrieving phenotype data include standardized assessment instruments that are harmonized across the sites, maintaining clinical records and dealing with missing phenotype data due to lack of information gathered from the participants in the study data. However, it is possible to fill the missing information using imputation techniques (see 2.4).

1.3.2. Genotype data: Types and Technologies

Genotype data comprises of genetic variants, which can be varying stretches of several megabases, i.e. Copy Number Variants (CNVs) down to Single Nucleotide Polymorphisms (SNPs) or Single Nucleotide Variants (SNVs). To obtain genotype data, there are two widely used technologies, i.e. array-based and next-generation sequencing technology described as follows:

Array-based technologies

Millions of SNPs can be genotyped using oligonucleotide (short DNA molecules)-probes with the main purpose to differentiate between alternative alleles at the SNP locus and determining the nature of the allele based on the signal generated from genotyping. The two key players in this technology are Affymetrix and Illumina. Both technologies are based on the biochemical principle that nucleotide bases bind to their complementary bases based on Watson–Crick base pairs, i.e. A (Adenine) pairs with

T (Thymine) and C (Cytosine) pairs with G (Guanine). Moreover, both the technologies call for the hybridization (annealing) of fragmented single-stranded DNA to arrays which contain millions of unique nucleotide probe sequences designed specifically to a target DNA subsequence. However, Illumina has a higher probe density that encompasses millions of markers.

Affymetrix arrays take a short DNA sequence targeting a single SNP allele. There are unique nucleotide probes which are designed in a way that they serve as perfect complementary to one of the two or more target alleles, e.g. A or B of a genetic variant (Major alleles conventionally referred to as allele A). Besides that, there are also negative probes that are identical to a perfect matching probe except that the allele-specific base is altered such as not to be complementary to any of the annotated alleles [35]. After the hybridization of target DNA to these unique nucleotide probe sequences, a signal is generated, and its intensity is measured. The intensity is proportional to the amount of target DNA in the sample and depending on the affinity between the target and probe. These intensity measures can depict the SNP genotype, i.e. AA, AB or BB [35]. Since intensity measures of all probes and individuals are assessed on multiple arrays, the intensities are normalized to account for non-biological differences. This aims at standardizing the intensity distributions across the arrays. The standardized approach is quantile normalization. It ranks the data and makes each quantile the same across the sample by calculating mean or median. In this manner, an average of the distributions is generated. So the highest values in the samples are the mean highest values. This ensures that all arrays in the study have precisely the same probe intensity distribution [35]. This can be achieved by implementing normalization algorithms in any programming language such as R, MATLAB, etc.

Illumina Bead-Arrays are based on the single base extension technology Infinium. Here, two allele-specific probes are designed to bind adjacent to the SNP of interest. The last base of the probe matches the alleles of interest. A single base extension is used to confer the allele specificity of the probe. For example, if a probe is a perfect match to allele A, a nucleotide with a green fluorophore is incorporated and a red fluorophore for the B allele. Illumina uses silica beads (a few microns in size) and a longer probe sequence than Affymetrix. In addition, a genetic barcode is attached to the bead in the form of another oligonucleotide with a fluorescent dye to be able to allocate the specific probes [36]. For each variant, beads with specific probes (one per bead) are synthesized and spread randomly on to a glass slide with silica coating having small etched holes for the beads to reside [37]. Thus, each SNP is interrogated with a single bead type covered by one unique probe designed to target the sequence spanning the SNP of interest. The signal intensities from each bead type are measured with a scanner [38]. A number of algorithms are available for processing the raw signal from these arrays into genotype calls such as GenCall [39] and BeadStudio/GenomeStudio software; Illumina [40]. Normalization steps are performed at the level of sub-bead pools level [39] (SNPs that share similar properties and are usually clustered together) using Illumina BeadStudio software, which provides the normalized intensities as a pair of coordinates corresponding to the signals for the two alleles at each SNP [40].

NGS technologies

NGS (Next-generation sequencing) is a DNA sequencing technology that performs millions of sequencing reactions of multiple small fragments of DNA to determine the sequence. Thus due to the speed of sequencing and the amounts of data generated this technology is also termed “high-throughput”. It has massively reduced the time and cost required to generate sequence data. The sequencing methods vary depending on the retrieval of DNA/RNA samples such as healthy vs. affected, different time points and experimental conditions, etc.

NGS provides large-scale DNA sequencing and is an efficient technique to identify novel SNPs [41]. NGS is used for sequencing a whole-genome or targeted regions of the genome, e.g. coding regions, exome-sequencing, which are sheared into small fragments. Barcodes and adapters are attached to each of the fragments for sequence identification, and each fragment is converted into a sequencing library. In the next step, the individual sequences are amplified multiple times and are sequenced. These sequences are then mapped and aligned onto annotated reference genomes, e.g. the human genome 19 reference (hg19). After aligning the fragments, SNP or genotype calling can be performed to identify SNPs and genotype for each individual respectively [42].

Array technology uses pre-selected targets whereas sequencing provides better coverage of the entire genome. Since the focus of this research is on common variants, which can also be covered by SNP genotyping technologies and are less expensive than the sequencing technology, we performed SNP genotyping only.

1.3.3. Transcriptome data

Transcriptome data is a representation of the complete set of RNA transcripts produced by the genome under specific circumstances such as the effects of a drug at specific time intervals or in a specific cell. For example, this data can contain information about the gene expression at certain time points and/or tissues in an organism. The two widely used platforms for generation of transcriptome data are microarrays and RNA-sequencing, both relying on the conversion of RNA into cDNA, i.e. the complementary DNA sequence to the respective transcript.

Microarrays are cost-effective and measure the abundance of transcripts via hybridization of the cDNA to an array of complementary probes, similar to the genotyping arrays, but targeting cDNA specific sequences. RNA-Seq is an NGS method, short pieces of cDNA (adapters) are attached to these fragments which contain the sequences to amplify the genomic fragment. These adapters also contain short sequences that serve as identifiers to avoid the samples being mixed. The cDNA library is then analysed by NGS, which produces short sequence segments corresponding to either one or both ends of the fragment. These short segments are then reconstructed and aligned with the help of a reference genome such as 1000 Genomes to map the genes. In the end, raw counts are produced, which are the number of reads that overlap with a transcript. In both cases, the data is normalized and analysed with the help of various bioinformatics tools available, e.g. the data analysis package *limma* in R [43] and also as standalone software that can analyse gene expression data and identify specific patterns, e.g. dCHIP [44] for microarrays, ArrayAnalysis [45] and AltAnalyze [46].

1.4. ASD

1.4.1. ASD prevalence and diagnosis in research

ASD is a neurodevelopmental disorder marked by impairments in two domains, i.e. (A) social interaction and communication, and (B) restricted or repetitive patterns of behavior and interests.

The estimated prevalence of ASD was 2.47% among the United States children and adolescents in the years 2014-2016 [47]. The median of global prevalence estimates of ASD was 62/10,000. This estimated prevalence is four times higher in boys than girls [48]. Despite these high prevalence rates of ASD and efforts to reveal its genetic basis over the past decade, a clear understanding of the ASD mechanism is still unresolved.

Currently, there are two gold standards for the diagnosis of ASD, i.e. the ADOS [34] and the ADI-R [49]. They provide a diagnostic algorithm for the ICD-10 (International Statistical Classification of Diseases and Related Health Problems- 10th Revision) [50] and DSM-IV-TR (Diagnostic and Statistical Manual of Mental Disorders, 4th Edition-Text Revision) [51] definitions of ASD [52].

Both ADI-R and ADOS are well established and validated diagnostic tools for children and adolescents with ASD. As mentioned before that the data gathered from these diagnostic tools can be interpreted as quantitative or phenotype data. In this study, we used ADI-R data because it considers the actual state of the patient as well as information on the retrospective behavior over the years and is thus less prone to age effects. Furthermore, the ADI-R, in contrast to the ADOS, does not come with age or developmental specific versions.

1.4.2. Genetics of ASD

Heritability

ASD is one of the most genetically heritable mental disorders but lacks information available on its neurobiological causes and biomarkers. One of the biggest challenges in understanding the mechanism of ASD is its heterogeneous clinical and genetic architecture. Moreover, the strong interplay of genetic influences and environmental interactions makes it a topic of intriguing research. Twin studies have also assisted in estimating the genetic and environmental contributions of ASD phenotypes. These studies have shown that MZ (monozygotic) twins are more concordant (twins sharing the same genetic and environmental condition) for ASD than DZ (dizygotic) twins (twins sharing environmental conditions but only 50% of their genetics) suggesting strong genetic effects underlying the liability to ASD [54]. A meta-analysis of twin studies estimated heritability rates between 64% - 91% [55]. Another recent study estimated the heritability of ASD in population data from five countries and found an estimate of ~80%, further supporting the finding that variation in ASD occurrence in the general population is mostly attributed by inherited genetic influences [56]. Besides that, the risk of ASD has been shown to be increased by genetic variants [57], structural variations [28], and mutations [58].

Genetic architecture of ASD

The underlying causes of ASD remain largely unknown however twin studies have shown a high genetic contribution to ASD [59]. Based on the Human Reference Genome Project an individual on an average carries 3 million genetic variants that differ from the reference human genome [60]. These variants could be SNPs/SNVs, CNVs, and short insertions or deletions also termed as indels. All these variants contribute significantly to ASD liability. Moreover, the type of variants (common or rare), as well as the origin of variants (inherited or de novo), contribute to the ASD genetic risk. Though, common variants are known to have small effect sizes but increase genetic liability for ASD. Previously, a twin study in a Swedish sample has identified that the genetic variation accounts for ~60% of the liability for ASD with common variants accounting for ~49% of the liability [62]. On the contrary, *de novo* mutations, CNVs and gene disrupting point mutations (a single nucleotide base change that can disrupt gene function) collectively contribute ~5% of the ASD liability [73] and less heritability.

1.5. Genetic studies designs

1.5.1. Twin studies in ASD

These studies evaluate the involvement of genetic and environmental factors on complex diseases based on the findings that MZ twins share 100% of genetic makeup and DZ twins share ~50% of their genetic makeup, while both share the same environment. High co-twin correlations among MZs and low co-twin correlations among DZs would suggest a high genetic heritability. Similarly, a high co-twin correlation among both groups would indicate a strong environmental effect on the phenotype. Twin studies are generally used to assess the heritability of a phenotype and thus to inform the decision to investigate a trait at the genetic level.

The first twin study of ASD was performed by Folstein et al.,1977 in a cohort of 11 MZ twins and 10 DZ twins. The study identified that MZ twins were more concordant for ASD, i.e. 36% compared to 0% for DZ [77]. However, when a ''broader autism phenotype'' (individuals with personality and cognitive traits) was used, the concordance rate increased to 92% for MZ twins and to 10% for DZ twins [54,78,79]. In the later period, twin studies with comparatively larger groups than the previous studies showed high concordances for ASD in MZ twins (77–95%) compared with DZ twins (31%) [80]. Moreover, these studies have shown that the recurrence of having a child with ASD can increase depending on the proportion of the genome, which is shared between the individual and an affected sibling or parent.

Sandin et al. [81] showed that individual risk of ASD and autistic disorder is increased with genetic relatedness to an individual with ASD. They estimated the relative recurrent risk (RR) for ASD as compared to the general population was RR= 153.0 (95% CI (Confidence Interval), 56.7-412.8) for MZ twins, RR= 8.2 (95% CI, 3.7-18.1) for DZ twins, RR= 10.3 (95% CI, 9.4-11.3) for full siblings, RR= 3.3 (95% CI, 2.6-4.2) for maternal half-siblings, RR= 2.9 (95% CI, 2.2-3.7) for paternal half-siblings and 2.0 (95% CI, 1.8-2.2) for cousins. In this study, the heritability of ASD and autistic disorders is estimated to be ~50% for the additive genetic component and similarly, the non-shared environmental influence was also 50%. In a recent meta-analysis by Tick et al. [55], the correlations for MZ twins were 0.98 and for DZ

0.53 at a prevalence rate of 5%. Another study by Sandin et al. 2017 [8] included 37,570 twin pairs, 2,642,064 full sibling pairs, and 432,281 maternal and 445,531 paternal half-sibling pairs. Among these, 14,516 children were diagnosed with ASD. The ASD heritability was estimated to be 83%, non–shared environmental influence was 17%. In short, these studies have provided high heritability estimates of ASD. One limitation, however, is that these estimates are often overestimated due to the overlapping genetic makeup between MZ twins and the 50% similarity in DZ twins. Finally, these studies do not provide information on the chromosomal regions, genes or variants involved. For this purpose, linkage studies and whole-genome analyses are performed.

1.5.2. Linkage studies in ASD

The purpose of linkage studies is to evaluate the probability that an allele or set of alleles are inherited together with a disease or trait in a family or group of families and thus to map the phenotype onto a genomic location, rather than identifying causal variants. The analysis is conducted in large pedigrees and tests for genome-wide genetic markers. The results are expressed as LOD (logarithm of odds) scores which compare the likelihood of two loci are being linked to the phenotype, i.e. being co-inherited, with the likelihood of observing them by chance in a disease [82]. High LOD scores thus correspond to regions with strong linkage to the disorder, i.e. the unknown disorder locus is close to the linked variants and can contain several candidate genes that are then investigated further.

A large number of linkage studies have identified ASD risk loci on multiple chromosomes, i.e. 2q21-33, 3q25-27, 3p25, 4q32, 6q14-21, 7q22, 7q31-36, 11p12-13 and 17q11-21 [64]. A study by Liu et al. [83] showed that dimensional subphenotypes of ASD can also help in reducing the genetic heterogeneity and can lead to better identification of susceptibility loci. In ASD families with IQ (Intelligence Quotient) ≥ 70, they identified linkage to chromosome 15q13.3-q14, a region already known in SZ. Moreover, they also found linkage of chromosome 11p15.4-p15.3 with “delayed onset of first phrases”. Later, the same group identified loci in a large study cohort associated with specific phenotypes in ASD. For example, the region 19q13.3 was genome-wide significantly associated with repetitive sensory-motor behavior (RB) whereas 11q23 was associated with joint attention (JA) [84]. Later, Weiss et al. [85]

performed a genome-wide linkage study and identified suggestive and significant linkage on chromosomes 6q27 and 20p13, respectively. Further analysis showed SNP on chromosome 5p15 between *SEMA5A* (Semaphorin 5A) and *TAS2R1* (Taste 2 Receptor Member 1) was significantly associated with ASD (*P*= 2x10^{-7}). They also identified that the expression of *SEMA5A* is reduced in the brains of autistic individuals.

Linkage analyses are suitable to detect loci and subsequently genes with potentially rare variants of high penetrance. However, they are not able to detect common variants that have small individual effects on risk [86]. GWAS is a powerful method to detect common variants with small effect as seen in Figure 1.

1.5.3. Genome-wide association studies in ASD

Though association studies are designed for any type of genetic variants, SNPs are mostly used because of their spread across the genome. GWAS methods can analyse variations in a case-control or trio-based (parents and offspring) setting. GWAS is efficient in detecting common alleles that contribute to common multifactorial diseases [87], however not only limited to common variants. GWAS is based on genotyping data usually generated using Chip- Array technology (see 1.3.2). Since the number of SNPs is limited to these arrays **genotype imputation** is further used to infer the missing genotypes based on linkage and thus increasing the number of SNPs to be analysed (see 1.7.2).

In trio-based studies, an affected individual is recruited along with the parents to compare the alleles transmitted from the parents to the case versus the non-transmitted. This is performed by using the TDT (transmission-disequilibrium test), which looks for the linkage between a marker allele and a disease locus. One limitation of TDT is the difficulty to recruit parents-case data.

Association studies based on case-control design have controls that are either unrelated or are the family members of the individual. In this study design, the occurrence of a given allele in cases versus the controls is observed to see the association between the phenotype and the disease. In contrast to a Chi^2 (chi-square)-based association test as used in case-control studies, the TDT approach is independent of potential stratification effects, i.e. findings that might relate to the differences in ethnicities between cases and controls rather than the group status.

A caveat in GWAS studies is that millions of SNPs are tested. Testing for multiple corrections is therefore mandatory to minimize the chances of false positives. The two widely used methods are FDR (False discovery rate) [88] and Bonferroni [89] correction which calculates the expected rate of type I errors when performing multiple comparisons which then provide a corrected p-value (see Appendix). Generally, the larger the sample size, the more likely a study will find a significant relationship if it exists. As the sample size increases, the impact of the random error is reduced and the overall variability is decreased. This allows the measures to become more precise for the complete dataset. However, with large study cohorts, more bias can be introduced in the analysis, such as various confounding factors including population stratification (see 2.6.8), inadequate quality control and genotyping errors. As well as performing GWAS on small underpowered samples can result in false-positive findings. Examples for successfully identified associations have been reported for several complex disorders such as ASD [90,91], Alzheimer [92], Parkinson's [93], stroke [94], and SZ [95].

There has been a drastic increase in ASD-GWAS since the first successful GWAS in ASD by Wang et al. 2009 [96] who identified six significant SNPs mapping to *CDH10* (Cadherin 10) and *CDH9* (Cadherin 9) genes which encode neuronal cell-adhesion molecules. Another study by Anney et al. [97] found a genome-wide significant SNP rs4141463 located within the gene *MACROD2* (Mono-ADP Ribosylhydrolase 2). Later, a study by Connolly et al. [98] selected individual items from the ADI-R, ADOS, and the Social Responsiveness Scale (SRS) in the Autism Genetic Resource Exchange (AGRE) cohort to perform GWAS. They reported eight genome-wide significant ($P< 5\times10^{-8}$) hits, i.e. rs10239799 (*KCND2:* Potassium Voltage-Gated Channel Subfamily D Member 2) , rs2056412 (*C8ORFK32*: Family With Sequence Similarity 135 Member B), rs2779251 (*NOS2A*: Nitric Oxide Synthase 2), rs1429793 (*NELL1*: Neural EGFL Like 1), rs11899372 (*BIN1*: Bridging Integrator 1), rs4925506 (*MPN2*: Serine Protease 38), rs17134117 (*SDK1*: Sidekick Cell Adhesion Molecule 1) and rs3797817 (*FER*: FER Tyrosine Kinase) associated with "serious facial expressions", "concentrating on parts of object rather than whole picture”, “loss of motor skills”, “faints or blackouts”, “association of loss of skills with physical illness”, “too tense in social settings” and “loss of motor skills”, respectively.

A study by Smoller et al. [99] analysed five psychiatric disorders namely ASD, ADHD, BD, Major depressive disorder and SZ. SNPs at four loci mapping to regions on chromosomes 3p21 and 10q24 passed the genome-wide significance threshold. A more recent GWAS focused on the seven items of the restricted and repetitive behavioral score of the ADI-R in 3,104 ASD-affected individuals. It identified a genome-wide significant association of the SNP rs2898883 ($P< 6.8\times10^{-9}$) with the degree of the repetitive use of objects or interest in parts of objects[100]. This SNP is located within the sixth intron of *PHB* (Prohibitin). On further investigation, they identified candidate target genes of the associated SNPs at that locus and found three more genes: *SLC35B1* (Solute Carrier Family 35 Member B1)*, CALCOCO2* (Calcium Binding And Coiled-Coil Domain 2) and *DLX3* (Distal-Less Homeobox 3).

In short, to date several studies have investigated the association of SNPs with ASD via GWAS but with limited replication success. The reason is the limited sample size and small effects of disease variants, and as a result, these associations are not replicated in other studies. With the advent of large-scale international collaborations to combine genotyping data from different sites, the statistical power has been improved. A recent genome-wide association meta-analysis of 18,381 ASD cases and 27,969 controls identified five genome-wide significant loci with the variants rs910805, rs10099100, rs201910565, rs71190156 and rs111931861. It is the first study to robustly associate common variants with ASD and further highlighted biological insights relating to neuronal function and corticogenesis [57].

1.5.4. CNVs studies in ASD

Beside SNPs, CNVs are another class of genetic variants that are being analysed. Overall 4.8-9.5% of the human genome is affected by CNVs [101]. Since CNVs include deletion, duplication or insertion of DNA fragments their effect on gene expression could also be large. Therefore, they might also be related to phenotypic variations in a genetic disorder. One problem with these studies is the accurate determination of CNVs and their boundaries since they can vary among individuals [102]. CNV studies, similar to SNP studies rely on Array data comparing the intensity of signals across the genomic markers to identify deletions or duplications. CNV studies are mostly done in trios to identify rare *de-novo* CNVs in the affected individual that have not been transmitted by the parents. The term *de-novo* refers to the new mutation, i.e. germline origin of the variant in the affected study participant. CNV studies have found regions in genes associated with ASD[103], type-2 diabetes [104], and SZ [105].

In addition to SNPs, CNVs are an important susceptibility factor for ASD. Studies have shown that the proportion of *de novo* CNVs is three to five times higher in ASD families when compared to controls. Altogether, they explain only 1% genetic heritability of ASD [28,68]. *De novo* CNVs were found in ~ 27% of individuals with syndromic ASD (associated with chromosomal abnormalities or mutations in a single gene) [69]. Individuals with two or more *de novo* CNVs typically have a more severe phenotype. Previous studies have shown that in ~ 7-8% of individuals with ASD chromosomal anomalies were found [70]. Among the most common CNVs in ASD, there are the maternally derived duplications of chromosome 15q11-q13, as well as deletions of 16p11.2 and 22q13. Studies have also found a considerable enrichment within CNVs in ASD for neuronal synaptic complex genes such as *SHANK2* (SH3 And Multiple Ankyrin Repeat Domains 2)*, SHANK3* (SH3 And Multiple Ankyrin Repeat Domains 3)*, NRXN1* (Neurexin 1)*,* and *NLGN4* (Neuroligin 4) [71,72].

CNV studies have provided important regions and genes associated with the ASD phenotype [3,68,72,106]. Previously identified genetic variants included CNVs associated with 7q11.23 [107], 15q11–13 [106], 16p11.2 [68], and 22q11.2 [28] loci, as well as genes *NRXN1* [108], *CNTN4* (Contactin 4) [109]*, SHANK3* [110], and *NLGNs* genes [72]. Among the pioneer studies for CNV analysis, a study by Szatmari et al., 2007 [111] identified 254 highly significant CNVs. Out of these, four CNVs were highlighted and among them, a 300 kb sized CNV deletion on chromosome 2p16 was identified in two families. This region contains coding exons of the *NRXN1* gene, which interacts with neuroligins in synaptogenesis. Hence, disruption of this region can affect the function of *NRXN1*, which might affect ASD or its phenotypes.

Later, a study by Sebat et al., 2007 [71] identified 17 *de novo* (occurs in children but not in their parents) CNVs in 16 individuals. They identified a 4.3 Mb (Megabase) sized *de novo* deletion at 22q13.31-q13.33, which includes the *SHANK3* gene. This region has also been previously associated with ASD [112].

Another recurrently reported CNV region associated with ASD is located on the chromosomal region 16p11.2. Studies have reported microdeletions and microduplications of 16p11.2 which has been validated further to be associated with ASD [28,113].

A whole-genome CNV analysis by Glessner et al.[72] identified CNVs in the loci 15q11–q13, 22q11.21, containing the ASD susceptibility genes *NRXN1* and *CNTN4*. Other new susceptibility genes identified in this study were *NLGN1* (Neuroligin 1) and *ASTN2* (Astrotactin 2).

Furthermore, Pinto et al.[106] analysed the genome-wide features of rare CNVs in ASD. Based on 996 cases and 1,287 controls, they identified 5,478 rare CNVs. By examining parent-child transmission, the authors found 226 *de novo* and inherited CNVs that were not present in controls. As a whole, ASD cases were found to carry a higher number of *de novo* CNVs than controls (1.69 fold, P= 3.4x10^{-4}).

A number of novel genes such as *SHANK2* (SH3 And Multiple Ankyrin Repeat Domains 2), *SYNGAP1* (Synaptic Ras GTPase Activating Protein 1), *DLGAP2* (DLG Associated Protein 2) and the *DDX53* (DEAD-Box Helicase 53) – *PTCHD1* (Patched Domain Containing 1) were found to be associated with ASD in this study.

In another study in Han Chinese population, pathogenic CNVs responsible for ASD were investigated [114]. Genome-wide study of CNVs in 335 ASD cases and 1,093 healthy controls was performed. They identified six CNVs at 6q26 that were extended on different exons of *PARK2* (Parkin RBR E3 Ubiquitin Protein Ligase) gene. *PARK2* was one of the important genes with several case-specific regions overlapped on it.

A recent study investigated 1,108 ASD and 2,458 SZ cases in a Japanese population. 29 clinically significant loci were common in both disorders. Disease-relevant genes were identified in eight known ASD and SZ associated loci, i.e. 3q29, 7q11.23, 15q11.2, 15q11.2-q13.1, 15q13.3, 16p11.2, 17q12, and 22q11.2 [103].

1.5.5. NGS studies in ASD

There are a number of NGS methods available, however, in genomics, the most commonly used methods are whole-genome sequencing (WGS), whole-exome, and *de novo* sequencing. WGS attempts to sequence the whole genome, however, due to sequencing technically difficult regions of the genome, it can capture only 95% of the genome. WES only considers the protein-coding sequences (i.e. exome) for sequencing and offers less coverage than WGS. As WES only focuses on ~1.5% of the genome that constitutes the exomes, the cost to sequence it is ultimately reduced compared to WGS. *De novo* sequencing refers to the sequencing of a primary genetic sequence of a particular organism for which there is no reference sequence available. NGS has been widely used in the identification of variants associated with ASD [115], SZ [116] and depression [117].

Nowadays, NGS studies in ASD are extensively performed and have identified disruptive variants in the protein-coding regions of the genome. One of the earliest NGS studies in ASD is from Sanders et al., 2012 [118]. They performed WES of 928 individuals, which included 200 phenotypically discordant sibling pairs with *de novo* mutations in brain-expressed genes associated with ASD. They identified a total of 279 *de novo* coding mutations and one gene named *SCN2A* (sodium channel, voltage-gated, type II, α subunit) with *de novo* mutations in two affected individuals. Later, a study by Rubeis et al., 2014[119] performed exome sequencing in 3,871 autism cases and 9,937 ancestry-matched or parental controls individuals. They identified 22 autosomal genes at an FDR < 0.05, along with 107 autosomal genes. Moreover, they identified that these genes are enriched for developmental pathways of chromatin remodeling, synaptic function, etc.

Another WES study from 787 ASD families reported that ASD is associated with *de novo* indels (insertion/deletion of a nucleotide base). The study also identified *de novo* indels in the genes of *KMT2E* (lysine methyltransferase 2E), and *RIMS1* (regulating synaptic membrane exocytosis 1) involved in synaptic function and chromatin modification [120].

1.5.6. eQTL studies in ASD

An eQTL (Expression quantitative trait loci) represents a genomic locus or variant, e.g. a SNP that influences the expression level of a gene. eQTLs can act *in cis* if the respective SNP is present near the gene whose expression is influenced or they can act *in trans,* i.e. the SNP is not in close proximity to the gene [121]. Genome-wide eQTL mapping thus identifies the association between gene expression levels and DNA variants (i.e. SNPs or CNVs) by performing a direct association test between markers of genetic variation with gene expression levels across individuals. The analysis requires genetic markers that can be genotyped in a population as well as data on the gene expression in the tissue of interest.

A direct association test is performed between markers of genetic variation with gene expression levels. These analyses can help in identifying the underlying genetic mechanisms of diseases. For example, when SNPs are associated with the expression of a gene in eQTL mapping and with a disease in GWAS. This implicates that the expression of the gene mediates the effect of SNP on the disease [122]. eQTLs have been widely associated with ASD [123], BD [124], and SZ [125].

The relevance of eQTLs in neuropsychiatric disorders has been shown by a study which identified 21 of the *cis*-eQTL variants of genes expressed in the fetal brain, that are located within a region of chromosome 17q21.31 and are enriched among risk variants for ASD, ADHD, SZ and BD disorder [124]. Another study identified global enrichment of brain expression quantitative trait loci among top SNPs from an ASD-GWAS including individual genes *SLC25A12* (Solute Carrier Family 25 Member 12)*, PANX1* (Pannexin 1) *and PANX2* (Pannexin 2) [126]. Furthermore, a meta-analysis of 424 brain samples across five different studies was performed to identify regulatory variants that influence gene expression in the human cortex. They found that 28% of ~1000 autosomal genes encode proteins required for mitochondrial structure or function were eQTLs (enrichment P= 1.3x10^{-9}). Thus, the information generated by eQTLs can provide important insight to understand the underlying biology of associations with psychiatric disorders. Moreover, integrative strategies are also used combining results from GWAS and eQTL to gather information on susceptible SNPs in GWAS such as in Crohn's disease, SZ and psoriasis [127–129].

1.6. ASD data

1.6.1. Quantitative data

This type of data is gathered from clinical interviews such as ADI-R [49], or ADOS [34]. which are the two gold standards in ASD diagnosis (see 1.3). ADI-R is an investigator-based interview for parents or caregivers of individuals with ASD. It comprises 93 questions, which are categorized based on (i) the child's early development; (ii) acquisition and loss of language; (iii) language and communication functioning; (iv) social development and play; (v) interests and behaviors and (vi) general behaviors. ADI-R focuses on behaviors that are less frequent in non-affected individuals, and therefore it is more useful as an ASD-specific measurement. Studies have shown that ADI-R is influenced by the IQ, language of the child, and age, as ADI-R is not recommended for children with non-verbal mental ages of 18 months or below as well as children who have not started to walk [130,131]. In addition, some questions are only for verbal individuals. In ADI-R two separate scores are generated from social communication (verbal and non-verbal communication) and the other for repetitive behaviors. The answers are coded numerically between 0 and 9. 0 denotes that the behavior type specified in the coding does not exist. 1 shows that the behavior type specified is present but not in severe form whereas 9 denotes unknown or not asked question. A total algorithm score is then calculated for each of the areas. An individual is diagnosed with ASD if the scores in every area exceed the cutoff threshold for ASD.

1.6.2. Genotype data in ASD

SNPs and CNVs, both have an important role in the etiology of neuropsychiatric disorders, however here, we only focus on SNP genotype data. The SNP genotype data is generally coded as A, C, G, T or 1, 2, 3, 4 but also as 1 or 2 for the major and minor alleles. The widely used genotype data formats are as follows:

Merlin: This format contains a pedigree and a data file. The pedigree file includes the phenotype and genotype relationships per individual per row. The first four columns contain identifiers for family, individual, father and mother followed by gender information, where 1 is coded for male and 2 for female. Next, the phenotype information is provided in the form of a qualitative or quantitative trait. After this, genotype information for each individual is provided. The data file contains marker information (M), affection status (A), quantitative trait (T) and covariate (C).

PLINK: This format consists either of files for pedigree (fam), SNP genotypes (bed) and SNP information (bim), or flat format consisting of pedigree (ped) and SNP information file (map) (see Appendix).

Vcf (variant calling file): This format contains meta-information lines at the beginning of the file, a header line consisting of chromosome number, SNP position, SNP id, alleles information, a quality score, filter status (if the SNP is called at this position), and additional information followed by genotype encoding.

1.7. Data analysis

1.7.1. Quality Control

For quality assurance of genotype data, QC is a mandatory step before conducting any kind of analysis. Quality thresholds are crucial and strongly dependent on the study design. Such as for performing GWAS, a deep pre-processing and QC steps are required. Biases in study design and errors in genotype calling can introduce a proficient amount of errors and information loss, which can increase the number of false-positive and false-negative associations. To date, there are various QC pipelines and protocols available, specifically used in psychiatric studies such as provided by the Ricopili [13] and the ASC (Autism Sequencing Consortium) framework [119], as well as publicly available protocols [133]. However, there are only a few tools available to perform the QC followed by downstream analysis for researchers with limited knowledge on handling complicated bioinformatics tools.

PLINK is one of the most widely used genetics tool which provides individual commands and options for performing quality checks. The available automated tools to perform QC of genotype data include SNPQC; an R-based pipeline for quality control of Illumina SNP genotyping array data [9]. The pipeline uses the direct output from Genome studio software that allows visualization and analysis of data generated from Illumina [134]. Since SNPQC is designed for Illumina arrays, it is dependent on files that are directly provided by Genome studio and therefore might not be straightforward for the new users with a limited programming background. Another available tool for QC is QCTOOL [135] but it is not updated anymore and currently is legacy software.

1.7.2. Genotype imputation

Some individuals might have missing genotype data at loci, which are actually genotyped for another fraction of individuals. The other scenario could be that the loci are not covered by the analytical platform used. This missing data in association studies can be a limiting factor in terms of sample inclusion and genotyping resolution. For example, these studies exclude individuals with missing genotypes considering a complete case analysis [136]. This not only reduces the sample size but can also cause potential bias and loss in efficiency of further downstream analysis [137]. Imputation of genotype values at loci which are untyped in samples can thus help in improving the mapping of the disease-causing variants, e.g. identify variants, which are not genotyped but are actually associated with a disease phenotype. Imputing these untyped variants can thus finally highlight fine association signals by imputing the un-typed causal variants based on SNPs in LD (Linkage Disequilibrium), i.e. the SNP alleles or DNA sequences that are physically close together in the genome tend to be inherited together and are in high LD rather than the SNPs far apart.

The quality of imputed data largely depends on the reference data selected for imputation, as the unobserved genotypes in the study data set are predicted based on the haplotype (a particular set of alleles that tend to be transmitted together) patterns in the reference panel. The two widely used reference panels are **HapMap and 1000 Genomes:** The HapMap reference dataset was one of the most used reference panels for imputation analysis in the beginning era of Genome-wide association analysis. Phase 2 of the HapMap project contained 270 unrelated individuals from Africa, Asia, and Europe. However, in phase 3 of the HapMap project, the number increased to 1,301 unrelated individuals and also covered individuals from 11 different populations. The dataset included 3.5 million commonly occurring genetic variants. This dataset had a deep coverage as it contained samples from a variety of different populations. The **1000 Genomes** dataset phase 1 was released in 2012 whereas phase 3 was released in 2015. This is the largest reference dataset available for imputation with 2,504 individuals and 84.4 million variants. It provides wide coverage as it contains many more SNPs than the HapMap data.

Imputation of genotype data relies on efficient and correct estimation of haplotypes which is improved by the correct identification of an individual's alleles inherited on one strand from one parent (phased strands). The computationally most intensive step during imputation is pre-phasing; which estimates the strand-based haplotypes (i.e. allele combinations inherited together on one strand) based on the called GWAS genotypes. Pre-phasing before imputation speeds up the imputation performance [138], and the pre-phased data can be used in the future on the availability of a new reference dataset. Thus, having the pre-phased data saves time for imputation and before imputation, since, for each set, the haplotype is estimated based on all the phased alleles. Haplotype estimation can also be performed in unrelated individuals by modeling the haplotype frequencies. Since several haplotype combinations are possible for an individual's genotypes, one can estimate the probability of any given haplotype configuration and choose the most likely configuration or output a set of configurations sampled from the posterior distribution (see 2.7).

SHAPEIT is a widely used tool, which performs phasing. The other widely used tool to infer haplotypes is Phase v2.1 [139]. SHAPEIT differs from it as it uses binary trees to represent the haplotypes for everyone, which overcomes the haplotype inference limitations by speeding up the computations for calculating posterior probabilities of the haplotypes compared to Phase v2.1. In addition, using the binary trees, it looks for the most plausible haplotypes for haplotypes estimation. SHAPEIT has also outperformed the previously used tools like Fastphase [140] and Gebril [141] in terms of speed and accuracy.

To date, there are several genotype imputation pipelines available such as the "genipe" [142], "Molgenis-impute" [11] and "Gimpute" [143] pipelines. Genipe uses PLINK [144], SHAPEIT [145] and IMPUTE2 [138] software to perform complete imputation. Molgenis-impute is a command-line tool that can be run on local servers as well as high computational clusters and is also based on the SHAPEIT [145] and IMPUTE2 [138] tools. Gimpute is an extension to the genipe [142] but with extensive pre and post imputation steps. All these imputation tools are well established and widely used for genotype imputation, though considerable efforts and time are required in setting up a complete framework that includes the necessary pre- and post-processing imputation steps. Minimac3 has been shown to perform better than the other imputation tools available [146] because of its reduced computation time paralleled with a high validity of the imputed variants [146,147].

A short overview of imputation is shown in Figure 2.

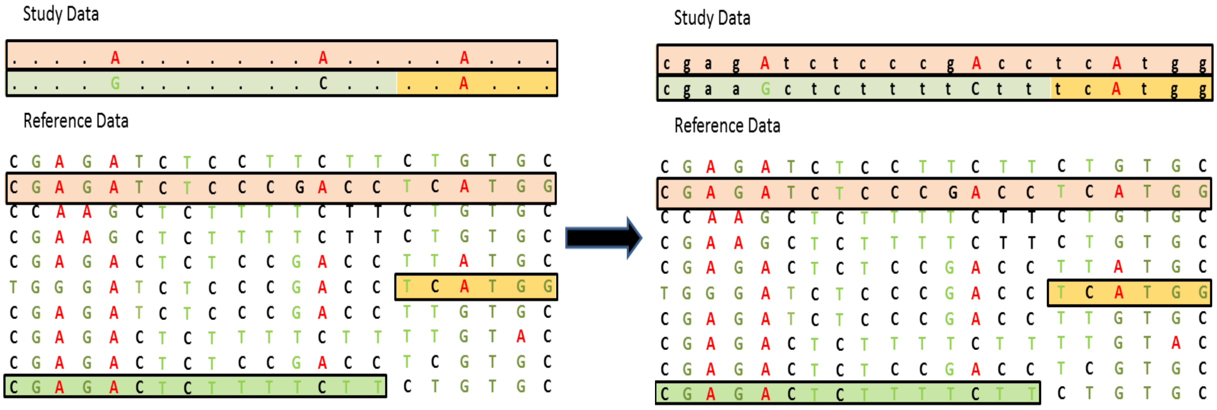

Figure 2 Genotype imputation

The upper panel represents the observed pre-phased data. The reference data consists of genotypes or haplotypes with shared regions identified between study and reference data. Based on this set of information the missing genotypes in the study data are imputed. Figure adapted from Li et al., 2009.

1.7.3. Association analysis

Genetic association analyses are widely used to identify the susceptible genetic variants that are associated with specific traits. The most commonly used association analyses are **candidate gene association** analysis and **genome-wide association** study (GWAS). In the former analysis, candidate genes and polymorphisms are chosen beforehand along with appropriate DNA samples and phenotype for analysis. However, in the latter, the entire genome is scanned for genetic variation. GWAS have superseded candidate gene study in terms of informative and reproducible data on the genetic basis of psychiatric and other complex disorders [148]. Moreover, due to the drastic decrease in genotyping cost, it is possible to genotype hundreds and thousands of genetic markers in large cohorts. However, as large number of SNPs are being analysed in GWAS the number of statistical tests performed is also increased and thus, statistical power is the main issue in these studies. Another notable issue is the effect size of the genetic variants, which goes together with the statistical power. As the individual variants carry only a small risk in disease traits, the effect size is smaller and more statistical power (larger cohorts) is required to detect significant associations at the genome-wide level. To handle these issues, gene-based analyses are applied after performing GWAS (see next section).

To perform GWAS analysis, there are existing pipelines like GWASpi [12], easyGWAS [149], and GWASTools [150]. GWASpi is an application written in Java and can be used under Linux, Mac or Windows. It can be used for pre-GWAS data quality control and conducting GWAS but has not been updated in recent years. Another tool is easyGWAS, which is a web application that allows a user to upload the genotype data and later retrieve the GWAS results. However, in most of the cases, genetic data is restricted to be shared online. There are also several R packages and MATLAB functions available such as "GWASTools", "GWAS", or one can also write own functions to perform GWAS depending on the regression model and covariates.

1.7.4. Gene-based analysis for GWAS

In a GWAS, several millions of SNPs are tested and thus the significance threshold is set to a p-value of $5x10^{-8}$, based on the structure and best estimate of independent SNPs in the human genome. This stringent threshold reduces the number of false-positive findings but also increases the number of false negatives. However, the combined effect of weakly associated SNPs, which may or may not be statistically significant on their own can predict the disease status or symptoms [151]. Thus, to maximize the use of GWAS, gene-based analysis provides an efficient way of combining the effects of individual genetic variants to identify the collective effect at gene level [152]. For polygenic traits, there is more than one gene involved with thousands of genetic variants individually of small effects. This ultimately requires large sample sizes to detect them. When analysing the collective effect of genetic variants, the number of tests needed to be performed is considerably reduced thus allowing the effects of weaker associations to be considered.

The success of GWAS analysis depends greatly on the available sample size. Here, gene-based analyses have the potential to account for multiple independent functional variants within a gene that can thus lead to an increase in power to identify the genes that are actually associated with the trait.

Among the most prominent tools used for gene-based analysis are MAGMA (Multi-marker Analysis of GenoMic Annotation) [153] and VEGAS2 (Versatile Gene-based Association Study 2) [154]. The functionality of both tools is comparable. MAGMA can analyse both raw genotype data as well as summary SNP p-values from a GWAS or meta-analysis. VEGAS2 is available as a web and command-line tool that takes the GWAS summary file (output from GWAS) with SNP IDs and the association p-values. It first assigns the SNPs to genes (17,787 autosomal genes) according to positions on the UCSC Genome Browser hg19 assembly. It then searches for regulatory regions and SNPs which are in LD within defined gene boundaries and positions around. The approach is permutation-based for testing the enrichment for highly associated markers using the LD information from a reference panel so that all the association signals from shared variants in LD can be detected.

MAGMA can use raw genotype data as well, where it first performs a principal component analysis (PCA) for all the markers in each gene. MAGMA then performs a linear regression where it uses the PCA eigenvectors as predictor variables and phenotype as the criterion variable. In this way, MAGMA overcomes the problem of low statistical power which comes into existence when a gene contains many markers and some of them are in strong LD. MAGMA also provides the option of performing gene analysis on GWAS summary data (see 2.9). Thus, MAGMA is reported to be a distinctive tool compared to other methods like INRICH [155], ALIGATOR [156], VEGAS [157] and MAGENTA [158] specifically because of more statistical power, less affected by linkage disequilibrium and multi-marker associations due to its multiple regression approach and being computationally less demanding [47]. One of the main differences between MAGMA and VEGAS2 is that MAGMA provides additional gene-set analysis methods that can be categorized into self-contained and competitive analysis. The former tests whether the gene set contains any association at all with a phenotype of interest and the latter tests whether the phenotype association in the gene set is greater than in other genes.

1.7.5. Pathway enrichment analysis

Once the SNPs and their respective genes are associated with a disease phenotype, a further insight into the functional effect of a SNP can serve as prime importance for understanding the underlying mechanism of a disease. Such as at the biological system level by analysing their effect on signaling pathways. To gain a mechanistic overview of any set of genes associated with a phenotype, pathway analysis is an excellent approach. It can help to identify the underlying pathways and mechanisms. The basic principle behind the analysis is to identify the biological pathways and gene ontology that are enriched in a gene list more than what is expected by chance. For example, when looking for annotations in the gene ontology, a standardized annotation platform of gene products, the frequency of individual annotations in the significant gene list is compared to the complete list of all genes on the array or in the human genome. In this way, a set of enriched biological processes annotated with the respective genes is identified and allows to draw the conclusion that the trait of interest is underlying alterations thereof. There are numerous pathway enrichment analysis tools, gene set enrichment analysis (GSEA) and R packages available for performing these analyses such as Database for Annotation, Visualization and Integrated Discovery (DAVID) [159], MetaCore [160], Ingenuity Pathway Analysis (IPA) (QIAGEN Inc., https://www.qiagenbioinformatics.com/products/ingenuity-pathway-analysis), Panther [161] and so on. MetaCore and IPA are high-end tools with very detailed information of the pathways, its drug targets and interactive maps however these are not freely available. One of the limitations of most of the tools is that it uses limited resources that are not timely updated such as DAVID. In comparison, GO-Elite [162] is a web-based and a command-line tool that performs over-representation analysis (ORA) and also accounts for the hierarchial semantic-structure of the GO annotation terms. These GO annotations are always updated and automatically downloaded in GO-Elite by default.

1.8. Aims of the study

Genetics and neuropsychiatry are two individual fields, but to unveil the pathomechanisms underlying complex neuropsychiatric disorders there is a strong urge to strengthen the methods and to develop tools that can integrate data from different disciplines. These tools should be central for researchers in genetics and neuropsychology to grasp and apply in research.

ASD is one of such complex developmental disorder that is diagnosed based on deficits in two domains: (A) social interaction and communication and (B) restricted and repetitive behavior. In this work, we incorporated two large ASD cohorts, i.e. AGP (Autism Genome Project) and a German cohort. The overall aim of the study is to develop and evaluate an integrative bioinformatics Big-Data Pipeline for the analysis of complex genetic traits in neuropsychiatry.

Therefore, we defined the following aims:

1. To elucidate the genetic architecture of quantitative ASD traits we first aimed at identifying and validating independent behavioral subdomains based on available clinical assessments.
2. Generation of an integrative bioinformatics pipeline which can perform the following analysis:

   i.Quality Control of the genotype data

   ii. Genotype imputation

   iii. Genome-wide association analysis

   iv. Gene-based enrichment analysis

   v.Brain enrichment analysis

3. To validate the implemented pipeline we applied MAGNET on the identified ASD subdomains in two ASD cohorts to identify underlying genetic pathomechanisms associated with these individual subdomains.
4. Further, our goal was to investigate if the phenotypically defined ASD subdomains are genetically independent or are correlated with each other and if they share genetic etiology with ASD risk.

2. Materials and methods

2.1. ASD quantitative data

In this study, we included a German cohort with individuals from n=705 families (n=625 parent-child trios, n=53 parent-child duos, and n=27 singletons) recruited at the Departments of Child and Adolescent Psychiatry at Goethe-University Frankfurt am Main, University Hospital Bern, Saarland University Hospital, and University Hospital Freiburg. The other cohort is the AGP (Autism Genome Project) cohort including n=2,730 trio families, and n=5 parent-child duos collected at 15 clinical sites across the US, Canada, and Europe. Overlapping German samples were excluded from the AGP cohort. The diagnosis was established by experienced clinicians based on thorough clinical assessment, the Social Communication Questionnaire (SCQ) [163], ADI-R [49] and/or ADOS [164]. Exclusion criteria and sample quality checks were based on the AGP cohort [97]. For the final analysis, only one affected individual per family, i.e. the index patient, with complete ADI-R and genotype information available was included.

Written informed consent was obtained from all participants or caregivers, and the study was approved by the local ethical committees (decisions 162/99 (Frankfurt); 147/10 (Aachen); 214/10 (Bern); 73/04 (Homburg), 237/09 (Frankfurt)). All ASD individuals were diagnosed according to ICD-10 [165] by experienced child psychiatrists or clinical child psychologists. The diagnosis was confirmed by the ADI-R [49,166] and/or ADOS [34]. Individuals with SZ, BD, a neurodegenerative disorder, a known cytogenetic finding, fragile-X Syndrome, Angelman syndrome, Prader-Willi syndrome, Rett syndrome or any other genetically diagnosed disorder, IQ<35, history of a severe medical condition, birth weight <1,500 grams or cerebral palsy were excluded. Sample quality checks and exclusion criteria are published elsewhere [97].

2.2. SNP genotype data

In this project, we focused on SNPs genotype data. The German cohort was genotyped using Illumina HumanOmniExpress 12v1-H bead arrays at Life and Brain (Bonn, Germany). The AGP cohort was genotyped on 550K Illumina, 510K Illumina, 1M Single and 1M Duo Illumina Chips [97]. The methods implemented for performing QC of the genotype data are detailed in 2.6.

SNP genotype data carries information of each SNP with an identification number, i.e. an “rs” number or the chromosome number and genomic position, e.g. 7:24926377 where 7 is the chromosome number and 24926377 is the genomic position. Besides this information about chromosome number, physical position (Distance between two markers measured by the number of nucleotides between them) and genetic position (Distance between chromosome positions) is also provided. Moreover, it also includes a file consisting of sample information encompassing the pedigree and individual information. The raw intensities from the array are then normalized and SNPs are called using specific algorithms [167]. The information can then be coded in PLINK format, i.e. as a ped and map or as bed, bim and fam files. For a detailed description of the SNP genotype files that can be provided as input to our developed pipeline please see Appendix.

I. Preliminary data analysis of phenotype data

2.3. Quality assurance of ADI-R data

We focus on ADI-R data in our study which has a total of 93 items organized into specific categories (see 1.4.1). Among these 93 ADI-R items, 42 are methodically combined in the form of a formal, diagnostic algorithm for autism or a general diagnosis of ASD. We selected 28 “ever/most abnormal” items from ADI-R questionnaire based on the study by Liu et al. [84], where “ever” denotes if a behavior ever occurred and “most abnormal” represents whether the behavior was present at a specific, defined period between 4 and 5 years of age. A list of these 28 items is provided in Table 3 in the results section. These items are available for both verbal and non-verbal individuals. ADI-R diagnostic algorithm scores of 3 were recoded as 2 to limit the impact of severity before performing phenotype imputation. Moreover, it was made sure that all items use the same coding in both cohorts such as item "Repetitive use of objects" used 7 as a score, which means that the individual shows a not age-related interest in a toy, but this play cannot be designated into a high-grade stereotype, therefore it is coded as 0 in both cohorts. Similarly, item 31: "Use of others body to communicate" codes 8 for little or no spontaneous communication, which was then coded as 0 in both cohorts. Besides these instances, all 8 and 9 scores were coded to NA (Not available). All individuals who had >10% missing items in the 28 selected items were excluded from both cohorts. The item with the highest value between the ever or most scores was selected for imputation. As the sample size is an important factor affecting the statistical power and for reliable estimates, respective ADI-R items from AGP and German cohorts were combined for phenotype imputation.

2.4. Phenotype imputation of missing ADI-R data

In psychiatric research, it is a common problem that the clinical interviews used for diagnosing the disorder, e.g. in ADI-R some questions are left unanswered. Multiple imputation (MI) is a statistical technique for analysing incomplete data sets. MI fills the missing values multiple times and creates multiple "complete" datasets. Multivariate imputation by chained equations (MICE) was implemented in R using mice [168] package.

MICE is one of the most powerful techniques in current research to deal with such data [169]. We performed MI based on predictive mean matching (pmm) which is a semi-parametric imputation approach. It aims at reducing the bias introduced in a dataset because of imputation and looks for real values sampled from data[170]. MI using pmm is performed as follows:

i. Let us assume a variable ***Y*** which is to be imputed based on ***X*** predictors.

ii. Estimate a linear regression of ***Y*** on ***X*** producing β.

iii. A random draw from the posterior predictive distribution of β is made to generate a set of $\beta*$. Based on Bayesian inference, the information about unknown parameters is expressed as a form of the posterior probability distribution to create random variability in the imputed values [168].

iv. Using $\beta*$, the missing values are predicted for all cases with and without data missing on ***Y.***

v. In each case where ***Y*** is missing, the closest predicted value is identified among the cases where ***Y*** is observed.

vi. pmm then randomly draws one of the three close cases and imputes the missing value $\boldsymbol{Y_i}$ with the observed value of this close case.

vii. Depending on the ***m***, i.e. number of multiple imputed datasets, to generate the algorithm, the process is repeated ***m*** times in a chain. As a result, ***m*** complete datasets are generated.

We created 10 imputations, a number between 5-10 is suggested as computationally feasible as suggested by Horton et al. [171], one dataset out of these ***m*** multiply imputed datasets was selected for further analysis.

2.5. Identifying ADI-R subdomains

An interesting approach for looking at the quantitative data is to identify meaningful groups or subgroups to target the underlying genetic associations. Commonly used approaches to dissect the heterogeneous architecture of ASD is to perform factor analysis [84,172] or principal component analysis [173,174]. These analyses can firstly help in reducing the number of variables to more representative and meaningful factors. Secondly, specifically looking at the individual subgroups helps in decreasing the overall heterogeneity of the disorder and working on more homogenous groups.

PCA was preferred over the classical EFA (Exploratory factor analysis) approaches to preserve the maximum amount of variation and independence in the resulting factors. This can play a role in determining that the genetic factors might be independent of each other. EFA does not account for the maximum variation and estimates interdependence between variables to find common factors, which might not necessarily be independent of each other.

Following criteria were satisfied before performing PCA:

i. **Sample size:** A sample size of total n=50-400 is recommended to yield reliable estimates [175,176].

ii. **Factorability:** Checks that some correlations should exist among the variables so that coherent factors can be identified. It is expected that the variables have a degree of co-linearity among the variables but not an extreme degree or singularity among the variables. The following two tests are performed for structure detection:

a. **Bartlett's test of sphericity:** The null hypothesis is that the correlation matrix calculated for the variables in the samples is an identity matrix. Whereas the alternative hypothesis is that they are related and a structure could be detected. The purpose is to identify if there are redundant variables in the samples, which can be summarized into a few numbers of components. The test checks if the observed correlation matrix R= $(r_{ij})_{(pxp)}$ (where p is the number of variables) diverges significantly from the identity matrix. A significant result indicates that a principal component analysis is appropriate for the data set.

b. **Kaiser Maier Olkin (KMO) test:** KMO also indicates the suitability of the data for structure detection. The KMO measure of sampling adequacy is a statistical test that indicates the proportion of variance in the items that might be caused by the underlying components. High values close to 1 indicate that performing a PCA would be useful.

A partial correlation is calculated first which is the relation between two variables and removes the effect of remaining variables. In the next step, KMO index compares the values of correlations between variables and those of the partial correlations. If two variables share a common factor with other variables, their partial correlation will be small, indicating the unique variance they share.

$$KMO = \frac{\sum\sum r_{ij}^2}{\sum\sum r_{ij}^2 + \sum\sum a_{ij}^2}$$

where r_{ij} is the correlation matrix and a_{ij} is the partial covariance matrix

Based on the Kaiser's criteria a KMO value between 0.9 -1 is considered best[177].

2.5.1. PCA

PCA is a powerful tool to highlight similar patterns, similarities, and differences in the data. This approach is very useful when dealing with multidimensional data. After the identification of patterns, the data is compressed by reducing the total number of dimensions. We applied PCA to identify the structure and dimensions of the quantitative trait data. The steps performed in PCA are as follows:

i. All initial variables are standardized so that each contributes equally to the analysis. Mathematically this is done as follows:

$$Z = \frac{value - mean}{standard\ deviation}$$

ii. Calculation of the covariance matrix to identify the variation in variables from the mean with respect to each other. Moreover, it reveals the relationship of the variables among each other. Also if they are highly correlated in such a way that they contain redundant information. A covariance matrix is then simply a symmetric matrix with ***nxn*** dimensions and has all possible combinations of variables. For example, for a 3-dimensional data set with 3 variables x, y, and z, the covariance matrix is a 3×3 matrix ***A*** of this form:

$$A = \begin{bmatrix} cov(x,x) & cov(x,y) & cov(x,z) \\ cov(y,x) & cov(y,y) & cov(y,z) \\ cov(z,x) & cov(z,y) & cov(z,z) \end{bmatrix}$$

Whereas cov(x,x)=var(x) in the main diagonal and cov(x , y) = cov(y , x) so the upper and lower half of the diagonal is the same.

iii. Computation of the eigenvectors (principal components) and eigenvalues (explains how much variance is present in the data) of the covariance matrix ***A***. This can be expressed as:

$$Av = \lambda v,$$

where ***v*** is a vector, ***λ*** is the eigenvalue associated with eigenvector ***v*** of ***A***. The eigenvalues of ***A*** can be rewritten as $\det(A - \lambda I) = 0$, where ***I*** is an identity matrix. Simplifying the matrix and calculating the determinant will provide the eigenvalue of the matrix and the corresponding eigenvector.

iv. Arranging the eigenvectors in descending order of eigenvalues will provide principal components in order of significance. Eigenvectors with the lowest eigenvalues contain the least information about the distribution of the data. The number of components is equal to the number of dimensions of the data. But, PCA tries to put maximum information in the first component.

v. Rotation

For a meaningful interpretation, it is necessary to spread the variability more evenly among the components. Rotating the components will help in serving a simple structure. We chose "varimax" rotation, which is an orthogonal rotation of the component axes to maximize the variance of the squared loadings of a component (columns) on all the items (rows) in a components matrix. The loadings from PCA are the weights and correlations between each variable and the component. The higher the loads the more relevant it is in defining the component. PCA was performed with varimax rotation on 28 ADI-R items using the R package psych [178] as in previous studies [173,174].

vi. Component extraction

Components are extracted based on the following three criteria:

-Scree plot and Eigenvalue: A scree plot shows the eigenvalues of the principal components on the y-axis and the number of factors on the x-axis. The point where the slope of the curve is leveling off ("the elbow") indicates the possible factor solution.

-Communalities: The proportion of variance accounted for each variable by the principal components variables. Small values indicate variables that are not well represented in the common factor space and vice versa.

-Total variance explained: Total amount of variability of the original variables explained by each principal component.

vi. Interpretation of component loadings

The rotated factors should make a theoretical sense to the researcher. Each of the identified components should have at least three variables with high loadings and each variable should load highly on only one component.

The best solution for the number of components to be included was identified based on Kaiser's criterion i.e. to exclude all components with eigenvalues under 1.0 [179], and scree plot [180]. Components were retained if (i) each component have at least three items loaded onto it [181,182], however, additional variables improve stability [183]; (ii) loadings of respective items >0.4, which is more stringent than otherwise defined criteria (>0.35) [184]; and (iii) they are interpretable. The respective items were summed up to provide a combined score, which will be used for subsequent analysis.

II. The MAGNET tool: Implemented methods

Development of MAGNET was divided into five main parts, i.e. I) quality check (QC) of the genotype data, II) imputation of genotype data, III) GWAS, IV) enrichment analysis, V) integration of transcriptome data. This section details all the methods and algorithms implemented within MAGNET and the respective criteria used within each part. The list of software used for the analysis is provided in Table 1.

• Tool	Description
PLINK v 1.9 (Purcell *et al.*, 2007)	Genetic data analysis
liftOver (Tyner *et al.*, 2017)	Converts between genome builds
SHAPEIT v2.727 (Delaneau *et al.*, 2011)	Haplotype estimation of SNP genotypes
Minimac3 (Browning and Browning, 2016)	Imputation
MAGMA v1.06 (Leeuw *et al.*, 2015)	Gene-based test
GO_Elite v1.2.6(Zambon *et al.*, 2012)	Gene Ontology & KEGG pathways

Table 1 Software used in MAGNET

2.6. QC

QC plays a crucial part in data analysis. Although, the initial quality checks are mostly performed at the genotyping centers but a second thorough quality check will assure that the data produced is of high quality. QC steps in our framework are based on the most widely used pipelines for QC in psychiatric studies provided by the Ricopili lab and the ASC (Autism Sequencing Consortium) framework [119]. The data for GWAS requires a sufficient amount of pre-processing and QC steps. Any biases in study design and errors in genotype calling can introduce errors and loss, which can increase the number of false-positive and false-negative associations. All the QC steps are implemented in PLINK and QC plots are generated in R. The standard steps and thresholds used in QC are detailed as below:

2.6.1. Genotyping rate

The distribution of the missing genotypes is analysed using PLINK. We chose a minimum classical genotype rate of 95% based on the ASC guidelines [97], it would filter all SNPs having more than 5% of missing data. Similarly, if an individual has more than 5% of missing genotypes, this individual would be excluded from the study dataset. This is lower than the other suggested thresholds of 98% -99% [186,187].

Thus, our framework allows the inclusion of more variants and individuals, which increases genomic resolution (more SNPs) and reduces beta errors (more samples). This is done by using “--geno” option in PLINK to exclude SNPs based on the missing genotype rate. Similarly, individuals with missing genotype data can be filtered using the “-- mind” command. It is recommended to first filter the SNPs and then individuals with high missing genotype data.

2.6.2. Application of the Hardy Weinberg Equilibrium

The Hardy Weinberg Equilibrium (HWE) principle assumes that the genetic variation in a population will remain constant from one generation to the next without any evolutionary influences. It has been known that potential genotyping errors, population stratification, and inbreeding indicate extreme HWE deviations. HWE p-value thresholds used are $< 10^{-8}$ [119], if both cases and controls are present, then $<1e^{-10}$ in cases and $<1e^{-6}$ in controls[186]. We select a HWE threshold of p-value $< 10^{-8}$ based on the ASC framework. Our framework is optimized for quantitative/qualitative traits, and thus differentiation between cases and controls is not applicable.

It would be also worthwhile to identify the rates of homozygosity (two identical forms of an allele, one inherited from each parent), as high rates of homozygosity can reflect poor genotyping due to a poor-quality sample, or sample contamination generating an additional variation. Extreme outliers for heterozygosity should be discarded.

Let us suppose that the minor allele frequency is represented as “***q***” and the probabilities of the three possible genotypes is denoted as ***aa, Aa*** and ***AA*** at a biallelic locus which is in hardy Weinberg equilibrium, this can be represented as follows:

Let $x = AA$, $y = Aa$ and $z = aa$ and $N = x + y + z$ where N is the sample size.

So it can be written as:

$$f(AA) = \frac{x}{N} \quad ; \quad f(Aa) = \frac{y}{N} \quad ; \quad f(aa) = \frac{z}{N}$$

$$f(A) = \frac{(2x + y)}{2N} \quad ; \quad f(a) = \frac{(2z + y)}{2N}$$

Or $f(A) = f(AA) + \frac{1}{2}f(Aa)$

$$f(a) = f(aa) + \frac{1}{2}f(Aa)$$

Let $\mathrm{p} = \mathrm{f(A)}, \mathrm{q} = \mathrm{f(a)}$ where p and q are allele frequencies of allele ***A*** and ***a*** in the population.

The sum of the allele frequencies for all the alleles at the locus must be 1 so:

$$p + q = 1 \quad ; \quad p = 1 - q \quad ; \quad q = 1 - p$$

$$(p + q)^2 = p^2 + 2pq + q^2 = 1$$

$$(1 - q)^2 \ + 2(1 - q)(q) + q^2 = 1$$

In this equation, p^2 represents the frequency of the homozygous genotype AA, q^2 represents the frequency of the homozygous genotype aa, and 2pq represents the frequency of the heterozygous genotype Aa. One can calculate the frequencies of the three genotypes if the frequencies of p and q are known.

p and q are used interchangeably as A and a, however, q is usually used for the rarer, recessive or deleterious allele. A Pearson's chi-squared test is performed to test if the observed genotype frequencies obtained from the data deviate from the expected genotype frequencies based on the Hardy-Weinberg principle. Low p-values indicate that a SNP is out of HWE. This can be calculated as follows:

$$\chi^2 \ = \Sigma \frac{(O - E)^2}{E}$$

where O denotes observed frequency and E the expected frequency, calculated for $f(AA), f(Aa)\ and\ f(aa)$ and summed up to get a χ^2 distribution-based p-value. Degrees of freedom (DF) is calculated using the following formula:

$$DF = (r - 1)\ (c - 1)\ ,$$

where r = number of rows and c = number of columns.

Each SNP is tested for HWE since poor-quality genotyping can cause heterozygotes being called as homozygotes, which can lead to generating more homozygotes than expected. In individuals, high rates of homozygosity can indicate that the quality of the sample is poor or the sample is contaminated. SNPs extremely discordant with HWE and extreme outliers for heterozygosity should also be discarded. This is performed in PLINK using the “--hwe” command.

2.6.3. Minor Allele Frequency (MAF) filtering

Minor allele is defined as the less frequent of two variants of a gene. MAF removes SNPs, which fall below a specific threshold. Minor alleles are more often to be risk alleles in GWAS on complex diseases [188]. MAF can also help to distinguish between common and rare variants. The power to detect genetic effects expressed as 1-beta error frequency is dependent on the MAF. Moreover, MAF depends on the study design and sample size. The widely used thresholds are between 1%-5% [119,186]. These variants explain most of the genetic variance in complex traits [253]. However, the rate of false negatives decreases with an increase in MAF and sample size values. We selected only common SNPs and therefore limited SNPs to a MAF ≥ 2%. In addition, we performed a power analysis using G*Power 3.1.9.2 [185].

The frequency of an allele can be defined as:

$$\text{Frequency of allele A } = \frac{\text{Number of copies of allele "A" in population}}{\text{Total number of alleles "A" and "B" in population}}$$

The frequency of both alleles should add up to 1. The MAF threshold can depend on the sample size since larger samples can use lower MAF thresholds. Very low-frequency alleles are more likely to represent genotyping error and can give spurious association results. PLINK uses the “--maf” command to perform this step.

2.6.4. Sex check

This step ensures that the self-reported gender from the individuals matches the genotyped gender, i.e. the gender reported based on the X-chromosome from the dataset. We used here the most commonly used threshold for sex-check, i.e. the males should have an X chromosome homozygosity estimate >0.8 and females < 0.2[189] or for males an estimate of 1[97]. This step was also implemented in PLINK using the command “--sex-check” command to detect if the SNP and pedigree data gender are different. If the gender information of an individual varies from the input dataset provided gender, the family and individual id are reported in the list of individuals with gender discrepancies. We implemented in our pipeline to remove samples, that have inconsistencies between the genotype-based gender and the reported gender. However, it asks the user to update the gender information for the reported individuals. A wrong gender annotation might lead to the omission of data ultimately leading to a reduction in sample size.

Moreover, this information also reveals sex chromosome anomalies, which are difficult to detect phenotypically. High levels of heterozygosity rate or low levels of homozygosity within an individual will be an indication that the sample quality is low and there is a chance of sample contamination or inbreeding as discussed in the next section.

2.6.5. Inbreeding and contamination

The step was implemented to identify inbreeding and contamination in the sample, which can occur due to mixed DNA samples. The probability of two alleles at a given locus in an individual is calculated based on the population data to identify if they are identical by descent from a common ancestor. This is the probability that an individual is homozygous for an ancestral allele by inheritance and not by mutation, i.e. inbreeding coefficient (F) [190]. Samples with an F > 0.2 have a high rate of homozygous alleles and are thus considered to be likely inbred, while a coefficient < -0.15 marks samples with too few homozygous alleles and are thus likely to be contaminated with other DNA [186]. These thresholds are based on the ASC criteria. We use a stringent lower bound value to avoid any risk of contamination in the sample. The inbreeding coefficients are calculated using the "--het" command in PLINK.

2.6.6. Mendelian error

This step was implemented to test if the alleles of an individual could have been inherited from one of the individual's biological parents, following laws of Mendelian inheritance, in particular, the law of segregation and the law of independent assortment [191]. SNPs>4 Mendel errors and individuals in trio dataset with >10,000 Mendel errors are suggested to be removed[186]. Based on ASC guidelines for trio datasets the Mendel errors threshold for SNPs is >1% and individuals is > 10,000 Mendel errors. We selected a Mendelian error threshold of >1% for individuals and a Mendelian error frequency > 10 % for SNPs. Individuals and SNPs below these thresholds will be excluded. However, the user can adjust the thresholds based on the study design. We implemented PLINK command "--me" to filter individuals based on Mendel error rate.

2.6.7. Identity by descent (IBD)

To account for any duplicate individuals in a dataset we applied IBD criteria. It determines if two individuals share alleles that are inherited from common ancestors, to identify any duplicate individuals.

For monozygotic twins or duplicates, the IBD= 100%. An IBD of 50% corresponds to first-degree relatives (individual's parents, siblings or child), an IBD of 25% represents second-degree relatives (such as uncles, nieces, or grandparents of an individual) [133]. An additional IBD-derived measure is $\hat{\pi}$ (pi-hat), a reference value for measuring genome-wide estimates of IBD [192]. It gives the summary statistics of overall IBD proportion to tell if the samples are related or unrelated. Due to genotyping errors, a non-random association of alleles between different loci occurs, i.e. linkage disequilibrium variation around the theoretical values. We perform relatedness testing using $\hat{\pi}$, where one of the two individuals with $\hat{\pi}$> 0.8 (two genetically identical samples) is excluded. Thresholds were based on the ASC thresholds

[119]. The other thresholds include an IBD measure of > 0.9 to report identical samples and > 0.2 for reporting closely related members[133,186].

Genome-wide IBD-sharing coefficients are calculated between individuals from whole-genome data. Probabilities of sharing 0, 1 or 2 alleles can be provided as a metric to calculate the hidden Markov model which provides multipoint estimates of allele-sharing IBD for each pair of individuals in a homogeneous sample. We require the conditional probability of IBD for z = 0, 1, or 2 at a particular position, given the marker genotypes ***M*** of all ***K*** markers on a chromosome, ***P(Z = z|M)***. This can be re-expressed, using- the Bayes theorem, as

$$P(Z = z|M) = \frac{(P(M|Z = z)(P(Z = z)}{\sum_{z' = 0}^{2} P(M|Z = z')P(Z = z')}$$

In this equation ***Z*** denotes the possible states being 0, 1, and 2. The global IBD sharing probability for the whole genome is ***P (Z=z)***, and the summation is over the three possible IBD states.

In most studies, there are discrepancies between pedigrees provided and relatedness inferred from the genotype data. To infer genetic relatedness, we estimate coefficients of IBD. It is important to identify and take into account unannotated relationships. In this way analyses assuming all subjects are unrelated can use a filtered subset of samples. This step is performed in PLINK using the "--genome" command.

2.6.8. Population stratification

Performing GWAS analysis with a huge sample size can often lead to bias, which might be due to confounding factors such as population stratification. We implemented population stratification analysis within our pipeline to identify the presence of multiple subpopulations (e.g., individuals with different ethnic backgrounds) in a study. As allele frequencies can differ between subpopulations, population stratification can lead to false-positive associations and/or mask true associations. Therefore, as a result of varying frequencies of minor alleles in genetically distant ancestries, population substructures could be visualized. We implemented PLINK to perform population stratification and applied the multidimensional scaling (MDS) methods to identify ***n***-dimensional representation of the population. Following steps were performed:

i. The SNPs after passing all the quality checks are used for the analysis.

ii. Pairwise IBS distance is calculated for all the autosomal SNPs.

iii. Nearest neighbors are identified based on the pairwise IBS distance.

iv. This distance is then transformed into Z-score.

v. An ***n*** number of dimensions can be extracted using the MDS-plot.

vi. The values for each *n* dimensions can be then used as covariates in the downstream analysis.

For *N* individuals in a sample, a ***N x N*** matrix of genome-wide IBS pairwise distances is generated and MDS is performed using the "--mds-plot" and "--cluster" options collectively. At this step, the quality check is completed and all plots with pre and post QC analysis and final QC data are saved.

2.7. Genotype imputation

This section refers to the methods and algorithms used in the development of second part of our pipeline. Data handling steps are integrated within MAGNET to directly provide the QC output as in input for genotype imputation. The following steps are implemented within MAGNET:

2.7.1.1. Matching genomic build

At this stage, it is essential to check the SNP names and their genomic positions to see if they match the genome build of the reference genome. In case the genomic build of the targeted and the reference data set do not align with each other, it can result in mismatched SNP positions and wrong annotations. MAGNET uses 1000 Genome data as reference data [19], i.e. GRCh37 or build 37 (Genome Reference Consortium Human build 37). For correct matching, MAGNET implements liftOver [193] and performs the following steps in an automated manner:

i. Generates a liftOver format bed file, which is in the following format

Chromosome Number	Starting position	Ending position	SNP name
chr1	743267	743268	rs3115860

ii. Chooses the chain file (alignment file with chromosome number, chromosome size, strand, alignment positions of the reference and query sequence) to select for updating the genome build. Users can select among hg16, hg17, hg18 and hg38 annotation files depending on the study data (by default hg18). In case the data is already in hg19 format, the files remain unchanged.

iii. A list of SNPs with an unknown chromosome or position and are not in the hg19 reference is generated within the pipeline and these SNPs are ultimately removed using PLINK command "--exclude".

iv. SNP annotation is then updated by liftOver ensuring that the study and reference genome build are the same.

v. SNPs that were not updated after liftOver are again removed using the PLINK command "--exclude" from the PLINK data file.

For the next steps, only affected individuals are considered. By default, we set our pipeline to distinguish between affected and unaffected individuals using the PLINK coding provided for the individuals. However, the user is free to choose if all samples are needed for the study. The following steps will be performed for each chromosome within an automated loop to parallelize the process.

2.7.1.2. Strand checking

The lifted files in the PLINK format will then be provided for strand checking. For a successful and correct imputation, it is also important that the provided genotype data and the reference alleles are matched and are annotated based on the same strand. The difference in strands could arise due to differing genotyping platforms, which may use a forward strand of the human genome assembly, some use Illuminas's annotation while some use Affymetrix annotation.

For strand check, we integrated SHAPEIT [145] which highlights and corrects for any strand inconsistencies. It identifies the SNPs with the possible problem of strand flip and converts the forward allele to the "+" strand of the human genome reference assembly. It also considers if the alleles are changed to their complementary alleles (C-G and A-T) based on three criteria: (a) the observed alleles,

(b) minor allele frequencies (MAF), and (c) linkage-disequilibrium (LD) pattern within a specific SNP window [194]. SNPs with persisting problems and errors are then removed from the dataset.

The command used in SHAPEIT for strand checking is "-check". This provides file information in the following format:

type	**pos**	**main id**	**main A**	**main B**	**main flippable**	**ref_id**	**ref_A**	**ref_B**	**ref flippable**
Strand	Strand	18681293	A	G	1	rs1006881:18681293:C:T	C	T	0
Missing	Missing	19347892	C	T	1	NA	NA	NA	1

Here, a two-line example is shown, the actual file reports all the alignment problems detected between the study and reference data. The columns in this file represent the type of the alignment problem, the physical position, alleles and id of the SNP as well SNP id and alleles in the reference panel. Two separate SNP lists are generated based on the type, i.e."strand" or "missing", which are flipped or excluded, respectively. For the former, the "--flip" command is used whereas for the latter "--exclude" command is used in PLINK. In the end, PLINK files will be generated which can be used for phasing.

2.7.1.3. Phasing

For this step, scripts are automatically generated within our pipeline using Python to split the PLINK files for each chromosome in the study data and the reference panel files with SNP information, these scripts will run in parallel. Our pipeline implements SHAPEIT which uses compact hidden Markov model for sampling haplotypes for unrelated individuals. Let us suppose that an individual is selected from a population for phasing whose genotypes of three heterozygous markers (since there are two different alleles) are known. The parental information is missing and therefore each of the three markers has a probability of falling into a certain haplotype combination. If an individual has $\boldsymbol{N}$ heterozygous markers, there are $2^{\boldsymbol{N}}$ different haplotype combinations. But keeping in view that all humans are historically related there are common haplotypes present among many samples individuals. In order to infer haplotypes in unrelated individuals, it is necessary to identify common haplotype patterns.

Let ***G*** be the observed genotype and ***D*** as the unobserved diplotype of an unrelated individual. A diplotype here is a pair of haplotypes (*h1, h2).* Let ***H*** denote a set of ***K*** haplotypes defined over ***M*** markers. When updating the haplotypes for a given individual, ***H*** would be the set of current haplotype estimates of all other individuals. The total number of markers M are subdivided into non-overlapping subsets of consecutive markers also termed as "segments" in which the number of distinct haplotypes in ***H*** is limited. The haplotypes of ***H*** are split so that there exist ~***J*** haplotypes by segments with ***J < K***.

A graph $\boldsymbol{H_g}$ is built based on these haplotype segments, where edges are the probabilities. At each marker, there are ~***J*** nodes, one for each distinct haplotype in the segment in which the marker resides. The goal is to sample the diplotype for ***G*** conditional on the known haplotypes from $\boldsymbol{H_g}$ that is, by sampling from P($D/G, H_g$). The method used in SHAPEIT thus samples pairs of haplotypes from the probability of ***h*** given $\boldsymbol{H_g}$, i.e. P(h/H_g) that are consistent with **G**. If ***G*** has ***s*** heterozygous markers then the candidate haplotypes would be 2s, where ***S*** is used to denote the set of possible haplotypes. This method scales linearly with the number of haplotypes used in each iteration, i.e. O(*MJ*). The other HMM-based methods such as Impute2 and MaCH are O(MJ^2)[145].

At the end of this step, phased files are generated which are then converted to vcf (variant calling files) format automatically by our pipeline. This is a standardized format for performing imputation. It is stored in a compressed manner and can be used for fast data retrieval of genetic variants.

2.7.1.4. Imputation

For performing imputation we integrated a Python script which will automatically create 22 different jobs, to perform imputation, one for each chromosome. This is one of the main steps of the whole imputation pipeline. This step was implemented in Minimac3[146] because of its reduced computation time paralleled with a high validity of the imputed variants [147]. It is based on the "state space reduction" of HMM showing haplotype sharing. It looks for similarities among haplotypes in small genomic segments so that the effective number of states is reduced (see Figure 3).

Consider a chromosome region with *M* markers and *H* haplotypes, e.g $\boldsymbol{X_1....X_n}$. The region can be analysed by breaking it into consecutive genomic blocks based on the markers beginning from the left.

Let us assume that block 1 contains ***p*** markers and block 2 contains ***q*** markers. The haplotypes $\boldsymbol{X_1....X_n}$ contains two ***U*** unique haplotypes, i.e $\boldsymbol{Y_1}$ and $\boldsymbol{Y_n}$. The left probabilities of the original state space at first marker will be known $\boldsymbol{L_1 (X_1), L_1 (X_2) ....L_1 (X_n)}$. HMM can be applied to the reduced state space ($\boldsymbol{U_1....U_n}$) from marker 1 to last marker in the first block to get $\boldsymbol{L_1}$ ($\boldsymbol{Y_1}$) and $\boldsymbol{L_1}$ ($\boldsymbol{Y_n}$). At the end of block 1, the left probabilities of reduced state space at the last marker in the block i.e. $\boldsymbol{X_n}$, can be unfolded. Such as $\boldsymbol{L_n(X_1)....L_n(X_n)}$. The same procedure is then repeated for the next block, i.e. $\boldsymbol{L_6}$ to $\boldsymbol{L_9}$.

Each haplotype is imputed separately, assuming that GWAS haplotypes are conditionally independent. It should be kept in view before performing imputation that if the genotypes are coming from different platforms, then imputation should be performed separately for each platform.

At the end of this step, minimac output files are generated. For details, see 3.2.2.4. These files are converted to PLINK format and all imputed SNPs below an imputation quality threshold of 0.3 are discarded. Again QC of the imputed data is performed, and all chromosomes are merged in one PLINK dataset. Since this file includes millions of SNPs, SNP chunks are created to perform the downstream analysis in an efficient manner by our pipeline.

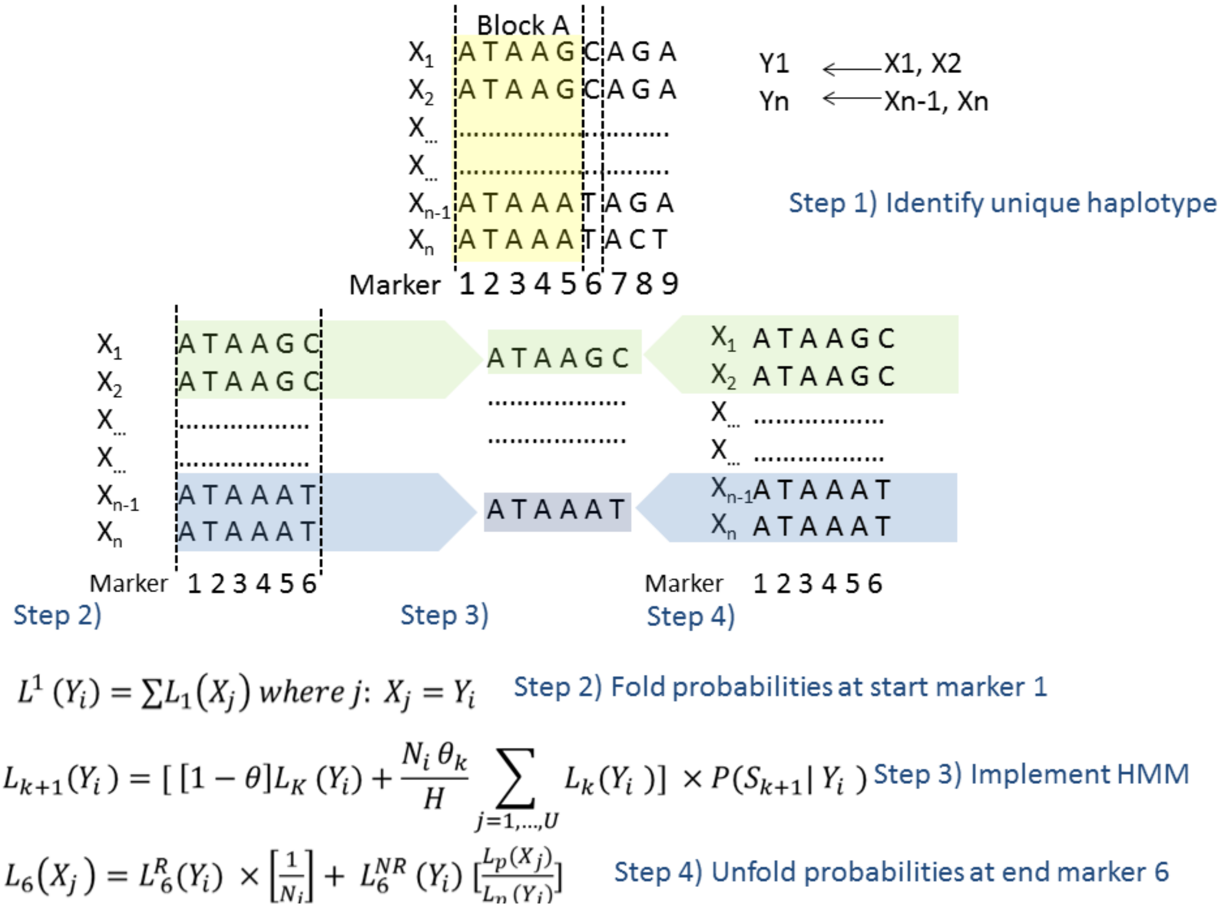
Block A
X_1 ATAAGCAGA
X_2 ATAAGCAGA
$X_{\dots}$
$X_{\dots}$
X_{n-1} ATAAATAGA
X_n ATAAATACT
Marker 1 2 3 4 5 6 7 8 9
Y1 ← X1, X2
Yn ← Xn-1, Xn
Step 1) Identify unique haplotype
X_1 ATAAGC
X_2 ATAAGC
X_{n-1} ATAAAT
X_n ATAAAT
Marker 1 2 3 4 5 6
ATAAGC
ATAAAT
Step 2)
Step 3)
Step 4)
$L^1(Y_i) = \sum L_1(X_j)\ where\ j\colon X_j = Y_i$
Step 2) Fold probabilities at start marker 1
$L_{k+1}(Y_i) = [\,[1-\theta]L_K(Y_i) + \frac{N_i\,\theta_k}{H}\sum_{j=1,\dots,U} L_k(Y_i)] \times P(S_{k+1}|\,Y_i)$
Step 3) Implement HMM
$L_6(X_j) = L_6^R(Y_i) \times \left[\frac{1}{N_i}\right] + L_6^{NR}(Y_i)\left[\frac{L_p(X_j)}{L_n(Y_i)}\right]$
Step 4) Unfold probabilities at end marker 6

Figure 3 Minimac3 workflow using state-space reduction

A block showing a chromosome region with nine markers and four haplotypes i.e. X_1, X_2, X_{n-1} ,and X_n. Two unique haplotypes, i.e.Y_1 and Y_n.are shown. Here *H* is the reference haplotype and a genomic segment bounded by markers *P* and *Q*, where *U* ≤ *H* and *U* are the unique haplotypes in that specific block. L_k and $\mathcal{L}_k$ denote the left probabilities for the original and reduced states, respectively, at *k* marker where P ≤ k ≤ Q. Step 3 in the figure is a modification of Baum-Welch's forward equations to obtain $\mathcal{L}_k$. θ_k denotes the switch probability between markers k and k+1. S_{k+1} is the genotype of the study data, $P(S_{k+1}|Y_i)$ is the genotype emission probability, and N_i the number of haplotypes matching Y_i in the original state space. Figure adapted from Das et al., 2016.

2.8. GWAS

This is the third part of the pipeline which incorporates R. Here, the aim is to identify the association between a trait and SNPs. Since the imputed genotype data consists of millions of SNPs, the data is parsed into small chunks. Each chunk creates a specific number of SNPs, which is provided for GWAS analysis. We provide the option to users if they would like to run a linear regression using ***lm*** or mixed regression analysis using ***lme4*** in R. Let us assume that the user wants to run mixed regression analysis for a quantitative trait, e.g. IQ from the German cohort as a function of SNP, which can be represented as:

$$IQ \sim SNP + \varepsilon$$

Here, “SNP” is a fixed effect and ε is the “error term” that describes the uncertainty in the model due to the random effects that are difficult to capture completely. Therefore, this error term could be expanded leaving the fixed part of the model undisturbed. There could be other factors in the model that could explain the uncertainty in the model, e.g. sex and age. Thus, we add these terms as fixed effects in the model. So now the model can be written as:

$$IQ \sim SNP + Sex + Age + \varepsilon$$

Let us further assume that IQ measures are contributed by individuals from different sites, e.g. 60 individuals contributed from Heidelberg, 20 from Freiburg and so on. Hence, each site had multiple IQ measures. Multiple IQ measures from the same site cannot be regarded as independent from each other. In order to deal with such situations, we included a random effect in the model that accounts for “site” from where the individual samples are included. Every site will have different IQ measures that will affect the measures. By adding random effects, we can get a structure for the error term ***ε***. In this example, adding a random effect for a site can characterize the distinctive variation, which is due to individual differences. We can now test for association of IQ with every SNP and controlling for the effect of recruitment site as an unobserved random intercept since affected individuals’ assessments might have been different across sites. So the above equation becomes:

$$IQ \sim SNP + Sex + Age + (1|Site) + \varepsilon$$

The intercept for each subject is different, and 1 stands here for the intercept. This will take into consideration the non-independence, which occurs from having multiple responses by the same site. This control captures the between-site differences, thus reducing the overall number of variables while increasing accuracy and statistical power for the parameters of interest. However, users will have the option to choose the model accordingly. The scripts were generated in R, and all required packages are automatically installed upon runtime. In the end, one regression output file is generated for each chunk. These files contain the effect sizes, nominal and adjusted p-values along with other information (see 3.2.3.4). All files are then merged. A text file containing only the SNP id and the p-value is extracted within the pipeline for further analysis.

2.9. Gene-based analysis

In this part, we implemented the gene-based analysis and directly take the text file with SNP and p-value information as input. The output of GWAS will be provided as input for gene-based analysis after arranging the file in the format for performing SNP-wise gene-based analysis. This analysis is performed using MAGMA.

Firstly, the SNPs are mapped to the corresponding gene, based on NCBI GRCh37/hg19 annotation within a window of 5 kilobases (kb) up and downstream of the respective coding sequence. However, we provided users the option to define a window-size.

It secondly analyses the individual SNPs in a gene and adds their respective p-value into a gene test-statistic. We selected the mean of the χ^2 statistic for the SNPs in a gene. The observed gene-statistic is computed from the regression output, i.e. SNP and p-values taking into consideration, only the SNPs, which are in the reference dataset. In our case, it is the 1000 Genomes dataset which is used to estimate the SNP statistic correlation matrix “R”.

A gene p-value is calculated by using a known approximation of the sampling distribution. For computing the approximate sampling distribution p-values, the correlation matrix “R” is required for SNP statistics. The correlations between the gene model sum of squares (SSM) values of the regression model are taken into account, which describes how well a regression model represents the modeled data. For single SNPs, a square of the correlation between the SNP genotype values is generated.

In general, the approximate sampling distribution is based on the basic properties of the multivariate normal distribution. Assuming under a null hypothesis of no association, the individual SNP Z-values z_i have a standard normal distribution, and therefore their joint distribution can be assumed to be a multivariate normal distribution with a mean of 0 and covariance equal to the correlation matrix R.

Besides a normal p-value, a permutation-based p-value is also calculated for all gene test-statistics. We selected adaptive permutations, which means that the number of permutation varies per gene. The genes are coded as Entrez gene, which are unique integers based on the gene-specific database (www.ncbi.nlm.nih.gov/gene) at the NCBI (National Center for Biotechnology Information).

Initially, for every gene 1,000 permutations are generated. MAGMA checks the number of P permutations with a gene test-statistic greater than the observed gene statistic. In case this value is greater than the pre-specified threshold P_{thresh}, the empirical p-value is calculated. In this way, an empirical p-value is calculated for all the genes.

In other cases, if the value is smaller, the number of permutations is increased to 5,000 and P is checked again, which will continue for checking at 10,000, 50,000 and so on until $P > P_{thresh}$ or the maximum number of permutations is reached, i.e. 1,000,000. At the end of the analysis, a file with significant genes along with a system code, i.e. *"L"* for Entrez gene ids is created for performing gene ontology analysis.

2.10. Gene Ontology analysis

In this step, we integrated Gene Ontology (GO) analysis. The significant gene list from the previous analysis, will serve as input for identifying the underlying biological pathways. Thus, the input file is (i) the list of all significant gene IDs (here, Entrez gene ids) named "input file", (ii) a file containing all genes tested in MAGMA named as the "denominator file", which is in the same format as the input file, which serve as the background gene list to test for enrichment.

Gene ontology ORA (Over-representation analysis) is a method to test if the set of biologically related terms occur more often than would be expected by chance in the dataset. This analysis provides information about the ontology id, the number of genes associated with the ontology id, Z-score, permuted and adjusted p-values. The gene lists are tested to avoid redundancy by using a robust pruning method to provide a set of non-overlapping terms. The statistics is based on Z-scores, p-values and gene counts, and look for unique branch paths from the overall ontology tree structure. This is performed via pruning to attain the node which has the largest Z-score in comparison to its corresponding child and parent nodes.

To identify functional profiles and underlying pathways of the genetic variants, we performed gene-based tests for GO-term and pathway enrichment. This step is performed using GO-Elite [162] and the R package *kegga* for identifying associated KEGG pathways. Z-scores are calculated, using the normal approximation to the hypergeometric distribution along with a permutation or a Fisher's exact test p-value. GO-Elite ranks each analysed term according to the Z-score. The method is detailed as follows:

A Z-score and permutation or Fisher's exact test p-value are calculated to look for the over-representation of genes within specific ontology terms and pathways.

$$Z = \frac{(Observed) - (Expected)}{Std.\,deviation\ (Observed)}$$

The probability of observed gene IDs (observed probability) from the significant gene list is subtracted from the probability of combined total gene IDs of all the MAGMA genes (expected probability) and divided by the standard deviation of the observed gene IDs (Observed probability). The statistics can be further explained as the following equation:

$$Z = \frac{\left[r - n\frac{R}{N}\right]}{\sqrt{n\left[\frac{R}{N}\right]\left[1 - \left[\frac{R}{N}\right]\right]\left[1 - \frac{n-1}{N-1}\right]}},$$

where

n = Total IDs associated with a biological term (denominator list)

r = Input IDs associated with a biological term (input list)

N = Denominator IDs examined (denominator list)

R = Total Input IDs (input list)

A Fisher's exact test is calculated by creating a 2x2 contingency table. The table will consist of (a) the number of input IDs within a biological term, i.e. “r”, (b) a number of non-input IDs in a biological term (n-r), (c) a number of input IDs excluded from that term (R) and (d) the number of non-input IDs excluded from that term (N-R-n-r).

In order to reduce the possibility of chance findings, permutation analysis is performed. A random number of source IDs are selected from the “input file” and “denominator file” in an equal amount. Again, Z scores are recalculated for all terms “X” times, where X is a user-defined value. By default, we provide an option of X= 2000. Now, the likelihood of a Z-score occurring by chance is calculated as the number of times a permutation Z-score is greater than or equal to the original Z-score divided by X. Further, a false-discovery rate (FDR) p-value is calculated from the Fisher’s exact test or permutation p-value based on the Benjamini-Hochberg (BH) correction (see Appendix).

The output file contains the name of the ontology, number of genes in the input and matching pathway/GO-term, gene names involved in the pathway, a Z-score, a permuted and adjusted p-value.

2.11. Brain enrichment analysis

The last step of the pipeline performs brain enrichment analysis. We integrated the Kang et al. [48] brain transcriptome data set within the pipeline. This will assist in gathering information on the brain-specific effects of associated genes at 16 different brain regions i.e. Orbital prefrontal cortex (OFC), Dorsolateral prefrontal cortex (DFC), Ventrolateral prefrontal cortex (VFC), Medial prefrontal cortex (MFC), Primary motor cortex (M1C), Primary somatosensory cortex (S1C), Posterior inferior parietal cortex (IPC), Primary auditory cortex (A1C), Posterior superior temporal cortex (STC), Inferior temporal cortex (ITC), Primary visual cortex (V1C), Hippocampus (HIP), Amygdala (AMY), Striatum (STR), Mediodorsal nucleus of the thalamus (MD), and Cerebellar cortex (CBC). Gene expression at these brain regions can be seen within a time frame, ranging from embryonic development to late adulthood of males and females. This dataset consists of 1,340 tissue samples collected from one or both hemispheres of 57 postmortem human brains. Co-expression pattern of genes within this dataset is distinguished into 29 co-regulated gene modules [4]. Enrichment analysis is implemented using Fisher’s exact test. Two-dimensional heatmaps with brain anatomical structures over time were plotted using the R package CerebroViz [49] to visualize the eigengene (first principal component) values for each module. Moreover, we generated gene networks of the modules, which highlighted the overlapping genes from each subdomain. Gene networks were plotted using the R package *igraph* [50]. For details on the output, please see 3.2.4.4.

We discussed till here all the parts of the pipeline with respect to the thresholds and methods implemented. Further, we used additional methods that are currently not part of the pipeline but were performed to answer the biological question using the combined ASD cohort (AGP and German). The PLINK files from the two separate cohorts were merged using the “--merge” command in PLINK.

III. Additional data analysis

2.12. Genetic correlation

Genetic correlation analysis depicts the genetic relationship between two traits. This analysis will provide an understanding if the genetic variants on the two traits are shared, as well as if the alleles that affect one trait might have an effect on a second trait.

The genetic correlation is defined as follows:

$$r_g = \frac{cov_g\ (t_1,t_2)}{\sqrt{var_g\ (t_1)\ var_g\ (t_2)}},$$

where

$var_g\ (t_i)$ is the additive genetic variance of trait i, and

$cov_g\ (t_1, t_2)$ is the additive genetic covariance between the traits.

For performing this analysis, the PLINK files were first converted into GRM (genetic relationship matrix) format. We used bivariate GCTA–GREML from the GCTA tool [195] to estimate the genetic correlation based on the combined (AGP and German cohorts) cohort containing the phenotypic and genotypic information from unrelated individuals. The GCTA bivariate method is an extension of the univariate model which relates the pairwise genetic similarity matrix to a phenotypic covariance matrix between the first trait of interest with the second trait of interest and allows for correlated residuals. Before calculating r_g, GCTA estimates the genetic relationship matrix (GRM) between unrelated individuals from the SNPs, which can be estimated as follows:

$$A_{jk} = \frac{1}{N}\sum_{i=1}^{N}\frac{(x_{ij}-2p_i)(x_{ik}-2p_i)}{2p_i(1-p_i)},$$

where

x_{ij} is the number of copies of the reference allele for the i_{th} SNP of the j_{th} individual,

j and k are individuals for which the genetic relationship between two individuals will be calculated,

p_i is the reference allele, and

N is the number of SNPs.

In this way, iteratively one individual of a pair is excluded, whose relationship is greater than a specified threshold. Genetic correlations are then calculated based on the GRM.

2.13. SNP-based heritability analysis

This analysis is performed to estimate the phenotypic variance explained by all SNPs in a GWAS based on unrelated individuals. The heritability analysis was also performed in GCTA using the combined ASD data in GRM format. SNP-based heritability (h^2_{SNP}) is calculated to estimate the total variance of a phenotype, which can be explained by all SNPs. We calculated the SNP-based heritability (h^2_{SNP}) based on unrelated individuals since this avoids the bias in estimates, which occur due to the effect of common environment (dominance/epistasis) of the related individuals, e.g. siblings or twins. Moreover, to attain the minimum sample size requirements, we performed the analysis in the combined cohort. SNP-based heritability for each quantitative trait (subdomain) was estimated as follows:

$$h^2_{SNP} = \frac{var_g}{(var_g+var_e)},$$

where

var_g is the genetic variance, and

var_e is the residual variance.

These variances are calculated using REML from the GRM as shown in the previous section.

The variance explained by genome-wide SNPs (i.e. variance explained by all the causal variants) is estimated based on two steps: (i) A GRM calculated for all SNPs. This is an NxN matrix where each element represents the genetic similarity of two individuals. (ii) REML analysis where GRM is used as a predictor in the mixed linear model with the individual subdomain as the dependent variable. This analysis is performed in GCTA [195].

2.14. Polygenic risk scores (PRS)

To identify the level of shared genetic etiology between ASD and the quantitative traits, we performed a polygenic risk score-based analysis in the combined cohort (i.e. AGP and German cohort) using PRSice which requires the GWAS output from individual subdomains [196].

In general, PRS is an estimate of an individual's predisposition to a trait. It is determined by the sum of their genome-wide genotypes and weighted based on the corresponding genotype effect sizes which are collected from the GWAS summary statistics.

For this analysis two datasets are required as input:

i. Base dataset: A reference GWAS summary statistics data. We used the PGC-ASD GWAS data consisting of 5,305 ASD cases and 5,305 controls. Data is publically available: http://www.med.unc.edu/pgc/downloads.

ii. Target dataset: GWAS summary statistics of the target dataset. In our study, we have six different GWAS summary statistics for each of the quantitative traits (subdomains), i.e. JA, SI, PI, NVC, RB, and RI.

iii. To avoid any bias in the results, we made sure that the individuals of the PGC-ASD GWAS are not part of our consortium as the inclusion of related individuals can result in inflation of output.

iv. We only selected the SNPs, which were overlapping in the base and target datasets.

v. Clumping of SNPs was performed using PLINK to attain SNPs that are largely independent of each other. We selected a significance threshold for index SNPs of 0.001; the secondary significance threshold for clumped SNPs was 0.01. The LD threshold was 0.1 and the physical distance threshold for clumping was 250 kb. This generated a list of clumped SNPs.

vi. Genomic profile scores will be generated in the target dataset, e.g. the sum of risk alleles weighted by base dataset effect size (betas, log odds ratio, etc.). It is possible that the causal SNPs in GWAS could not attain a significant p-value, therefore, PRS are calculated at a set of seven broad thresholds that are <0.001, 0.05, 0.1, 0.2, 0.3, 0.4, 0.5.

vii. Based on the above mentioned seven *P* thresholds, polygenic risk scores are generated based on all SNPs that were associated with the PGC-ASD data (base data).

viii. PRSice also calculated the *P* of shared genetic etiology, i.e. the extent to which the combined SNPs from each of the seven P-value threshold linked polygenic risk scores for ASD predict each of the six quantitative subdomains-between the base ASD phenotype and target phenotypes, i.e. the total autistic score as well as the score for each of the subdomain.

3. Results and Discussion

I. Preliminary analysis of phenotype data

3.1. Phenotype imputation

The selection criteria for performing this step are detailed in 2.3. Sample adequacy tests were performed to make sure that the data reaches the criteria for performing principal component analysis. Table 2 shows the results of the sample adequacy test. Both the tests satisfied the criteria.

Sample Adequacy Test	**Value**	**Cut-off value**
Bartlett' test of sphericity *P* -value	<0.0001	<0.05
Kaiser Maier Olkin	0.92	>0.5

Table 2 Sample adequacy tests.

3.1.1. Principal component analysis

Principle component analysis was performed to attain the independent components in the AGP cohort. The number of factors to be considered were decided based on Kaiser criterion [179], i.e. to include all components with an eigenvalue > 1 and a scree plot (Figure 4). This led to a six-component solution (Figure 5). The ADI-R items which were related to Domain A were labeled based on Liu et al. [84] as SI (Social Interaction; 5 items), JA (Joint Attention; 8 items), PI (Peer Interaction; 4 items), and NVC (Non-verbal Communication; 3 items). Similarly, ADI-R items related to Domain B were RB (Repetitive Sensory-Motor Behavior; 5 items); and RI (Restricted Interests; 3 items). Items that had a factor loading > 0.4 for a specific factor were considered. However, one item "*Conventional/Instrumental gestures"* loaded > 0.4 in two factors simultaneously, i.e. SI and NVC. We referred to the previously published factor analysis in the AGP cohort [84] which included the respective item into NVC only (see Table 3). The respective items for each subdomain were summed up to provide a combined score which will be used for subsequent analysis.

In order to confirm the structure of six factors/components attained from the AGP cohort, we performed a confirmatory factor analysis in the German cohort. The structure was successfully confirmed based on comparative fit indices such as TLI (Tucker Lewis index)> 0.90, CFI (Comparative Fit Index)> 0.90 [197,198], and absolute fit indices, i.e. RMSEA (Root Mean Square Error Approximation) < 0.08 [198,199] and SRMR (Standardized Root Mean Square Residual; see Table 4). The sum of the respective factor items was calculated for each participant. No difference with respect to SI, PI, and RI was observed for the AGP and the German cohorts (P_{all}> 0.1). However, the sum scores for JA and RB were lower in the DE compared to the AGP cohort, while the NVC score was higher in the DE cohort (P_{all}< 1 x10^{-03}) (see Table 5).

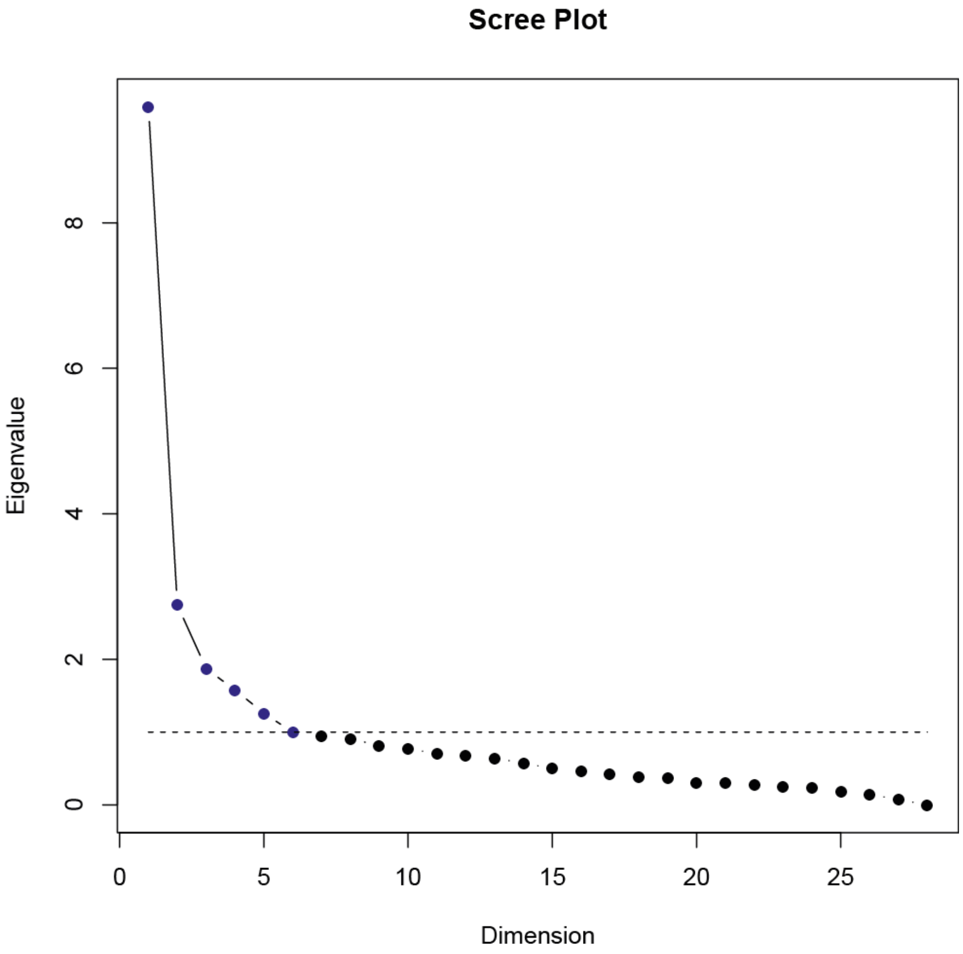

Figure 4 Scree plot of the AGP cohort

Scree plot for principal component analysis: The number of factors (dimensions) with the corresponding eigenvalue at the y-axis and the number of factors at x-axis. The dotted line marks an eigenvalue> 1 which shows in total six factors.

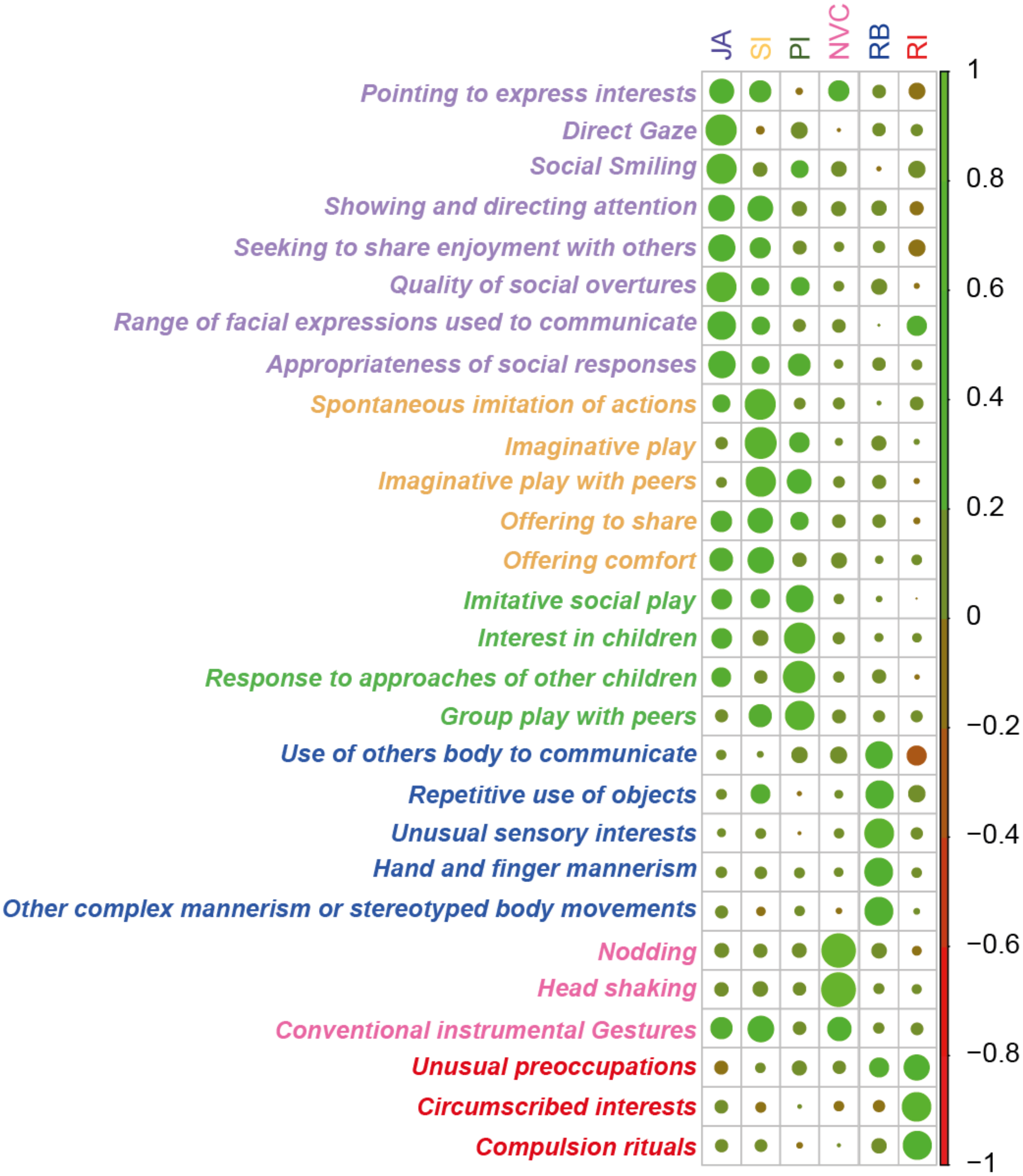

Figure 5 PCA based subdomains of the 28 ADI-R items

The color bar and size of the dots represent the intensity of correlation. Abbreviations: JA: Joint attention, SI: Social interaction, PI: Peer Interaction, NVC: Non-verbal communication, RB: Repetitive Sensory-Motor Behavior, RI: Restricted interests.

ADI item		JA	SI	PI	NVC	RB	RI
Pointing to express interest	ADI_A42	***0,43***	0,34	-0,03	0,31	0,12	-0,18
Direct Gaze	ADI_A50	***0,70***	-0,04	0,18	-0,01	0,11	0,09
Social smiling	ADI_A51	***0,65***	0,14	0,21	0,16	-0,01	0,19
Showing and directing attention	ADI_A52	***0,49***	0,46	0,15	0,14	0,15	-0,12
Seeking to share enjoyment with others	ADI_A54	***0,52***	0,30	0,12	0,06	0,09	-0,19
Quality of social overtures	ADI_A56	***0,64***	0,22	0,24	0,07	0,17	-0,02
Range of facial expressions used to communicate	ADI_A57	***0,58***	0,22	0,10	0,12	0,00	0,28
Appropriateness of social responses	ADI_A59	***0,52***	0,22	0,35	0,05	0,11	0,07
Spontaneous imitation of actions	ADI_A47	0,22	***0,69***	0,08	0,08	0,01	0,12
Imaginative play	ADI_A48	0,09	***0,72***	0,28	0,03	0,14	0,02
Imaginative play with peers	ADI_A49	0,07	***0,65***	0,43	0,08	0,12	-0,02
Offering to share	ADI_A53	0,32	***0,45***	0,22	0,12	0,11	-0,02
Offering comfort	ADI_A55	0,39	***0,49***	0,13	0,16	0,04	0,07
Imitative social play	ADI_A61	0,29	0,25	***0,54***	0,06	0,02	0,00
Interest in children	ADI_A62	0,29	0,16	***0,69***	0,09	0,05	0,05
Response to approaches of other children	ADI_A63	0,26	0,11	***0,75***	0,08	0,13	-0,01
Group play with peers	ADI_A64	0,10	0,37	***0,62***	0,12	0,09	0,09
Nodding	ADI_A43	0,14	0,13	0,14	***0,86***	0,15	-0,05
Head shaking	ADI_A44	0,13	0,16	0,11	***0,87***	0,07	0,06
Conventional/Instrumental gestures	ADI_A45	0,34	*0,49*	0,12	***0,41***	0,07	0,10
Use of others body to communicate	ADI_A31	0,06	0,02	0,18	0,19	***0,52***	-0,27
Repetitive use of objects or interest in parts of objects	ADI_A69	0,07	0,26	-0,01	0,04	***0,57***	0,20
Unusual sensory interests	ADI_A71	0,04	0,07	-0,01	0,06	***0,62***	0,09
Hand and finger mannerisms	ADI_A77	0,08	0,10	0,07	0,05	***0,58***	0,06
Other complex mannerisms or stereotyped body movements	ADI_A78	0,11	-0,05	0,06	-0,02	***0,59***	0,02
Unusual preoccupations	ADI_A67	-0,12	0,06	0,15	0,11	0,27	***0,48***
Circumscribed interests	ADI_A68	0,12	-0,07	0,01	-0,06	-0,09	***0,62***
Compulsion/Rituals	ADI_A70	0,11	0,10	-0,02	0,01	0,15	***0,60***

Table 3 Factor loadings in AGP data set

Bold italic value shows the factor loadings >0.4 that were considered for the subdomain. SI: social Interaction; JA: Joint Attention; PI: Peer Interaction; NVC: Non-verbal Communication; RB:Repetitive sensory-motor Behavior; RI: Restricted Interest

Measure	Value	Cut-off for good fit
TLI (Tucker-Lewis Index)	0.981	>= 0.95 good model fit[198]
CFI (Comparative Fit Index)	0.983	0.95 (great); 0.90 traditional[198]
RMSEA (Root Mean Square Error of Approximation):	0.039	< 0.08[200]
SRMR (Standardized Root Mean Square Residual)	0.048	<0.09 good[198]

Table 4 Confirmatory factor analysis in the German cohort

	AGP	DE	*P*	Combined
N total	1895	614		2509
Age at Diag. in months, mean (SD)	103.11 (58.52)	128.72 (74.19)	<0.001[a]	109.38 (63.66)
Male Gender, N (%)	1649 (87.01 %)	525 (85.50 %)	0.373[b]	2174 (86.64%)
Female Gender, N (%)	246 (12.98 %)	89 (14.50 %)		335 (13.35%)
IQ, Mean (SD)	78.63 (24.44)	88.96 (23.30)	<0.001[a]	80.99 (24.56)
IQ > 70, N (%)	1145 (60.42 %)	418 (74.51 %)	<0.001[b]	1563 (62.29%)
IQ ≤ 70, N (%)	750 (39.58%)	143 (25.50%)		893 (35.59%)
Subdomains, mean (SD)				
Joint Attention (JA), mean (SD)	12.86 (4.63)	11.92 (5.02)	<0.001[a]	12.63 (4.74)
Social Interaction (SI), mean (SD)	10.17 (3.24)	10.30 (3.43)	0.180[a]	10.20 (3.29)
Peer Interaction (PI), mean (SD)	7.31 (2.56)	7.30 (2.79)	0.815[a]	7.31 (2.61)
Non-verbal communication (NVC)	4.14 (2.24)	4.37 (2.21)	0.023[a]	4.19 (2.23)
Repetitive Sensory Motor Behavior (RB)	6.04 (2.97)	5.16 (3.25)	<0.001[a]	5.83 (3.07)
Restricted Interests (RI)	3.08 (2.03)	2.91 (1.90)	0.103[a]	3.04 (2.00)

Table 5 Descriptive statistics

a) Wilcoxon test b) Chi-square test, Abbreviations: DE German cohort AGP: Autism Genome Project cohort, diag. diagnosis; SD: Standard Deviation, P: nominal p-value comparing DE vs AGP cohort.

II. (a) The MAGNET tool: Methodological results

3.2. MAGNET implementation and architecture

We developed the MAGNET tool consisting of five main parts: I) quality check (QC) of the genotype data, II) imputation of genotype data, III) GWAS, IV) enrichment analysis, V) integration of transcriptome data, see Figure 6.

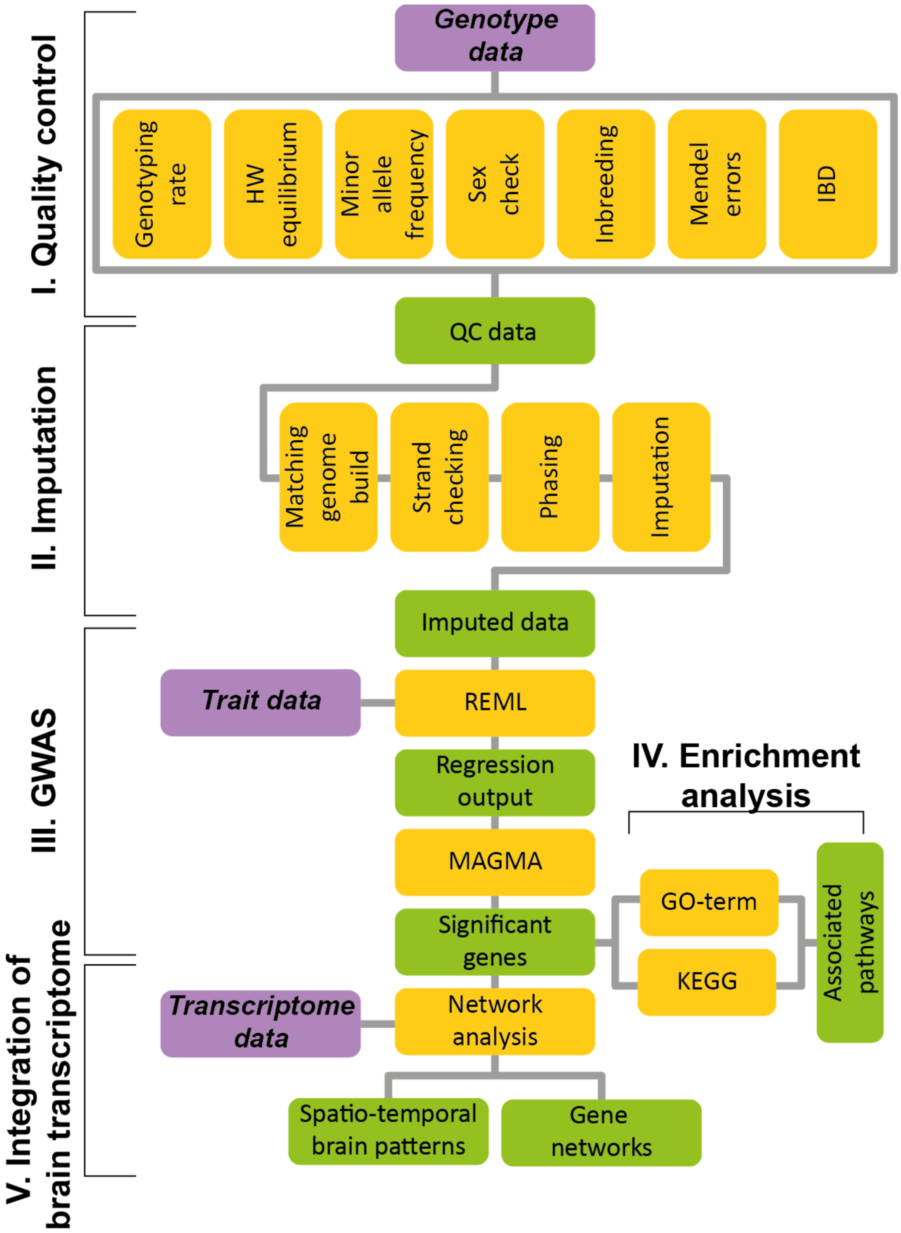

Figure 6 MAGNET workflow

The five main parts of MAGNET, i.e. (i) Quality control, (ii) Imputation, (iii) GWAS, (iv) Enrichment analysis, and (v) Integration of brain transcriptome data. Violet blocks represent input data, yellow blocks represent individual processing steps and green blocks represent outputs produced.

The framework was developed under Linux Distribution Red Hat 4.1.2-55 and implemented in bash, python, and R. The pipeline is freely available at GitHub https://github.com/SheenYo/MAGNET. The provided configuration options to run a complete MAGNET pipeline on a cluster is available for “SLURM” or “PBS” cluster management system with at least 128GB of memory. Stage 1: QC analysis, stage 4: pathway enrichment analysis and stage 5: transcriptome enrichment analysis are computationally less intensive and can be performed on any 64-bit x86 Unix based local system. However, stage 2: genotype imputation and stage 3: GWAS requires the use of a computing cluster. Prior to running MAGNET, it is required that R>=3.5, Perl, Python, gunzip and unzip utility for Linux are installed.

All the required parameters such as computational time or amount of memory required to run the framework are provided in Table 6. We will use the trait IQ from the German cohort for elaborating the architecture of MAGNET where ever necessary. Phenotype imputation (part of preliminary data analysis) was not performed on IQ trait data.

The user first needs to run “testPreMAGNET.sh” before running MAGNET. The script will create directories and install if any of the software in Table 1 is not installed.

Figure 7 shows the architecture of MAGNET. For each section of MAGNET, a bash script is defined or a complete script to run all the analysis together.

Each stage of MAGNET is described in detail listing the variable names for required input files, input parameters, reference data, and outputs produced as arranged in the configuration files and scripts.

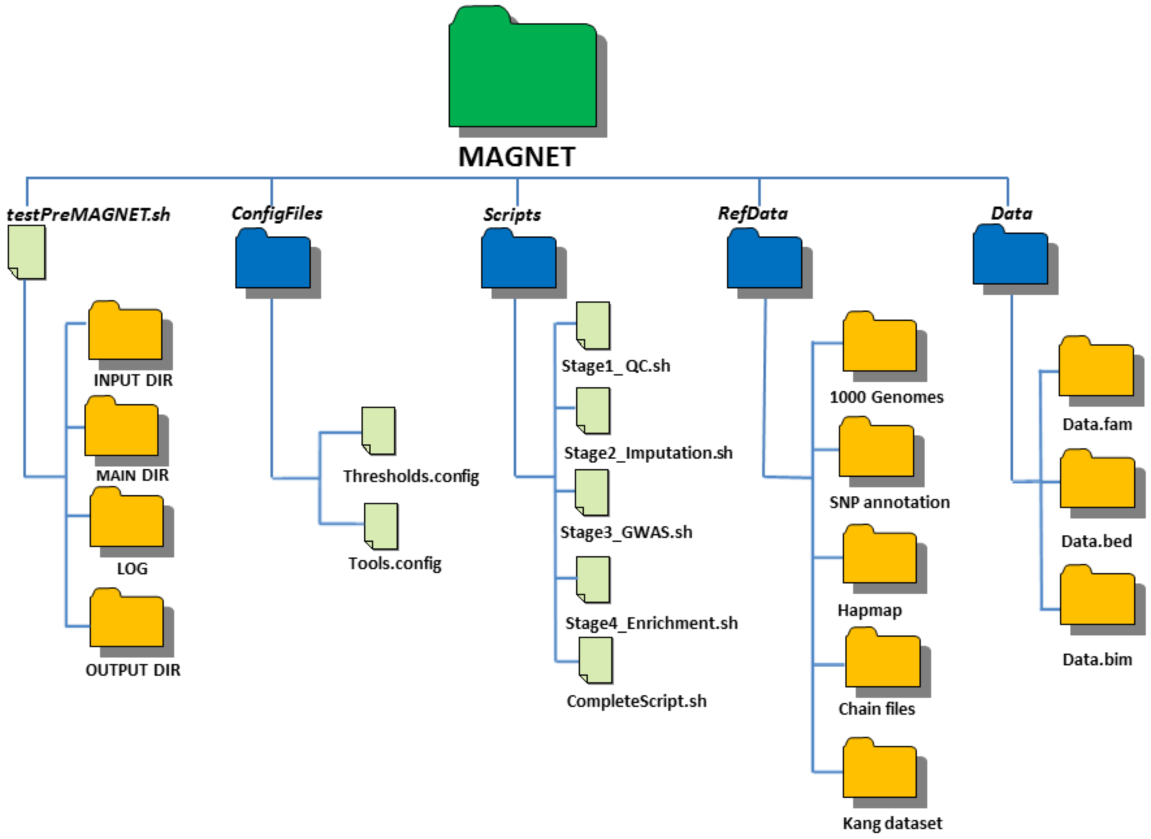

Figure 7 General architecture of MAGNET

MAGNET is composed of four main directories, i.e. ConfigFiles, Scripts, RefData and Data, and the main configuration file which will create the required folders needed to process and save the outputs from MAGNET. Config files contain the thresholds and tools configuration parameters. The scripts for each step are organized in separate files along with one complete script to perform the whole analysis. The required reference data for the different steps are saved as shown under the ref data folders. The data folder contains the study data to be analysed.

Parts	Computational Requirements	Sample Size	Time (h:mm)
1. QC pipeline	Required 7.2 GB memory (RAM) on an Intel(R) Core(TM) i7-3820 CPU 3.60GHz machine	3,343 Individuals (affected& non-affected), 715,726 SNPs	00:05
2. Genotype Imputation (Pre & Post steps)	Required 128 GB memory (RAM) on 1 computational node (slurm job scheduler) which consisted of four AMD Opteron Magny-Cours (twelve-core) CPUs	717 affected individuals, 622,344 SNPs	75:20
3.GWAS	Required 128 GB memory (RAM) on 1 computational node (slurm job scheduler) which consisted of four AMD Opteron Magny-Cours (twelve-core) CPUs	522 affected individuals with IQ information available, 8,261,813 SNPs	37:00
4. Gene analysis	Required ~8.50 GB memory (RAM) on an Intel(R) Core(TM) i7-3820 CPU 3.60GHz machine	522 affected indiviudals with IQ information avaialble, 8,261,813 SNPs	00:22
5. Transcriptome analysis	Required ~ 0.5 GB on Intel(R) Core(TM) i7-3820 CPU 3.60GHz	522 affected individuals with IQ information available, 996 significant genes	00:16
Total Time=~113:00			

Table 6 Computational requirements for MAGNET

For illustration purposes, we show here the computational requirements for running MAGNET on trait IQ in the German cohort. Since, part 1, 4 and 5 can run on any local machine as well, we show here the time taken on a local machine for these parts. Part 2 and 3 requires parallel computing on a computational cluster.

3.2.1. QC

This part is implemented in PLINK and R within the shell script “Stage1_GenoQC.sh”. This section reports the quality of user-provided data by generating reports for individual analysis. Results from these reports are generated as plots at the end of the analysis:

3.2.1.1. Input files

SamplesToQC: The user needs to provide PLINK formatted files either as .bed, .bim, and .fam or as.ped, .map input files. These are required to be ACGT/1234 allele coded. The program checks for their existence and exits if the files are not found. By default, the path is set to “Data” folder where the user can provide the PLINK files for analysis.

AffectedInds: PLINK normally defines ‘-9’ as the unaffected individuals and ‘2’ as affected individuals, in case the affected statuses are otherwise defined the user needs to provide a list of affected individuals and its respective path in the configuration file.

3.2.1.2. Input parameters

This section of the program consists of the following defined variables that can be changed by the user in the MAGNET/ConfigFiles/Thresholds.config.

installationDir: By default, the directory where the program is installed is considered as the installation directory, all further output folders will be created within this directory. This directory can be changed in the ToolsConfig, e.g. installationDir=/home/user/mypath.

GENO: Refers to PLINK missing genotype call rate threshold. By default we have set it to 0.05, all variants exceeding this threshold will be omitted from the analysis.

HWE: Refers to Hardy-Weinberg equilibrium exact test p-value threshold to filter out all variants below it, by default set to $10e^{-8}$.

MAF: Filter variants with a minor allele frequency less than a specific threshold. By default, it is set to 0.02. User can change it based on sample size and study design.

MIND: Excludes all samples which have missing genotype data greater than a specific threshold, here it is by default set as 0.05.

MEFam and MESNP: These options are used for family-based data only. Filters individuals and/or markers based on the Mendel error rate.

MEFam: By default discards all the families with more than 1% Mendel errors (considering all SNPs).

MESNP: By default discards all the SNPs with more than 10% Mendel error rate based on the number of trios.

3.2.1.3. Reference files

For this stage only HapMap data is required:

Hapmapfile: Hapmap genotype file for generating ethnicity plots

3.2.1.4. Output

QC1_report.imiss: A list reporting sample-based missingness, where F_MISS column details the missing call rate.

QC1_report.lmiss: A list reporting variant based missingness, where F_MISS column details the missing call rate.

PreQC_hardy.hwe: A statistic generated showing the Hardy-Weinberg exact test with p-values.

PreQC_AlleleFreq.frq: Lists all the SNPs with minor allele frequencies.

PreQC_Inbreeding.het: Generates the inbreeding coefficient estimates.

QC2_Sexcheck.sexcheck: Reports the individuals with mismatched gender.

FinalQC_Study: In the end, the user gets a clean quality checked PLINK data file, which will be directly incorporated for the next section. Altogether 9 graphs are produced at the end of QC, as an example six different QC output plots of IQ trait from the German cohort are shown in Figure 8.

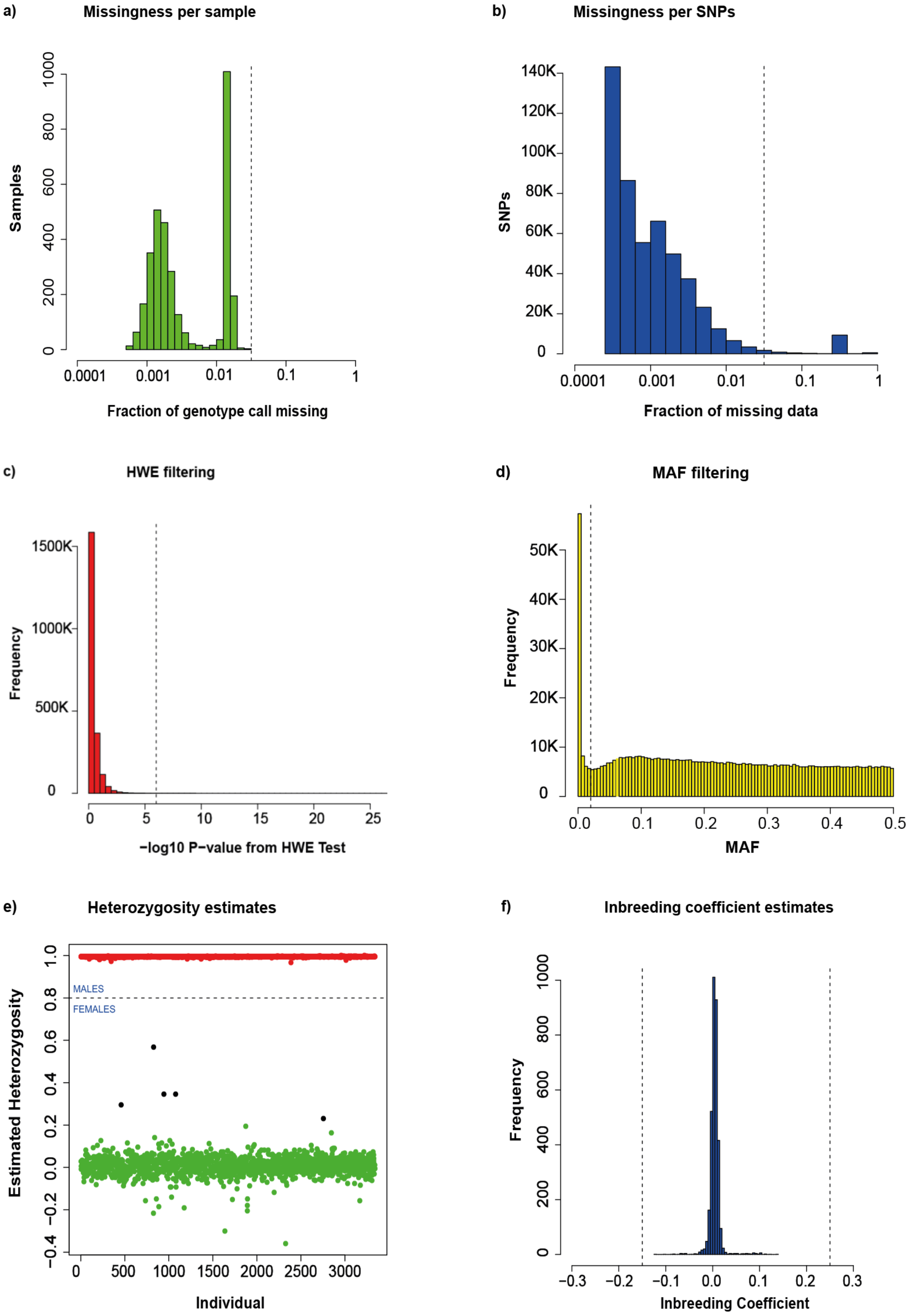

Figure 8 Quality check plots of IQ trait in German cohort

(a) and **(b)** show the histograms depicting the missingness per samples and SNPs respectively, **(c)** shows the Hardy-Weinberg equilibrium p-value threshold, **(d)** shows the MAF, **(e)** shows the heterozygosity estimates and **(f)** shows the inbreeding coefficient

3.2.2. Genotype Imputation

We implemented this section in R, PLINK, and python within the shell script “Stage2_Imputation.sh”. In this stage imputation of affected individuals was performed only for chromosomes 1-22 (autosomes) because of a lower proportion of genes on X chromosome and less coverage on current genotyping platforms in comparison to the autosomal chromosomes. Moreover, Y SNPs are approximated to be only ~0.07% of the biallelic SNPs within the genome and therefore might be underrepresented on genotyping arrays. The structure of this section looks as follows:

3.2.2.1. Input files

QCFile: Final quality check file (FinalQC_Study.bed, FinalQC_Study.bim, and FinalQC_Study.fam). For standalone imputation analysis, the user needs to provide a path of the QC PLINK formatted file (bed, bim, fam).

AffectedInds: In case the sample consists of unaffected and affected individuals, a list consisting of family and individual IDs of affected individuals only is needed which should have the following format:

FAMILY ID	INDIVIDUAL ID
FAMID_1	IID_1
FAMID_2	IID_2
……..	…………
FAMID_65	IID_65

3.2.2.2. Input parameters

ChainToChoose: By default Chain file (see 2.7.1.1) from hg18 to hg19 is selected to update the genome build. Users can select a genome build if it is not hg18 as detailed in the following section.

thresholdImp: Imputation quality threshold value of Rsq, default to 0.3.

chunkSize: Number of SNPs to be present in each SNP raw data file, by default each SNP raw data file consists of 5000 SNPs.

3.2.2.3. Reference files

The user needs to download the following reference files in “RefData” folder.

Hg19SNPs: Hg19 SNPs file containing SNPs rs ids (SNP name), starting and ending bp position, chromosome number.

Since the 1000 genomes dataset is based on the hg19 genome build, the study dataset needs to be updated to this genome build. All chain files are provided in the reference data, which a user can download.

Chain files can be downloaded from the links provided on the GitHub https://github.com/SheenYo/MAGNET and can be saved in the RefData folder.

MapFile: Genetic map for 1000 genome data Phase3 consisting of three columns containing the physical position (bp), the recombination rate (cM/Mb) and the genetic position (cM). This file along with reference files for SHAPEIT are required to be downloaded.

The folder will contain files in the following three formats:

ShapeitRefHaps: This file consists of SNPs and the haplotypes where each line corresponds to a single SNP consisting information about the two alleles of a SNP by each haplotype of an individual about the chromosome number, SNP id, SNP position, and the first and second allele.

ShapeitRefLegend: The file describes the SNPs, where the columns correspond to SNP id, SNP position, first and second allele.

ShapeitRefSample: The file contains information about reference individuals, i.e. Individual ID, population, group, and sex.

AnnotationFile: A complete instruction on downloading the annotation file is provided in the readme file at https://github.com/SheenYo/MAGNET. These files contain annotation based on SNP 142 genome build (SNP locations and alleles information extracted from the single nucleotide polymorphism database (dbSNP)) separated based on chromosomes, each file consists of chromosome number, base pair position, SNP name, and column with chromosome:base pair.

3.2.2.4. Output

Gwas.Chr (1-22)_Study.Imputed.Output.dose: Contains allele dosages (allele counts) for imputed and genotyped SNPs.

Gwas.Chr(1-22)_Study.Imputed.Output.erate: Contains estimated error rate for every imputed and genotype marker.

Gwas.Chr(1-22)_Study.Imputed.Output.info: Contains information on both genotyped and imputed SNPs.

Gwas.Chr(1-22)_Study.Imputed.Output.m3vcf.gz: Output file in vcf (variant calling file) format.

Gwas.Chr(1-22)_Study.Imputed.Output.rec: Recombination file containing switch error rate (Percentage of possible switches in haplotype orientation that is required to recover the correct phase in an individual [201]) per interval.

Gwas.Chr(1-22)_Study.Imputed.Output.hapDose.gz: Contains dosage for each haplotype separately.

Gwas.Chr(1-22)_Study.Imputed.Output.hapLabel.gz: Contains haplotype labels.

Merged_FinalQC_SNPs_Data (bed, bim, fam): PLINK formatted files consisting filtered (Rsq >0.3) and biallelic SNPs.

Data_SNPfile (1-22): Raw files with minor alleles each consisting of 5000 imputed SNPs.

3.2.3. GWAS

This step is implemented in R, python, and bash. The analysis is provided within shell script “Stage3_GWAS.sh”. This section uses the MAGMA tool to map the SNPs to their respective genes and perform gene-based analysis (see 2.9). Depending on the number of SNPs in the study, chunks are created with a default chunk size of 5000 each. However, the user is free to choose a chunk size in the configuration file.

3.2.3.1. Input files

Data_SNPfile.raw: Raw files consisting of 5000 SNPs each.

phenofile: The user needs to provide a reference file named “phenofile” consisting of family ID, individual ID and value of phenotype of interest (such as IQ) in the data folder, e.g in the table below:

FAMILY ID	INDIVIDUAL ID	TRAIT
FAMID_1	IID_1	49
FAMID_2	IID_2	103
………..	…………	………..
FAMID_65	IID_65	112

3.2.3.2. Input parameters

Pheno: Name of the phenotype to be analysed, required for the naming of results.

ColManhattan: Color to be used for Manhattan plot besides the grey color scheme used for every alternate chromosome, default is black color.

Further, the user needs to specify five arguments required for MAGMA analysis and plotting Manhattan plots that are as follows:

windowSize: The default window size to look for the genes around a SNP is 5kb upstream and downstream of the gene.

Covars: Name of covariates included in the regression model, the names should correspond to those in the phenotype file provided, e.g by default “Sex, Age” are the two covariates provided, these names are same as in the phenotype file.

Fixed: Names of random covariates included in the regression model, please note that the names should correspond to those in the phenotype file provided as explained above.

snpsOfInterest: Specific set of SNPs of interest which will be highlighted in the Manhattan plot, e.g. "rs377398625","rs557375998","rs10736578”

MagmaN: Sample size (Number of individuals) for which MAGMA will be conducted.

MagmaPERMP: Permuted p-value for MAGMA analysis, by default set to 0.05

3.2.3.3. Reference files

MagmaRef: 1000 genomes PLINK formatted reference file.

MagmaSNPloc: The file contains chromosome, SNP identifier, position in morgans or centimorgans (unit to denote the distance between two loci on a chromosome) which is mostly dummy coded as “0” of the reference 1000 genome dataset.

MagmaGeneloc: This file consists of location information about genes in NCBI37 (National Center for Biotechnology Information genome build 37), i.e. Entrez gene id, chromosome id, start and stop position, strand information, and gene.

3.2.3.4. Output

Results file: For each chunk, regression output will be saved in this file consisting of beta, se (standard error), t, p-value, and adjusted p-value.

Summary file: For each chunk regression output summary will be saved in this file.

Magma Result file: File consisting of complete MAGMA gene lists will be provided in the Magma_pheno.genes_tabseparated.txt file.

Pheno.SignificantGenes: List of significant genes resulting from MAGMA analysis below the default threshold of the empirical p-value of 0.05.

3.2.4. Enrichment analysis

The enrichment analysis is implemented in R-3.5, packages include kegga, WGCNA, igraph, and cerebroViz. The analysis is wrapped in shell script “Stage4_Enrichment.sh”.

3.2.4.1. Input files

Pheno.SignificantGenes: List of significant genes resulting from MAGMA analysis that are below the default threshold of empirical p-value of 0.05.

Magma Result file: File consisting of complete MAGMA gene lists will be provided in the Magma_pheno.genes_tabseparated.txt file.

R Pre-requisites: Requires R-packages "org.Hs.eg.db, annotate, WGCNA, igraph and purrr". These will be automatically downloaded upon script runtime.

Detailed commands for updating the packages are also provided at https://github.com/SheenYo/MAGNET.

3.2.4.2. Input parameters

GOeliteSpecies: The pipeline is based for human data only, by default the option is set to "Hs" for homo sapiens.

GOElitefolder: Name of the folder where GO elite inputs are stored.

Outputfolder: Name of output folder where results of the downstream analysis will be stored.

MAGNETHome: Name of the main directory where MAGNET is installed.

3.2.4.3. Reference files

Kang et al. [4] transcriptome data set is included as reference data for this stage. These files are provided with the tool.

Kang Universe: All genes from Kang dataset.

Kang genes: All genes which are in Kang modules.

KangData: File consisting of Kang expression data.

3.2.4.4. Output

The output produces the following files:

All_MagmaGenes_Symbols.txt: All MAGMA Entrez genes mapped with their gene symbols.

All_genesMAGMA_Imputed_Kang.txt: All genes which are present in MAGMA and in Kang dataset.

phenoEnrichment_ouput.txt: Output of enrichment analysis.

phenoGO_ElitePlot.pdf : Plots of top ten GO-terms.

phenoKEGG.pdf: Plots of top ten KEGG pathways.

phenoEnriched_Modules.pdf: Gene network plots of enriched modules.

Heatmap_EnrichedModules.pdf: Heatmap of enriched modules.

Cross sectional and sagittal Brain views: Eigen gene values of module genes in Kang dataset are also presented with respect to brain-specific regions.

We ran the MAGNET tool on an IQ trait from the German cohort and recorded the computational time required to process each stage of it. The results are summarized in Table 6. The computational requirements for each section are different. The QC section requires the minimum computational requirements and does not require a computational server. Moreover, a comparison with other state-of-the-art tools is provided in Table 7.

	Genipe	EZImputer	Molgenis-Impute	Our pipeline
Input Files	Genotype files, reference panel	Genotype files and reference panel	Genotype files and reference panel, chain files	Genotype files, reference panel, single trait file, chain files.
Tools used	PLINK, SHAPEIT and IMPUTE2	PLINK, Structure, SHAPEIT, Impute, Beagle StrandCheckUtility, Beagle Gprobs Utility	PLINK, liftOver, SHAPEIT, Genotype harmonizer, vcftools,tabix	PLINK; liftOver, SHAPEIT, Minimac3, R, Python
Tasks	QC, phasing, Imputation	QC, Upgrades input genotype build to genome build 37, SNP filtering, phasing and imputation	Upgrades input genotype build to build 37, phasing and imputation	QC, Upgrades input genotype build, strand check, SNPs filtering, Imputation
Additional Add-ons	Linear and logistic regression	Gives predicted ethnicity	-	Linear and logistic regression, GO and pathway analysis, maps gene expression to different brain regions, builds gene networks.
Samples in Test set	90 Samples	-	100 samples	717 samples
SNPs in Test set	2,278,357	-	1 to 10 million bp in chromosome 1.containing 4,836 markers	8,261,813
Reference	1000 Genomes project v3	1000 Genomes project v3	1000 Genomes Project (1 to 15 million bp in chromosome 1 containing 88,650 markers)	1000 Genomes project v3
Computing Server	10 nodes of 8 Intel® Xeon® E5620 CPUs 2.40 GHz, 48G of RAM per node	-	12 CPU credits, 2 GB memory	2 computational nodes each with 4 AMD Opteron Magny Cours (12 cores) CPUs with 128 G RAM for each core
Time required	4:25 h	-	11:63 h	128:08 h

Table 7 Comparison with state-of-the-art Imputation frameworks.

3.3. MAGNET-lite

We also developed a GUI (Graphical User Interface) for the enrichment analysis. The interface is developed in the R shiny package which builds interactive web apps using R. This interface was developed by Miriam Hana Ulbrich in her internship project under my supervision. Shiny is an R package that makes it easy to build interactive web apps straight from R.

Features

MAGNET-lite consists of the following features:

- The user only needs to provide a gene list consisting of Entrez ids or gene symbols.
- Pathway enrichment analysis is performed at the backend using GO-elite and R package kegga.
- Bar plots are created for the top ten most significant GO-terms and KEGG pathways
- Brain enrichment analysis is performed based on the user-provided gene lists.
- Heatmaps of enriched modules and topmost connected gene networks are created.
- All plots are downloadable in pdf format.

Magnet-lite can also be downloaded from https://github.com/SheenYo/MAGNET and then can be run as a web GUI.

3.4. Discussion

This section contains parts of the article “MApping the Genetics of neuropsychiatric traits to molecular NETworks of the human brain” available on bioaRxiv (10.1101/336776).

MAGNET performance

We developed a pipeline that integrates genotype, phenotype, and brain transcriptome data within a single framework. To illustrate the run time problem in data integration, we evaluated the run time for the different computation steps and the overall time required starting from the application of quality checks to the identification of associated genes for IQ trait in the German cohort, see Table 6. The complete framework for the ASD German cohort took ~4 days (i.e. ~113 hours) to complete on a computing server using 2 nodes with AMD Opteron Magny Cours with each 12 cores CPUs and with

128 GB RAM per node. Quality checks were finished within 5 minutes for a total of 715,724 SNPs and 3,343 individuals (German cohort before QC). The computational time directly depends on the sample size and number of genotyped SNPs and may vary with the preferences to include, exclude or modify flagged samples and SNPs. Imputation based on the 622,344 variants was done for the 717 ASD affected individuals only and took 48:22 hours increasing the number of SNPs to 8,261,813. For ~8 million SNPs, regression analysis took 37 hours. Overall, the gene-based association test took 19 minutes. Hence on an average MAGNET can save the time required to set up, configure, handle in between data generated and running individual steps. All scripts are arranged as easy to use command-line interface with the flexibility to perform individual stages separately. To run the analysis no high-end programming skills are required but a basic understanding of Linux and shell scripting might be helpful to run the scripts on a computational cluster.

Comparison with state-of-the-art tools

We also compared the features of MAGNET with other tools that perform QC, imputation and regression analysis such as "Genipe" [142], Ezimputer [202], and Molgenis-impute [11]. MAGNET provides an edge over Genipe as it provides extensive visual plots for each QC step and provides an additional pathway and brain enrichment analysis. Likewise MAGNET is beneficial for the users who do not want to provide their genetic data on an online server to perform genetic analysis due to legal issues. EZImputer besides performing QC and imputation also provides predicted ethnicity estimates. It actually provides a modular set of scripts for building an imputation workflow but does not provide an automated manner of performing it. Molgenis-impute is a well-established pipeline but only provides imputation workflow at the moment.

MAGNET is oriented towards researchers with limited computational skills of computing clusters who do not want to invest time in setting up workflows and data handling from different genetic analyses. Instead, MAGNET provides an automated pipeline within one shell. However, the user has the flexibility to run individual parts of the pipeline provided the input files are available in the correct format.

MAGNET availability and cluster usage

MAGNET is available freely at Github under https://github.com/SheenYo/MAGNET. with complete scripts that can be adjusted to the needs of the respective user. A web interface for MAGNET stage 4 called MAGNET-lite is also available for the users who are only interested to know the specific biological pathways behind their trait of interest and can also be downloaded from https://github.com/SheenYo/MAGNET and can be run as GUI. In addition, it can look for enrichment of the genes of interest with respect to 29 different modules associated with distinct spatio-temporal expression patterns of the human brain [4]. MAGNET-lite can be used as a normal GUI for which no programming or Linux experience is required.

To boost the processing time of MAGNET, the scripts for stage 2 and 3 are written to directly run on high-performance computing environments, i.e. SLURM and PBS. The user does not need to perform any further parallelization steps, as genotype imputation and regression analysis are adapted to run in an automated fashion on the cluster.

II. (b) The MAGNET tool: Biological results

3.5. Quality check of genotype data

MAGNET QC stage was run on AGP and German cohorts separately. MDS (Multidimensional scaling) analysis was performed using 11 populations from the HapMap dataset, the German and AGP cohorts to predict the dimension scores as shown in Figure 9.

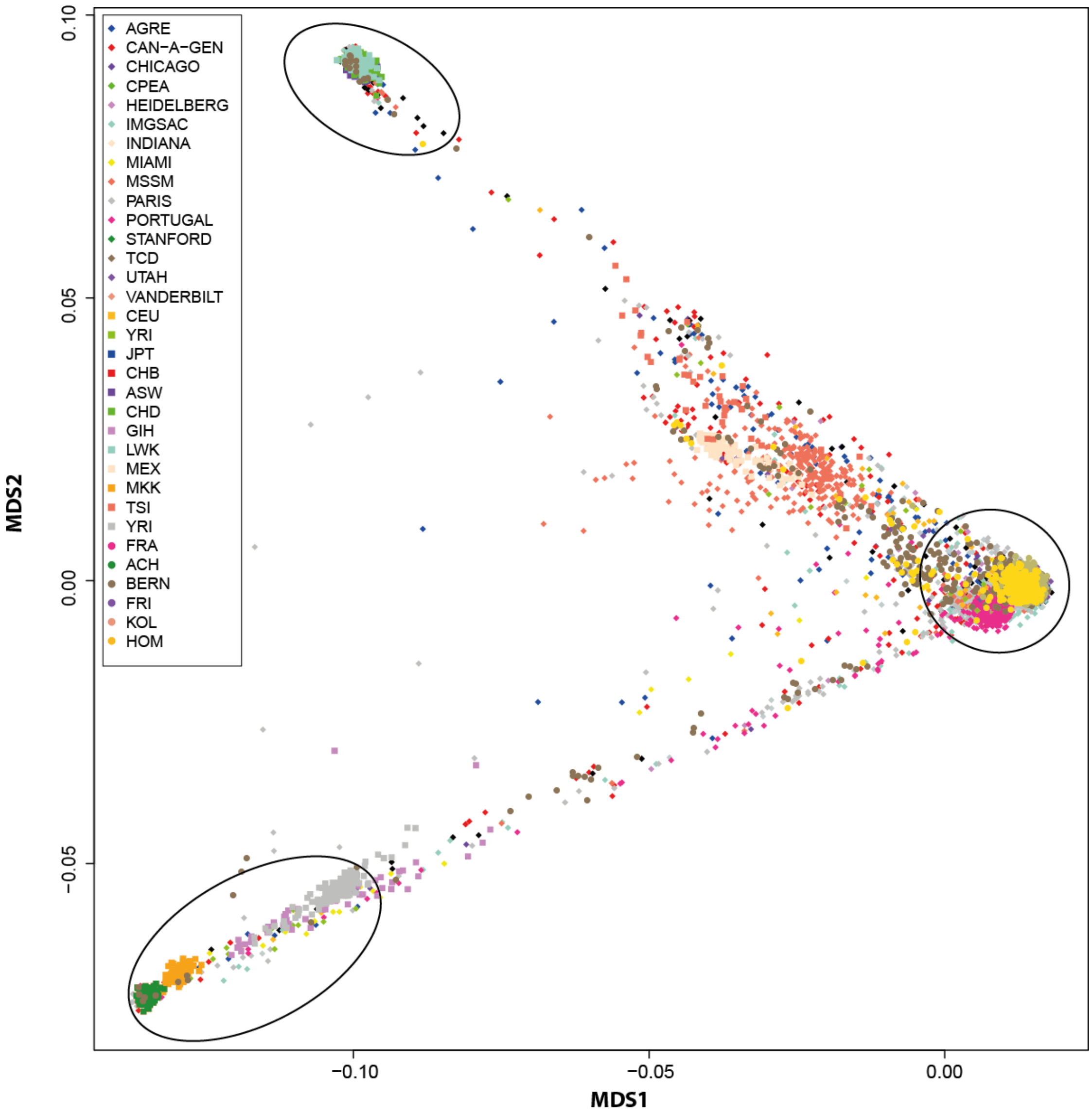

Figure 9 MDS plot of the first two dimensions

The diamond legend shows populations from the AGP cohort, the square blocks show populations from the HapMap dataset, and filled circles show the populations from the German cohort.

MDS plots showed the presence of three different clusters as the three main ethnicities, i.e. Asian, African, and European. We selected the first four ethnicity components to be included in our analysis for correcting population bias in the data. After QC, we only included affected individuals who had complete genotype and phenotype data, i.e. data available for age and recruitment site information. This resulted in 1,895 and 614 AGP and the German cohort affected individuals, respectively. A detailed summary of data description is provided in Table 5. There was no difference in gender distribution across cohorts (*P*= 0.373). The German cohort was older at diagnosis and showed a higher IQ compared to the AGP sample. Moreover, no difference was observed between SI, PI, NVC, and RI between the two cohorts. MAGNET provided a clean quality checked genotype file for each cohort. For the next steps, MAGNET was run individually on each subdomain and for each cohort separately.

3.6. Imputation of missing genotype data

The MAGNET imputation stage was run separately for each cohort and consisted only of affected individuals. As we used the 1000 Genomes phase 3 data which is annotated based on GRCh37 coordinates we used liftOver to remove any genetic sample data which did not correspond to GRCh37 annotation. Additionally, SNPs which were only in the provided genotype data and not in the reference data were also removed. SNP inconsistencies such as strand flip issues that cannot be resolved by flipping were removed during the imputation. MAGNET provided multiple imputation output files as detailed in 3.2.2.4, output was filtered based on the default imputation quality score of Rsq > 0.3 (removes > 70% of poorly-imputed SNPs at the cost of <0.5% well-imputed SNPs). The QC stage was run again at the end of imputation to remove any SNPs that fall below the thresholds of QC. As our aim was to identify the common variants observed in both cohorts, we manually selected SNPs that were overlapping in both cohorts and extracted them from the genotype files of AGP and the German cohort. This resulted in 6,900,500 SNPs overlapping in both cohorts with a MAF ≥ 2%. For efficient processing, MAGNET divided the SNPs into 1,381 files, each file consisted of 5,000 SNPs in contrast to the last file which contained 500 SNPs. This division and assignment of SNPs are performed automatically by MAGNET.

3.7. GWAS

MAGNET stage 3, i.e. GWAS was first performed in the combined (AGP and German) cohort to account for the power issues and to determine SNPs that might not reach genome-wide significance because of the sample size of AGP and the German cohort. Later, MAGNET was also run on individual cohorts. The sample size had a power of 1-beta > 80% to explain 6% of the variance (R^2= 0.06) in the German cohort, 1.5% in the AGP cohort and 1.2% in the combined cohort with a genome-wide significance threshold of alpha = $5e^{-8}$.

GWAS of the combined cohort resulted in eight genome-wide significant SNPs as shown in Table 8 and Figure 10. Out of the eight SNPs, four were found for SI, i.e. rs2095092, *P*= 4.3 x 10^{-08} at chr. (chromosome) 1p31.3 (closest gene *PATJ:* PALS1-Associated Tight Junction Protein); rs377634870, *P*= 4.8 x 10^{-08} at chr. 1p22.3 (no gene within 10kb); rs34459814, *P*= 2.5 x 10^{-08} at chr. 7q11.23 (closest gene *CLIP2:* CAP-Gly Domain Containing Linker Protein 2); and rs34083004, *P*= 3.7 x 10^{-08} at chr. 7q11.23 (closest gene *CLIP2*). One SNP was found in PI, i.e. rs10115292, *P*= 1.8 x 10^{-08} at chr. 9p21.1 (no gene within 10kb) and three in RB, i.e. rs13274146, *P*= 2.1x 10^{-08} at chr. 8p21.3 (no gene within 10kb); rs7837513, *P*= 4.2x 10^{-09} at chr. 8p21.3 (no gene within 10kb); and rs7824610, *P*= 2.0 x 10^{-09} at chr. 8q21.11 (no gene within 10kb).

In the AGP cohort we identified nine genome-wide hits, two were identified for SI, i.e. rs377634870, *P*= 4.8x10^{-08} at chr. 1p22.3 (no gene within 10kb), rs9333127, *P*= 4.75 x10^{-09} at chr. 10p13 (*ITGA8:* Integrin Subunit Alpha 8), five were identified for PI, i.e. rs7777015, *P*= 4.75 x 10^{-09} at chr. 7q21.11 (no gene within 10kb); rs6963792, *P*= 7.89x 10^{-09} at chr. 7q21.11 (no gene within 10kb); rs7783341, *P*= 3.25 x 10^{-09} at chr. 7q21.11 (no gene within 10kb); rs9969152 , *P*= 1.65 x 10^{-09} at chr. 7q21.11 (no gene within 10kb); and rs10115292, *P*= 4.73 x 10^{-08} at chr. 7q21.11 (no gene within 10kb). Two SNPs were identified for RB, i.e. rs441459, *P*= 4.53 x 10^{-08} at chr. 11p15.4 (*SLC22A18AS:* Solute Carrier Family

22 Member 18 Antisense); and rs388190, *P*= 1.44 x 10^{-08} at chr. 11p15.4 (*SLC22A18AS*). In the German cohort we identified one genome-wide hit, i.e. rs2151874, *P*=1.95 x 10^{-09} at chr. 1q42.2 (no gene within 10kb) for JA. None of the genome-wide significant hits from individual cohorts were replicated between the two cohorts.

GWAS for the trait IQ in the German cohort showed that none of the SNPs hit the genome-wide significance threshold. However, many SNPs survived FDR *P* < 0.001 such as rs10736578, rs1837768 belonging to the *CNTN5* (Contactin 5) gene as well as SNPs of *MCF2L* (MCF2 Cell Line Derived Transforming Sequence Like), e.g. rs66884214, rs534618502 and rs28459375.

	Pheno	**SNP**	**CHR**	**Gene**	**Comb. beta**	**Comb. Pval**	**AGP beta**	**AGP Pval**	**DE beta**	**DE Pval**
Combined Cohort	**SI**	rs2095092	1	*PATJ*	-0.530	*4.39e-08*	-0.466	2.39e-05	-0.704	4.10e-04
		rs377634870	1		0.532	*4.85e-08*	0.578	*1.58e-08*	0.165	5.57e-01
		rs34459814	7	*CLIP2*	0.492	*2.50e-08*	0.488	1.86e-07	0.461	5.87e-02
		rs34083004	7	*CLIP2*	0.488	*3.75e-08*	0.483	2.90e-07	0.461	5.87e-02
	PI	rs10115292	9		0.388	*1.83e-08*	0.361	*4.73e-08*	0.406	8.88e-02
	RB	rs13274146	8		-0.733	*2.15e-08*	-0.733	9.44e-07	-0.731	6.5e-03
		rs7837513	8		-0.776	*4.23e-09*	-0.783	2.28e-07	-0.753	5.27e-03
		rs7824610	8		-0.790	*2.00e-09*	-0.806	1.00e-07	-0.743	5.40e-03
AGP	**SI**	rs377634870	1		0.532	*4.86e-08*	0.578	*1.58e-08*	0.165	5.57e-01
		rs9333127	10	*ITGA8*	0.414	2.81e-06	0.556	*1.74e-08*	-0.092	6.36e-01
	PI	rs7777015	7		0.321	4.28e-06	0.447	*4.75e-09*	-0.119	4.4e-01
		rs6963792	7		0.299	2.73e-05	0.453	*7.89e-09*	-0.201	1.99e-01
		rs7783341	7		0.303	2.34e-05	0.466	*3.25e-09*	-0.228	1.44e-01
		rs9969152	7		0.316	8.07e-06	0.470	*1.65e-09*	-0.186	2.34e-01
		rs10115292	9		0.388	1.82e-08	0.361	*4.73e-08*	0.406	8.88e-02
	RB	rs441459	11	*SLC22A18AS*	-0.435	1.21e-06	-0.567	*4.53e-08*	-0.089	6.19e-01
		rs388190	11	*SLC22A18AS*	-0.438	3.16e-07	-0.553	*1.44e-08*	-0.099	5.76e-01
DE	**JA**	rs2151874	1		-0.495	6.63e-05	-0.160	2.40e-01	-1.600	1.95e-09

Table 8 Genome-wide hits in combined, AGP and German cohort

Genome-wide hits for combined and individual cohorts, italics show the P-values for genome-wide hits. DE: German, AGP: Autism Genome Project, SI: social Interaction; JA: Joint Attention; PI: Peer Interaction; NVC: Non-verbal Communication; RB: Repetitive sensory-motor Behavior: RI: Restricted Interest, Comb.: combined, CHR: Chromosome, Pval:p-value.

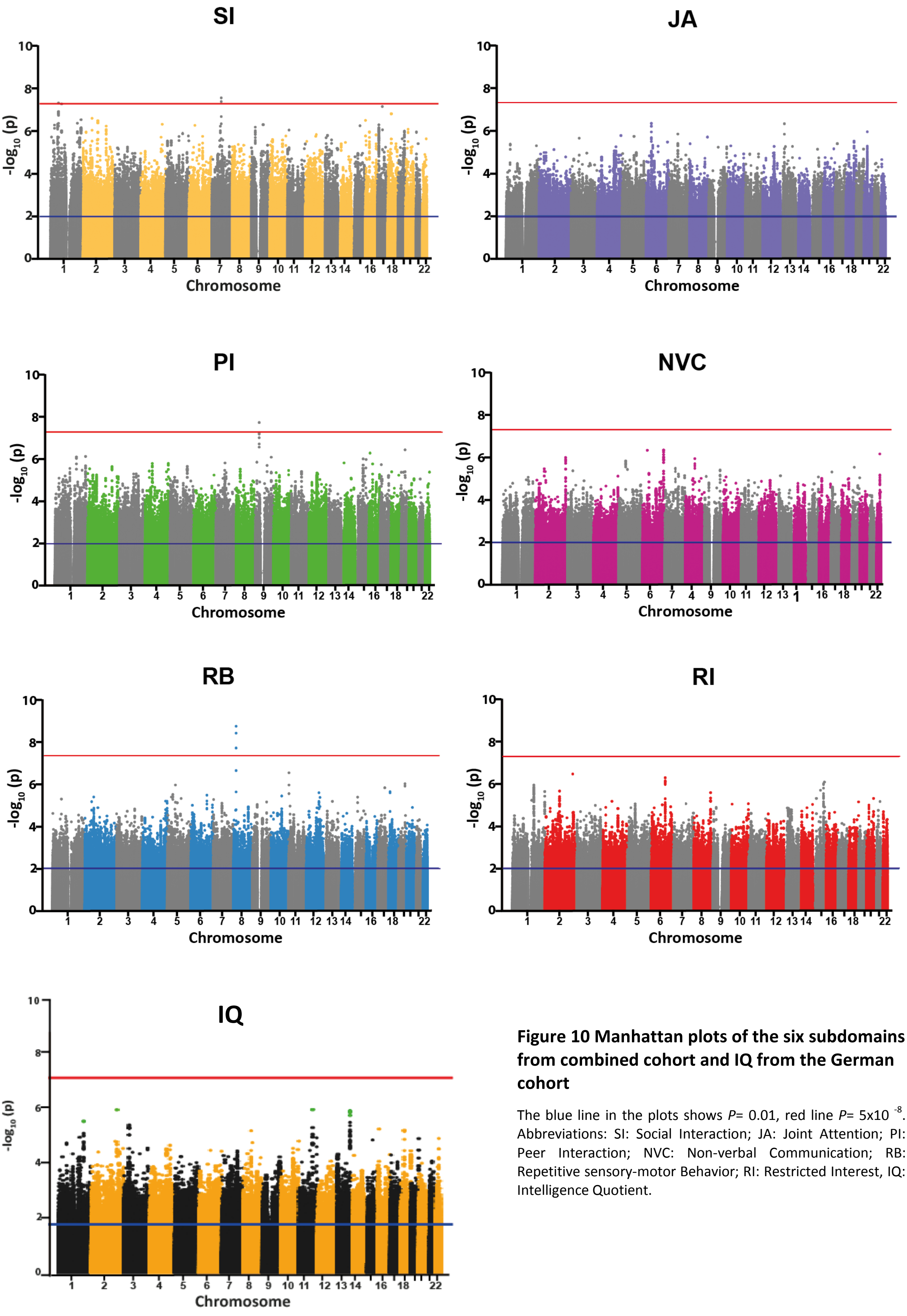

Figure 10 Manhattan plots of the six subdomains from combined cohort and IQ from the German cohort

The blue line in the plots shows P= 0.01, red line P= 5x10 $^{-8}$. Abbreviations: SI: Social Interaction; JA: Joint Attention; PI: Peer Interaction; NVC: Non-verbal Communication; RB: Repetitive sensory-motor Behavior; RI: Restricted Interest, IQ: Intelligence Quotient.

3.8. Gene and pathway analysis

MAGNET stage 4, i.e. gene-based analysis using MAGMA was performed on the individual GWAS outputs separately for each cohort. Since we wanted to identify the replicated genes in both cohorts, SNPs were mapped to corresponding genes within a window of 5 kilobases (kb) up and downstream of the respective hg19-annotated coding sequence. The significant genes (gene-wise empirical $P< 0.05$) to be associated with the subscores that also overlapped in both cohorts are shown in Table 9. These significant genes also contained some of the known ASD risk genes based on SFARI (Simons Foundation Autism Research Initiative) database (https://gene.sfari.org/). We identified 52 genes associated with SI which contained two ASD risk genes, i.e. *GNAS* (Guanine Nucleotide Binding Protein (G Protein)) and *PATJ* (Protein Associated To Tight Junctions). For JA, we found 35 overlapping genes that also contained the ASD risk gene *DAGLA* (Diacylglycerol Lipase Alpha). Similarly, in PI, 59 overlapping genes were identified having four ASD risk genes, i.e. *CECR2* (Cat Eye Syndrome Chromosome Region, Candidate 2), *MYO1E* (Myosin IE), *PGLYRP2* (Peptidoglycan Recognition Protein 2), and *SCN5A* (Sodium Voltage-Gated Channel Alpha Subunit 5). For NVC, we identified 47 genes encompassing the ASD risk genes *ICA1* (Islet Cell Autoantigen 1), *SCN8A* (Sodium Voltage-Gated Channel Alpha Subunit 8) and *THRA* (Thyroid Hormone Receptor Alpha). We identified 49 genes associated with RB including *CMIP* (C-Maf Inducing Protein) and *RNPS1* (RNA Binding Protein With Serine Rich Domain 1) which were previously identified as ASD risk genes. The 59 genes implicated in RI also include *ERBB4* (Erb-B2 Receptor Tyrosine Kinase 4) ASD risk gene.

For the trait IQ in the Geman cohort, MAGMA mapped ~ 8 million variants to 18,267 genes. Out of these genes, 996 significant genes were identified with an empirical $P< 0.05$. The identified top three most significant hits from MAGMA analysis are genes belonging to the S100 family, namely *S100A3* (S100 calcium-binding protein A3), *S100A4* (S100 calcium-binding protein A4), and *S100A5* (S100 calcium-binding protein A5).

Subdomain	Replicated Genes (ASD SFARI genes in bold)	Associated GO- terms
JA	API5, ATP12A, BMP5, C16orf91, CCDC39, CCNT1, COBLL1, COL23A1, **DAGLA**, DAPK3, ERMARD, GOLGA6L3, GYS1, JAK3, KANSL2, KMT2D, LHB, MKL1, MRPL24, MYOM3, OR5M8, PIEZO1, PIGQ, PPM1N, PSMD6, PYGL, RUVBL2, SCGB2B2, SLC15A5, SLC36A3, THOC7, TNFAIP3, TTC17, TTLL5	cellular polysaccharide metabolic process, cellular carbohydrate biosynthetic process, ATP metabolic process
SI	ABCA3, ALX1, ANXA3, ASNS, BCAR3, C17orf80, CA4, CA7, COCH, CPO, CYP3A7, EFNA2, ELSPBP1, FAM118A, FIGLA, FTL, **GNAS**, GYS1, HOXD3, HOXD4, HS3ST3A1, IBSP, IFI16, IL20, KPNA7, LY86, METTL24, MNS1, MRPL44, MYCBPAP, NAE1, NT5M, OR51Q1, **PATJ**, PPM1N, PSG7, PSPC1, RGS1, RGS10, RIBC2, SCNN1G, SEMA3E, SLC22A8, SMC1B, STK17B, TMCO4, TMEM86A, TTC17, TXNDC15, WDFY1, ZBTB12, ZFP37	embryonic skeletal system morphogenesis, sensory perception, anatomical structure development
PI	ADRB1, ANAPC15, ASB8, BLVRA, BRD3, C14orf119, CAMK2D, CCRL2, **CECR2**, CGB3, COPB2, COPS9, CRYZL1, DGUOK, DPP8, E2F7, ENPP3, EXOG, HACD3, HMGCLL1, HMOX1, HNRNPH1, IL18BP, IL20, IL7R, INTS14, ITGB5, KIAA0319L, LAMTOR1, LHB, LOC286238, LRTOMT, LTV1, MNS1, MTNR1A, **MYO1E**, NUMA1, OR2A4, PARVA, PCSK6, PFKM, **PGLYRP2**, PPP1R7, RNF121, RNF130, RSPO3, **SCN5A**, SLC24A1, STARD5, TDRD6, TM4SF4, TRPC4, TTLL1, UBAC1, UHMK1, UNC13B, WDR17, ZNF664, ZNF99	peptide hormone processing, hormone biosynthetic process
NVC	AMPD3, ARL14EP, CASC10, CCDC144NL, CCDC68, COBLL1, CPSF4, DNAJC1, DNAJC2, FAM96A, FBXW2, FIGNL2, **ICA1**, LIPJ, MLLT10, MPPED2, N4BP1, NAPEPLD, OR10G3, OXLD1, PES1, PID1, PLG, PMPCB, PSMC2, PSMD5, PSTK, PXN, RAB8B, RHAG, **SCN8A**, SKIDA1, SLAMF1, SLC26A5, SNX1, SOX21, SQOR, TCN2, TEX15, **THRA**, TM4SF4, TNFSF15, TNFSF8, ZKSCAN5, ZNF394, ZNF680, ZNF789	negative regulation of protein ubiquitination, regulation of protein localization
RB	ADAMTS10, AGA, AKAP13, APOD, ARMC12, ATP2C2, CLDN25, **CMIP**, DDX49, FAM153A, FKBP8, GALNT7, GATAD1, GLOD4, GPR21, HOMER3, HOXD10, HTR3B, KCNS2, KIZ, KLHL25, KLHL30, LGALS4, MAML3, MAT2A, MERTK, METTL6, MRGPRX3, MYOCD, MYOG, OPA1, OR2S2, PGC, PSG1, PTPRQ, PUS7, RAG1, RALGAPA2, RGS10, RINT1, **RNPS1**, SAAL1, SH3RF2, SLC16A5, SPATA31E1, TMPRSS5, TNFRSF10D, VAMP5, ZW10	skeletal muscle tissue development
RI	ACR, ACSBG2, AGAP5, AIM2, AK8, ANKK1, ARAP3, ARL15, ASIP, ATP1A2, C19orf70, C6orf132, C8B, CATSPERD, CDC37, CEP55, CIB4, COPG2, EMP1, **ERBB4**, FBXO22, GNG2, GRIN3A, HSD11B1L, IDH3B, KCNQ5, KIAA0319, KIAA1755, KL, KMT5C, KRT6A, KRT6C, LNPEP, LOC101929747, LONP1, MOB1B, MS4A13, MTMR14, NBPF7, NDST2, NLRP3, NSUN5, OR2B2, PPP1R13B, RPL36, SAFB, SEC11A, SERP2, SPN, SPSB1, SYCP2L, TMED5, TRPS1, TSGA13, TTC12, ZFYVE21, ZGLP1, ZNF814, ZSWIM8	generation of precursor metabolites and energy, intracellular receptor mediated signaling pathway, positive regulation of MAPKKK cascade
IQ (top 50 genes only)	S100A4, S100A5, S100A3, RAC2, PRR35, MDP1, NHLRC4, WDR38, CHMP4A, GOLGA1, S100A6, EIF1B, RPL35, NEDD8-MDP1, OPN4, PER2, S100A2, COX7A2L, PIGQ, MCF2L, C21orf59, WFIKKN1, ARPC5L, STK40, RAB40C, C16orf13, SND1, SHISA6, CLEC2B, IL23R, ENTPD3, ZKSCAN1, RPL14, NADSYN1, DCLK2, ZNF619, NEUROD2, PPP1R1B, KLHL40, PLD5, APOA4, NDUFS1, TTF2, LDB3, IBTK, NEDD8, EML4, MFSD2A, TSSK4, C14orf1	maternal process involved in female pregnancy, macrophage differentiation, epithelial to mesenchymal transition, response to cortisol stimulus, cerebellum morphogenesis

Table 9 Significant genes in both cohorts from MAGMA analysis

The bold genes are the known ASD SFARI risk genes. Abbreviations: SI: Social Interaction; JA: Joint Attention; PI: Peer Interaction; NVC: Non-Verbal Communication; RB: Repetitive sensory-motor Behavior; RI: Restricted Interersts, IQ: Intelligence Quotient.

3.9. GO-term analysis

Overlapping MAGMA genes from each subdomain were selected manually for the subsequent analysis. The overlapping gene list obtained for each subdomain was submitted to MAGNET stage 4. All together, unique and significant GO-terms (permuted p-value < 0.05) in SI, JA, PI, NVC, RB, and RI were 9, 14, 22, 11, 3 and 12, respectively. IQ which was only analysed in the German cohort showed 190 significant pathways. The top significant GO-terms are shown in Figure 11. These are diverse processes such as SI associated with the GO-term “sensory perception” among others. For JA the overlapping genes were enriched for “carbohydrate metabolism”, “energy metabolism” and “chromatin modification”. Similarly, in PI, enriched GO-terms included “hormone processing” and “plasma membrane”. For NVC we identified GO-terms related to “protein catabolism”. RB was enriched for the GO-terms “skeletal tissue muscle development” and “transmembrane receptor”. Enriched GO-terms for RI were related to “postsynaptic signaling” and “intracellular mediated signaling pathways”. The top GO-terms for IQ in the German data included GO-term analysis revealed processes such as “cerebellar cortex neuron differentiation” and cerebellum morphogenesis”.

3.10. KEGG pathway analysis

MAGNET provided the list of all enriched KEGG pathways, the number of genes in the KEGG pathway and the number of genes associated with the input list and p-value for over-representation of the KEGG term in the set. The KEGG pathways were limited due to the conservative approach applied for selecting the set of significant genes. A few interesting pathways include “Starch and sucrose metabolism” for JA, “Glucagon signaling pathway” for SI, “Metabolic pathways” for PI, “Sulfur metabolism” for NVC, “FoxO signaling pathway” for RB and “cAMP signaling pathway” for RI. Whereas for IQ from the German cohort, the enriched KEGG pathways include “VEGF signaling pathway”. The most significant KEGG pathways for IQ included “Basal cell carcinoma” and “Melanogenesis”. These pathways are shown in Figure 12.

3.11. Brain enrichment analysis

The final stage of MAGNET uses Kang et al. brain transcriptome data set to find enrichment of the significantly overlapping genes from both cohorts for each subdomain in 29 different modules that are co-regulated during the development of the human brain. Significantly overlapping genes from both cohorts in each subdomain were then looked for enrichment in the Kang dataset. Enrichment was found only for SI and NVC in Kang module 6 and module 27 respectively, showing a distinct pattern of gene expression across time and brain regions. Module 6 shows a gene expression pattern that is activated during toddlerhood and remains down-regulated between early and late childhood specifically in the hippocampus. However, in the frontal cortex and striatum, the genes are upregulated during childhood (Figure 13a). As per the information provided by Kang et al., module 6 is involved in GO-terms related to “transport”. On the other hand, the gene expression pattern of module 27 genes shows upregulation right after post-conception till middle childhood and then remains down-regulated from late childhood onwards except in the hippocampus which is down-regulated during early to late childhood (Figure 13b). Module 27 is related to GO-terms associated with “extracellular matrix” and “cell-adhesion”.

Similarly, IQ trait in the German cohort showed to be enriched for modules 4 and 14. Module 4 is up-regulated from early childhood to late adulthood in all brain regions other than the hippocampus, while the gene expression pattern of module 14 shows up-regulation between early and late childhood. Module 4 is involved in GO-terms related to “immune response”, and module 14 is associated with “mitochondria”. Gene interaction networks of the enriched modules are also provided to integrate the associated genes into the co-regulated modules. The provided graphs show the top 50 most connected genes and their transcriptomic correlation. Expression of the enriched modules and gene networks of topmost connected genes are shown in Figure 13.

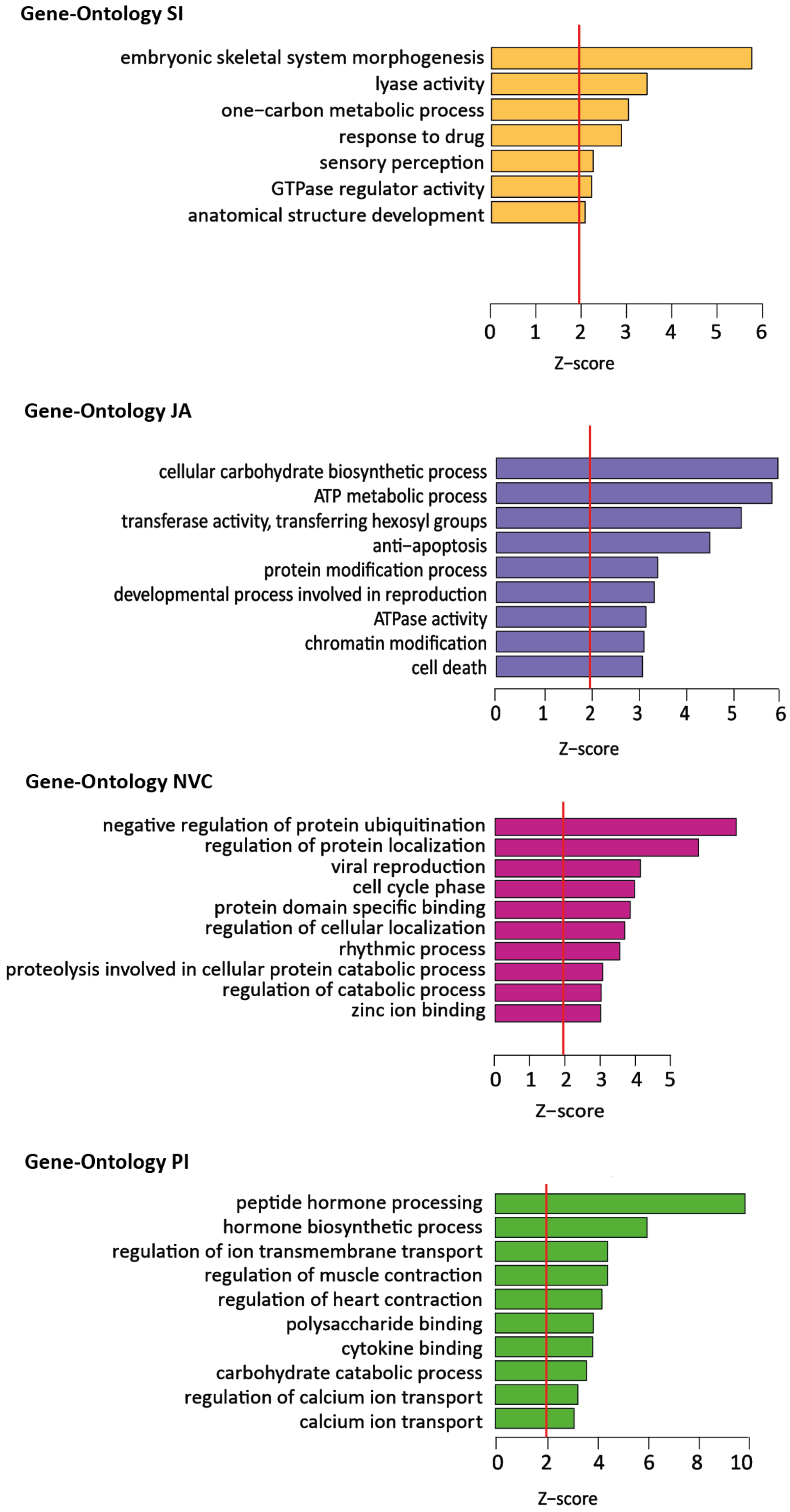

Gene-Ontology SI

Gene-Ontology JA

Gene-Ontology NVC

Gene-Ontology PI

…Figure continues on next page...

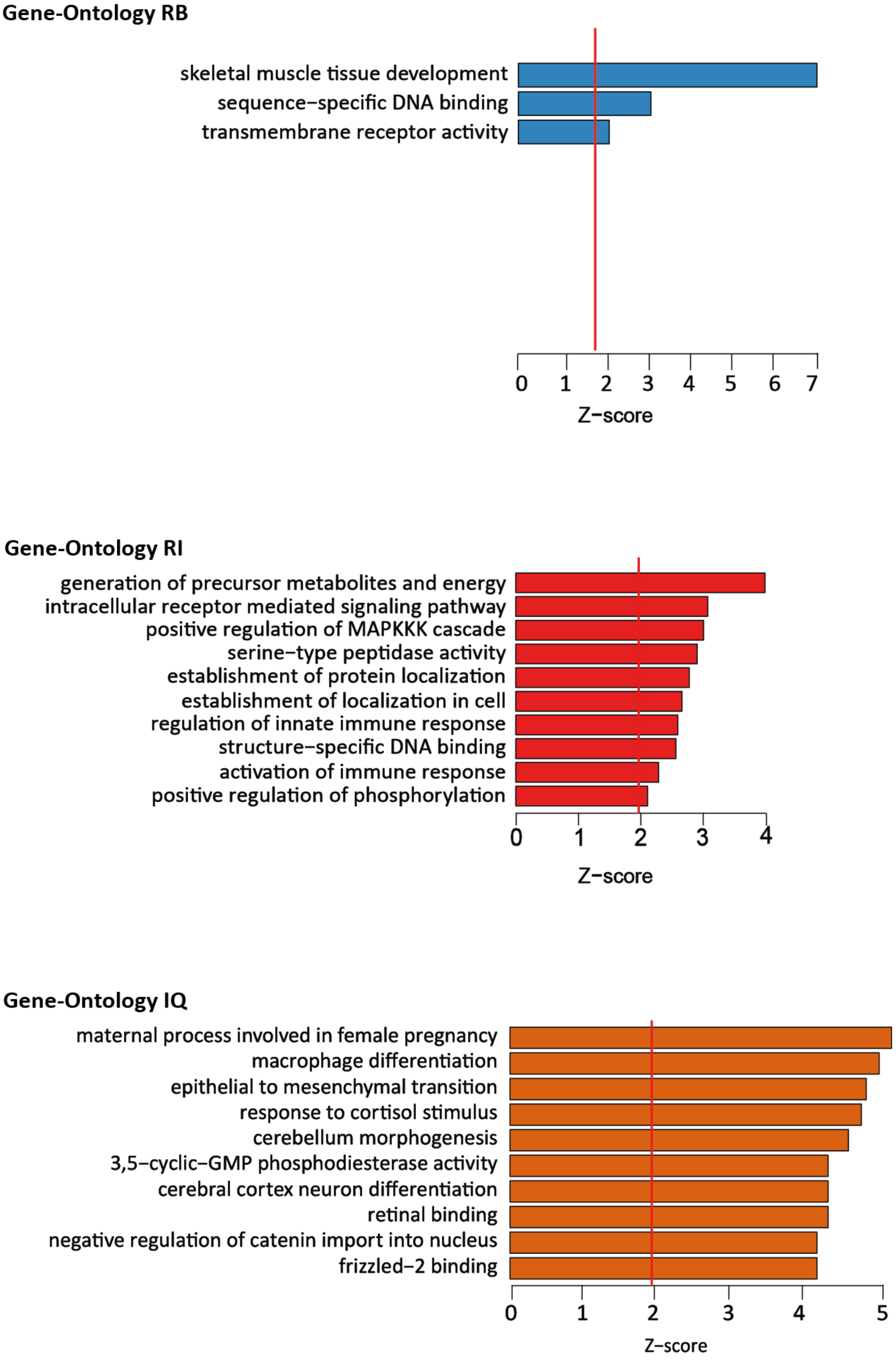

Gene-Ontology RB

Gene-Ontology RI

Gene-Ontology IQ

Figure 11 Gene Ontology (GO) analysis

Barplots showing the top GO paths. The red line marks significance threshold that is Z-score = 1.96. Abbreviations: JA: Joint Attention, SI: Social Interaction, NVC: Non-verbal Communication, PI: Peer Interaction, RB: Repetitive motor sensory behavior, RI: Restricted Interests, IQ: Intelligence Quotient.

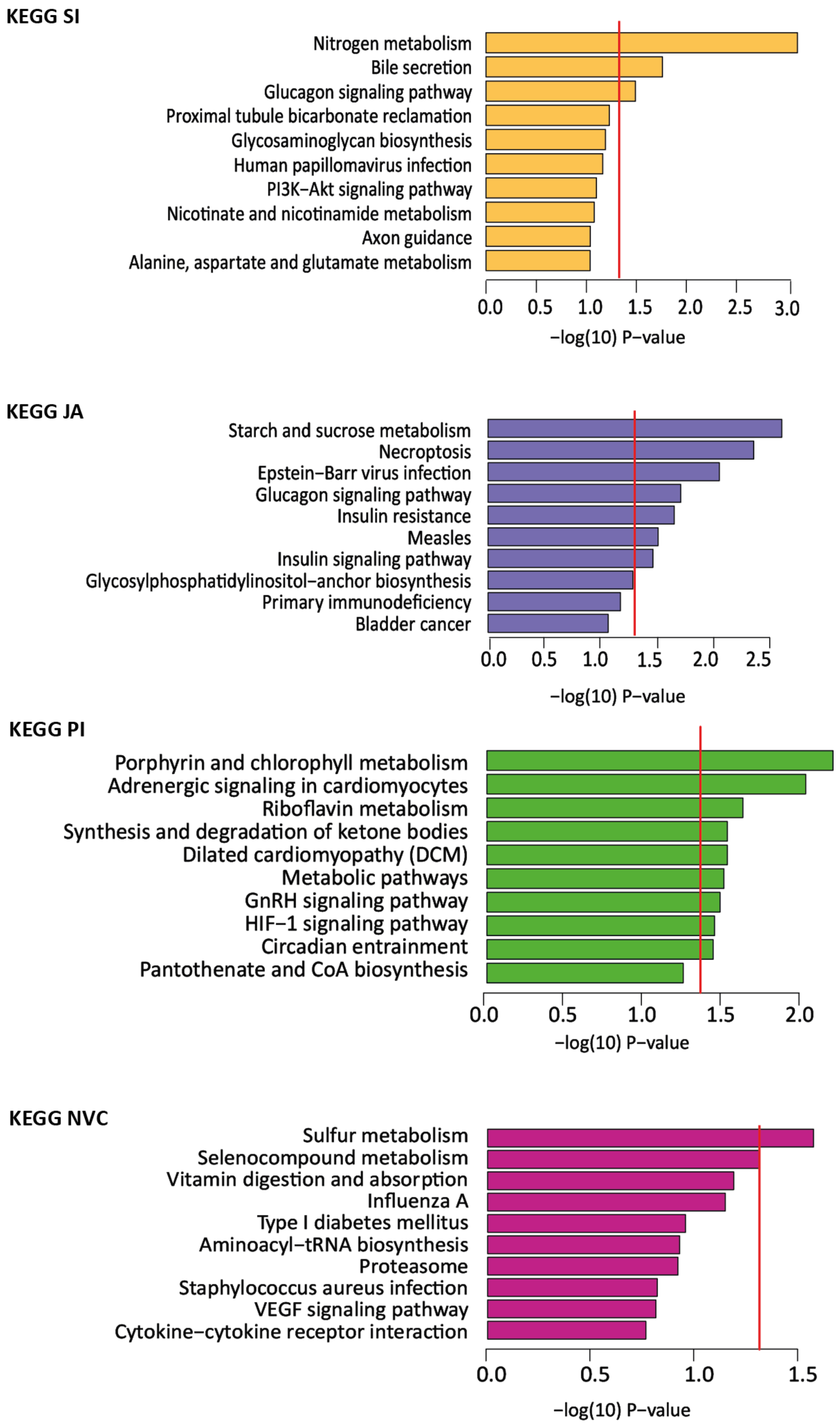

…Figure continues on next page...

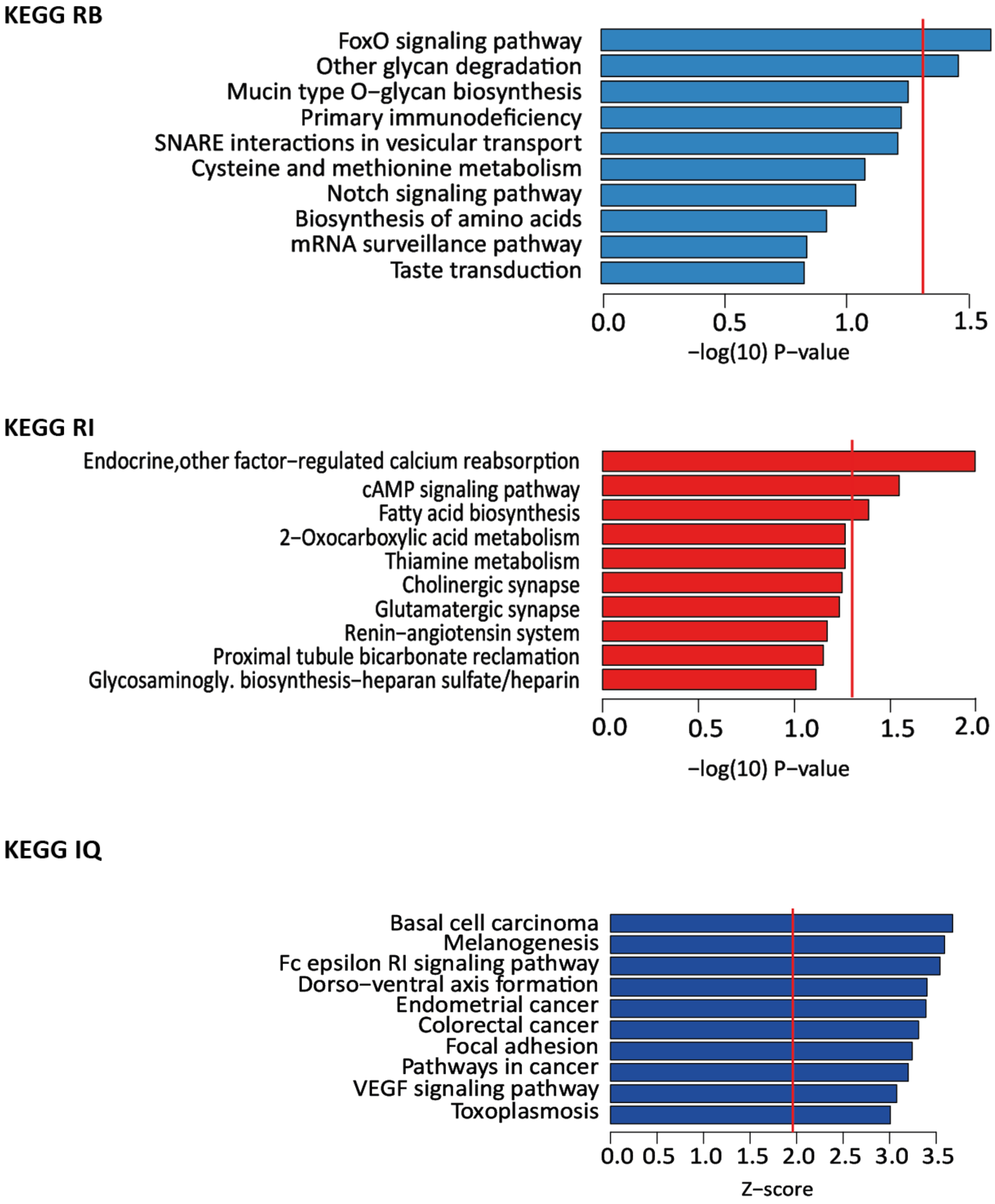
KEGG RB

KEGG RI

KEGG IQ

Figure 12 KEGG pathway analysis

Barplots showing the top GO paths. The red line marks the significance threshold that is P-value< 0.05 and for IQ Z-score= 1.96. Abbreviations: JA: Joint Attention, SI: Social Interaction, NVC: Non-verbal Communication, PI: Peer Interaction, RB: Repetitive motor sensory behavior, RI: Restricted Interests, and IQ: Intelligence Quotient.

(a) Kang module 6 enriched for SI

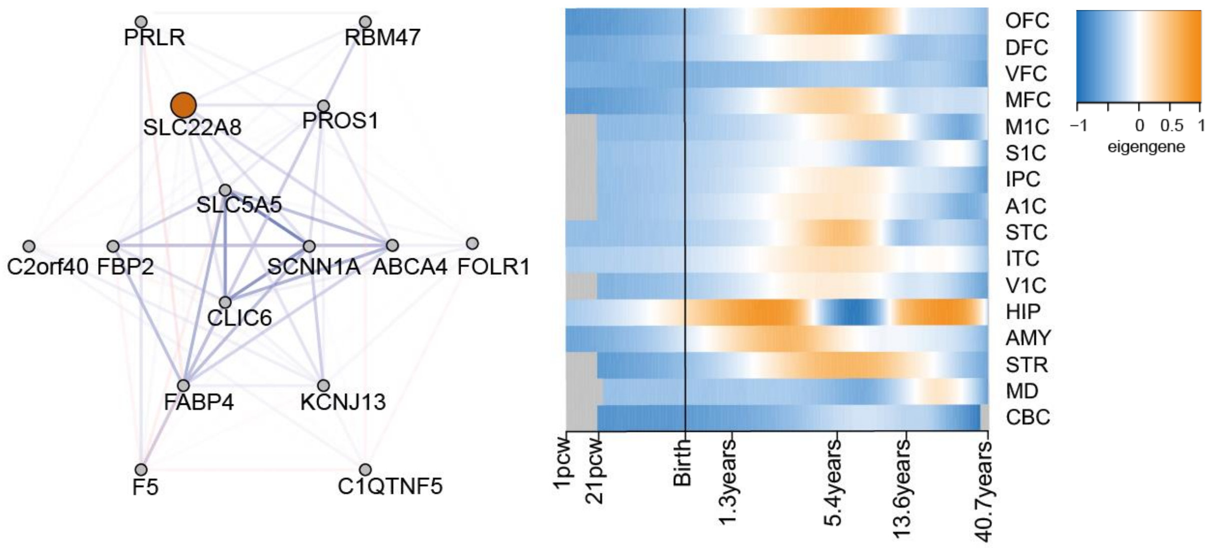

(b) Kang module 27 enriched for NVC

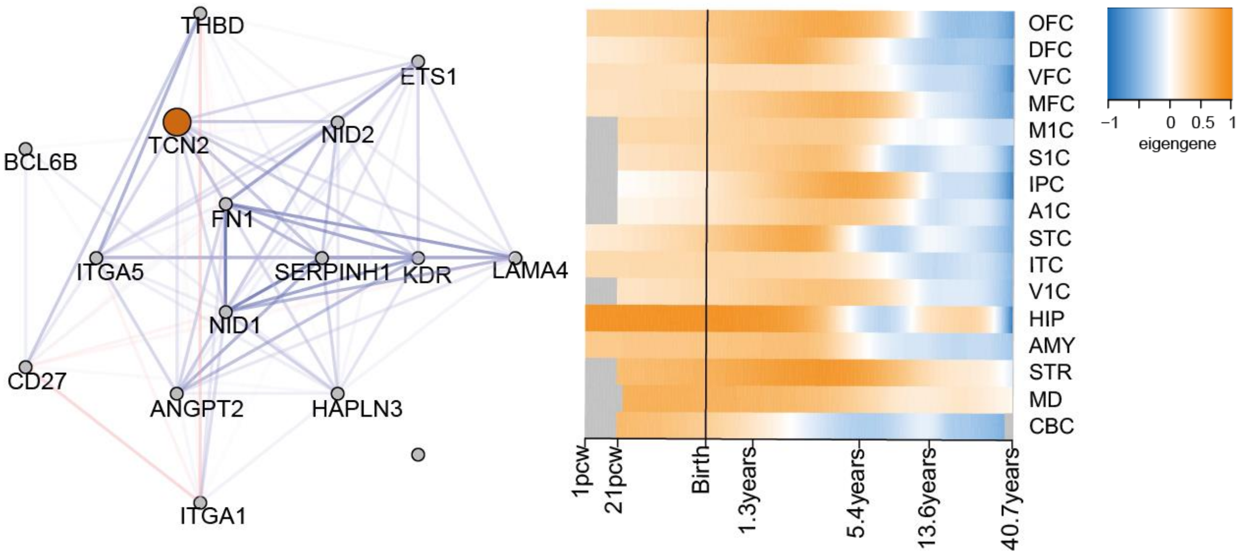

…Figure continues on next page …

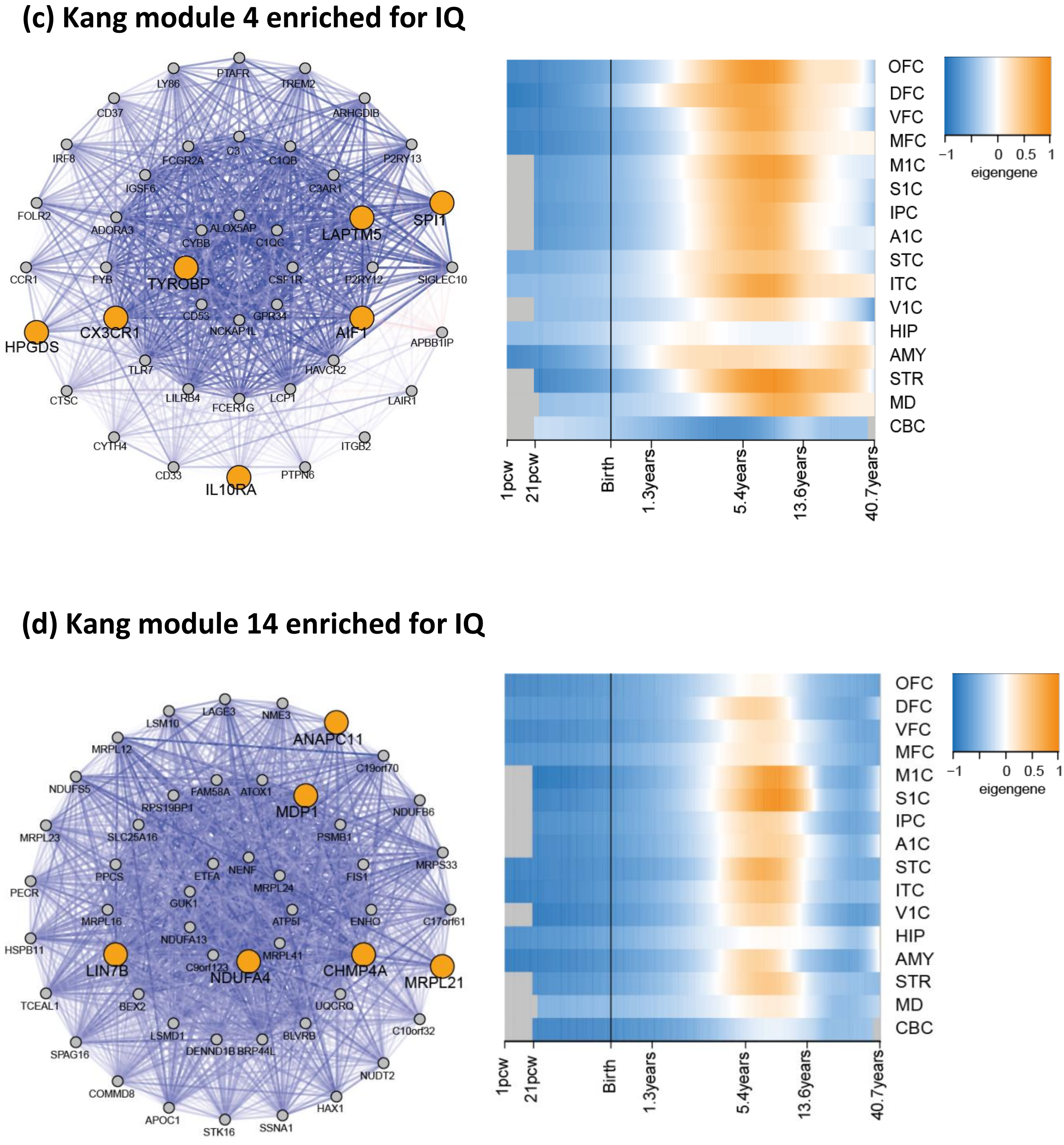

(c) Kang module 4 enriched for IQ

(d) Kang module 14 enriched for IQ

Figure 13 Expression profiles of associated brain gene modules

Eigengene expression of **(a)** Module 6 enriched for genes implicated in SI (Social Interaction), **(b)** Module 27 enriched for genes implicated in NVC (Non-verbal communication), **(c)** Module 4, and **(d)** Module 14 enriched for genes in IQ, where x-axis shows the developmental time frame, and y-axis shows the different brain regions ,i.e. OFC: Orbital prefrontal cortex; DFC: Dorsolateral prefrontal cortex; VFC: Ventrolateral prefrontal cortex; MFC: Medial prefrontal cortex; M1C: Primary motor (M1) cortex; S1C: Primary somatosensory (S1) cortex; IPC: Posterior inferior parietal cortex; A1C: Primary auditory (A1) cortex, STC: Superior temporal cortex; ITC: Inferior temporal cortex; V1C: Primary visual (V1) cortex; HIP: Hippocampus; AMY: Amygdala; STR:Striatum; MD: Mediodorsal nucleus of the thalamus; CBC: Cerebellar cortex.

III. Additional data analysis

The following analyses are not part of the MAGNET but were performed to investigate the genetic architecture of ASD subdomains at a further level.

3.12. Genetic heritability of ASD phenotypes

We also estimated the phenotypic variance explained by the common variants in our analysis among the six ASD subdomains (Figure 14). The estimates are lower than the twins-based heritability estimates but higher than previously reported ASD SNP-based heritability estimates [203]. The highest SNP-based heritability is observed for SI and the lowest for RB. All estimates were significant and were not corrected for any covariates.

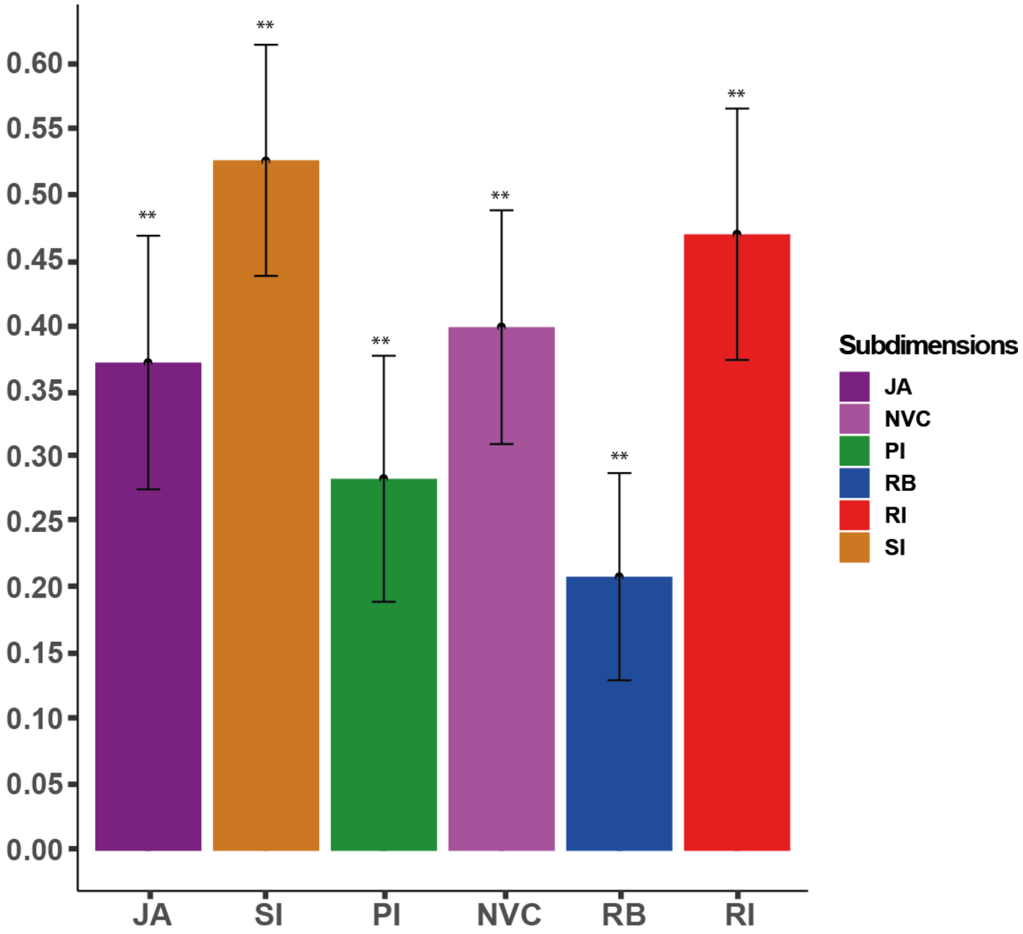

Figure 14 Heritability estimates

Bar plots showing the heritability estimates of the six subdomains. Asterisks indicate that the p-value is significant after multiple corrections. Abbreviations: SI: Social Interaction; JA: Joint Attention; PI: Peer Interaction; NVC: Non-verbal Communication; RB: Repetitive sensory-motor Behavior; RI: Restricted Interest.

3.13. Correlation among ASD phenotypes

We observed the phenotypic and genetic correlation among ASD subdomains. Phenotypically, the six ASD subdomains appear to be significantly independent of each other. However, the domain A subdomains of ASD, i.e. JA, SI, PI, and NVC are relatively closely clustered than the domain B subdomains, i.e. RB and RI. At the genetic level, we observe that SI pairs with NVC, PI with JA, and altogether, all these subdomains are also correlated with the exception of RB. The correlation of RB was weak with all other subdomains although none of the correlations was significant (Figure 15b).

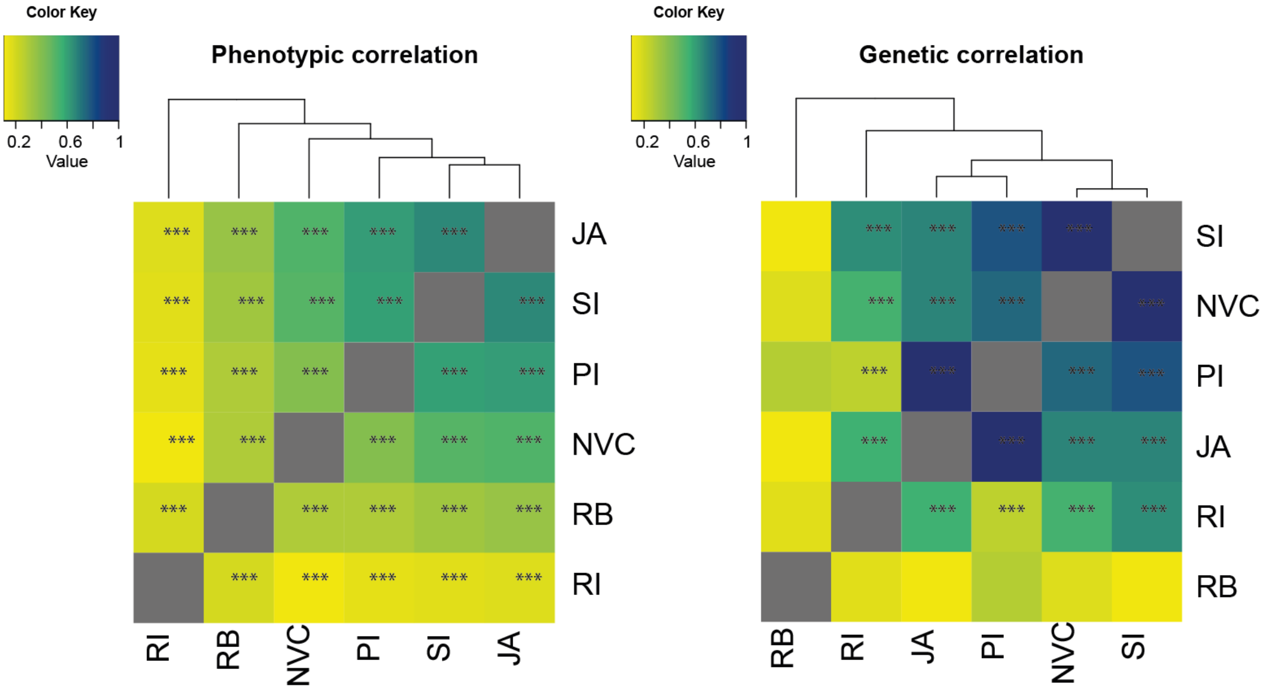

Figure 15 Heatmaps illustrating the (a) phenotypic and (b) genetic correlation among ASD subdomains

The color of squares represents the intensity of correlations depicted with a color range of yellow to blue showing a range of lowest to highest correlation respectively. Asterisks *** indicate p-values < 0.001. Abbreviations: JA: Joint Attention; PI: Peer Interaction; NVC: Non-verbal Communication; RB: Repetitive sensory-motor Behavior; RI: Restricted Interest.

3.14. PRS for ASD phenotypes

The PRS for ASD explained a significant (all *P*< $2x10^{-05}$) proportion of the genetic variance of all subdomains. Here, we report the best fit model for each of the subdomains. For SI the best fit explained 3.3% of variance (R^2), 2.3% in JA and in PI. For NVC and the domain B related subdomain RB, a much lower R^2 was observed, i.e. an R^2= 0.7% and R^2= 1.2%, respectively. In comparison, the other subdomain of domain B showed a higher R² for RI, i.e. 4.5%. P-values for the best models ranged from 0.031-0.411 (Figure 16).

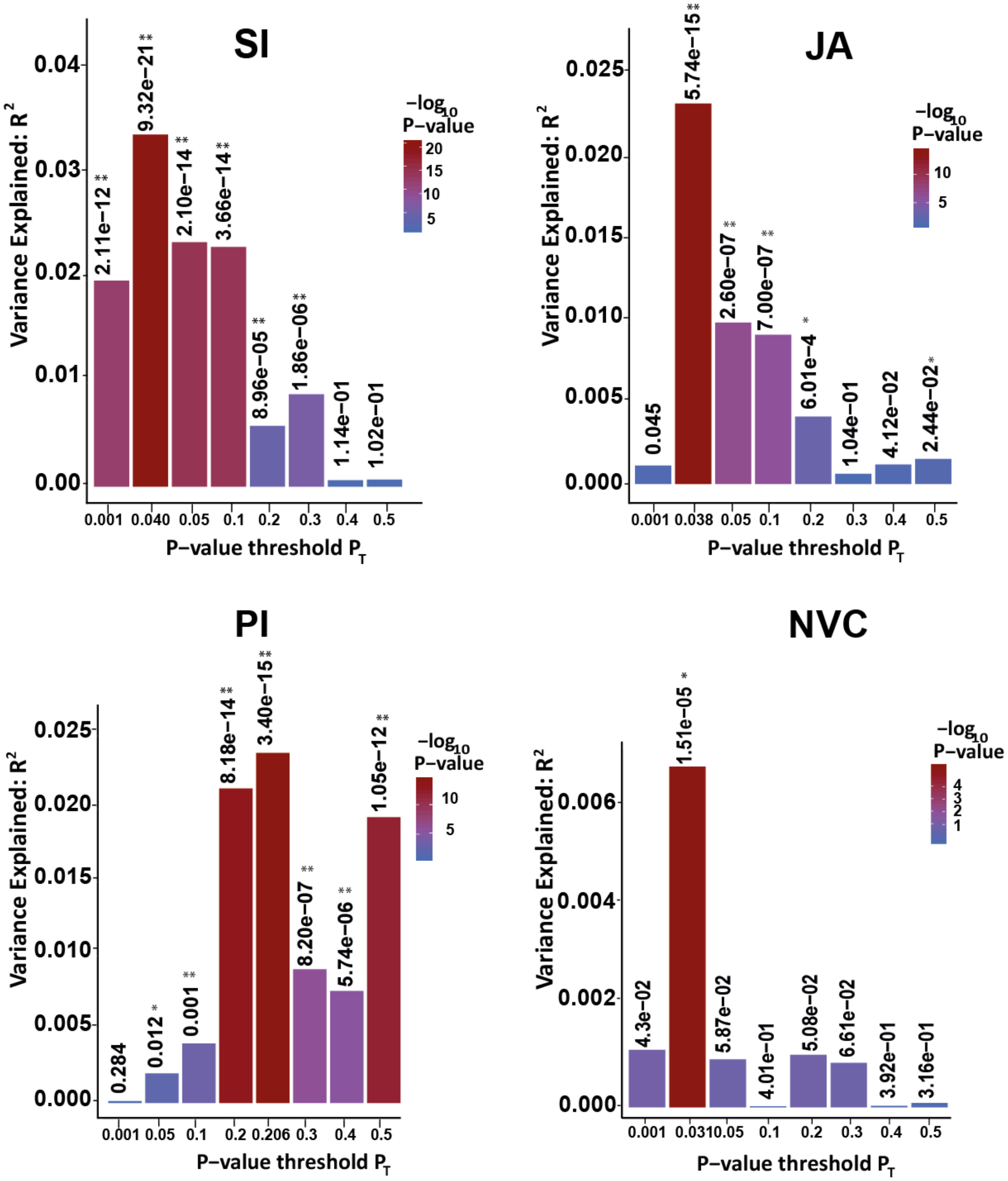

…Figure continues on next page…

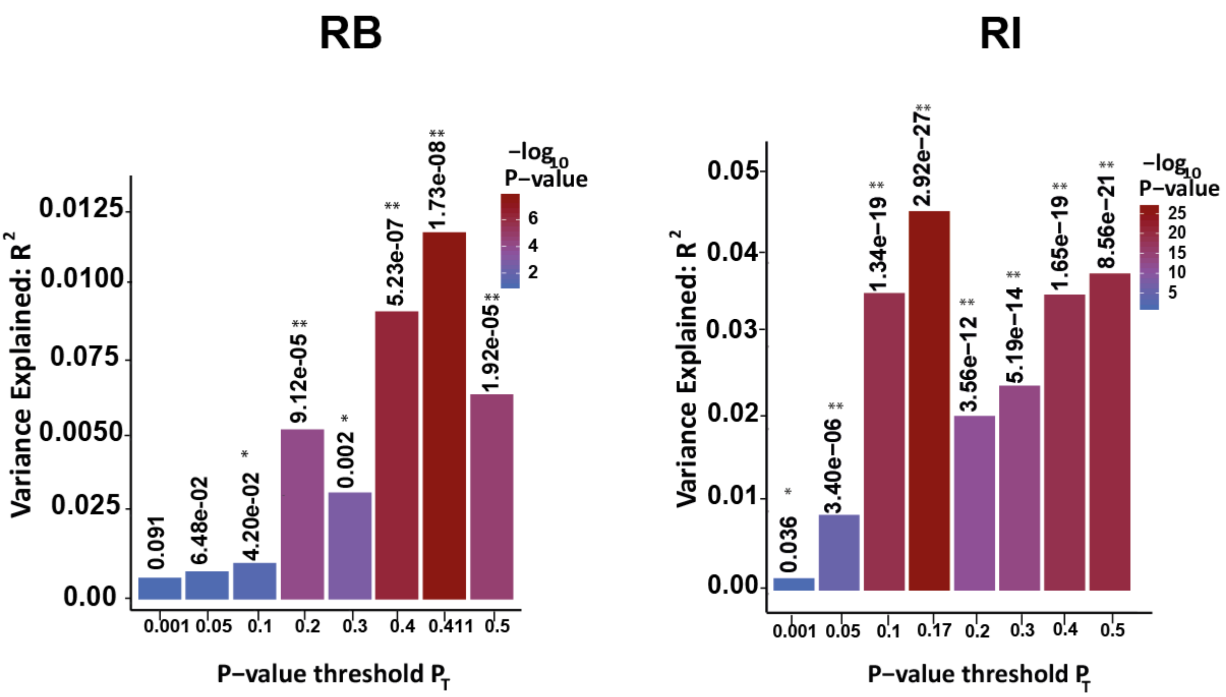

Figure 16 Polygenic risk score analysis

The shared genetic etiology between ASD diagnosis and individual subdomains. Each bar represents the respective P-value thresholds (P_T) whereas the numbers above bars denote the *P* value for the underlying model. Abbreviations: SI: Social Interaction; JA: Joint Attention; PI: Peer Interaction; NVC: Non-verbal Communication; RB: Repetitive Behavior; RI: Restricted Interest.

3.15. SNPs and genes overlap among the subdomains

We then compared the significant findings among the subdomains at SNP as well as at gene level. At the genome-wide significance threshold, none of the SNP overlapped among the subdomains. However, we found several nominal (*P*≤ 0.01) significant SNPs intersected among the subdomains (Figure 17a). We identified that the highest number of nominal SNPs overlapping were among SI, JA and PI, i.e. 149 SNPs, followed by 27 SNPs among SI, PI, and NVC. RI did not exhibit overlap with any other subdomain. At gene level, we found three overlapping genes significant for JA and SI (*GYS1*: Glycogen Synthase 1, *TTC17*: Tetratricopeptide Repeat Domain 17, and *PPM1N*: Probable Protein Phosphatase 1N), two genes overlapping between SI and PI (*MNS1:* Meiosis Specific Nuclear Structural 1, *IL20*: Interleukin 20), one gene significant for NVC and PI (*TM4SF4:* Transmembrane 4 L Six Family Member 4), and one gene associated with SI as well as RB (*RGS10:* Regulator Of G Protein Signaling 10), one gene in JA and PI (*LHB*: Luteinizing Hormone Beta Polypeptide) and one gene between JA and NVC

(*COBLL1*: Cordon-Bleu WH2 Repeat Protein Like 1) (Figure 17b). Overlaps between functional annotations were limited; we found only the GO-term “soluble fraction” as associated with JA and PI.

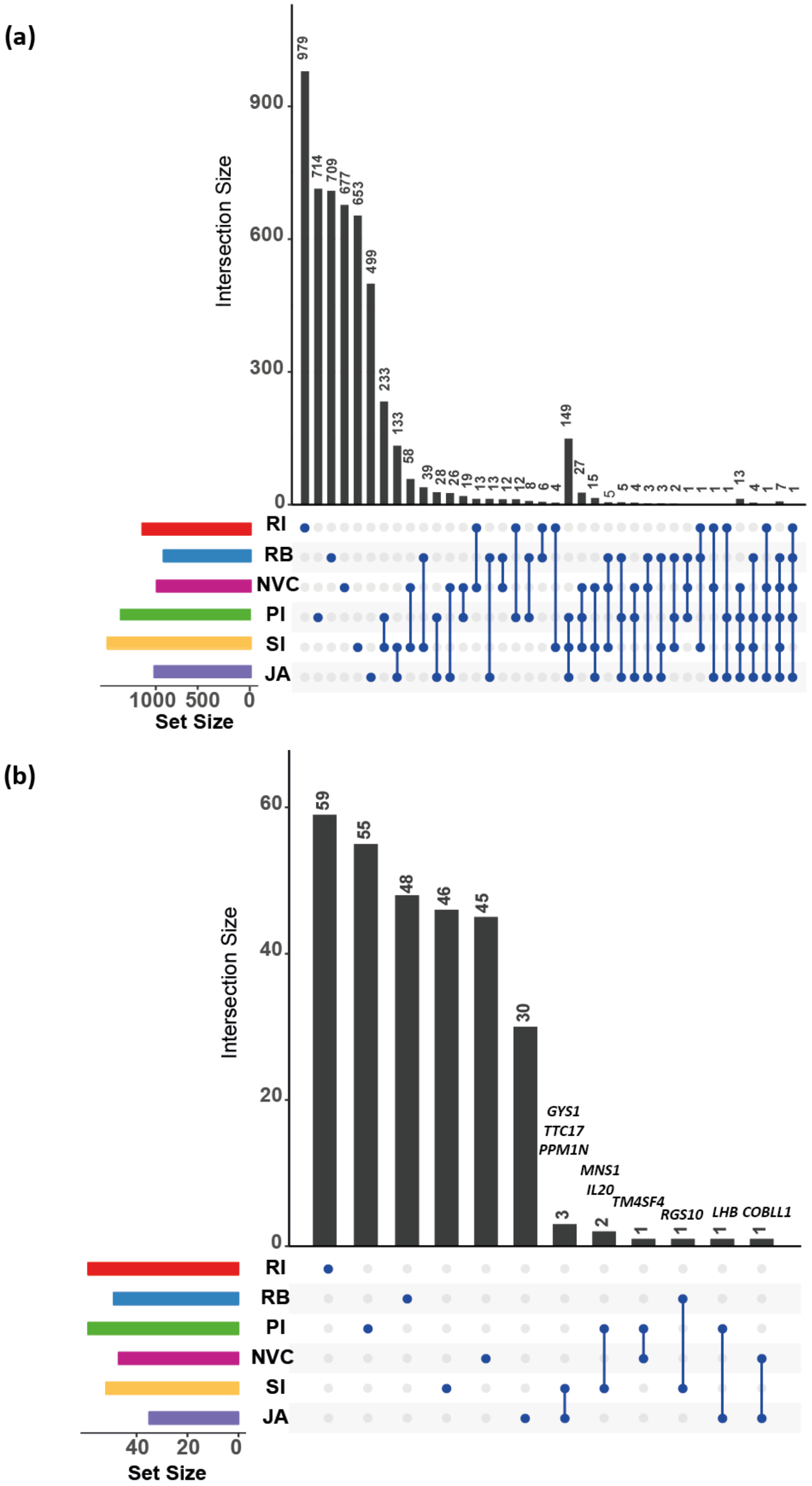

Figure 17 Overlap of significant findings

(a) Overlapping SNPs with a P< 0.01 between subdomains. **(b)** Overlapping genes with a significant empirical permutation P< 0.05 as identified using MAGMA. Bars correspond to the number of SNPs/genes intersecting between the subdomains as shown in the connection dot-plot below bars. Set Size is the total number of identified genes/SNPs for the respective subdomain. Abbreviations - SI: Social Interaction; JA: Joint Attention; PI: Peer Interaction; NVC: Non-Verbal Communication; RB: Repetitive Behavior; RI: Restricted Interest.

3.16. Discussion

This section contains parts of the article “Quantitative genome-wide association study of six phenotypic subdomains identifies novel genome-wide significant variants in Autism Spectrum Disorder” which has been submitted and is currently in the review process in the Journal of Translation Psychiatry. The biological question behind this study was to characterize the underlying genetic etiology and functional overlap behind ASD diagnostic domains and the respective subdomains. Moreover, clinical studies have also shown that the phenotypic heterogeneity can be studied as predictors of outcome in clinical trials [204]. However, only a few studies have looked at its association with the genetic underpinnings.

ADI-R defined ASD subdomains replicated previous structure

The two diagnostic domains of ASD defined by DSM-5 have been suggested as two separable domains, i.e. social and repetitive behaviors identified by using factor analysis and principal component analysis[205]. To date, information regarding the genetic etiology of these two domains remains limited and the individual findings are not replicated in other cohorts. The possible reasons can be the small genetic effect sizes and limited sample sizes.

Previously, it has been shown that defining separate ASD traits into more homogenous groups can reduce the genetic heterogeneity [206]. These subgroups might lead to direct expressions of gene effects and also contribute in improving the effect sizes and thus the statistical power. Moreover, it can assist in identifying susceptibility genes for ASD subgroups. In this study, we also identified a six-factor structure that has been previously reported by Liu et al.[84], as well as a similar structure was identified from 98 ADI-R items [207]. This six-factor structure was also confirmed in the independent German cohort in this study. Thus, we postulate that the classification of ADI-R diagnostic domains into these subdomains plays an important role and can serve as possible predictors in accessing the underlying etiology.

Association of common variants behind specific ASD subdomains in the combined, AGP and, German cohort

GWAS analysis using MAGNET identified several genome-wide significant common variants and respective novel candidate genes across the study. As GWAS was performed on the combined cohort for power issues, we later followed a conservative approach to consider only the genes which significantly replicated in both cohorts to be considered for the downstream analysis. We first discuss the findings from the combined cohort and the significant genes replicated from gene analysis in both cohorts.

Combined cohort (AGP and DE)

We identified four genome-wide common variants for SI. One mapped to an ASD-related gene *PATJ* (Protein Associated To Tight Junctions), which codes for a scaffolding protein CIPP and regulates the surface expression and/or function of ASIC3 (Acid-sensing ion channel 3) in sensory neurons [208].

A study found three case-specific loss-of-function variants (variants that disrupt the function of the resulting proteins) in association with *PATJ* [209]. Two other genome-wide hits map to *CLIP2* (Cytoplasmic Linker Protein 2) gene. This gene is located at chromosomal position 7q11.23 and duplication carriers of this region show a high rate of ASD [210].

Though no genome-wide hit was identified for JA, the GWAS analysis for JA identified one of the top three significant SNP peaks, consisting of rs10254837, rs4075496, and rs56263157 at 7q11.22 which maps to the gene *AUTS2*. Genomic rearrangements of this gene are associated with ASD and intellectual disability (ID) [211]. In a study by Gao et al., *Auts2*-KO (knockout) mice showed impairments in sensorimotor, cognition and communication behavior [212].

For PI we identified only one genome-wide significant SNP, i.e. rs10115292 mapped to an intergenic region at chromosomal position 9p21.1, which is known for ASD-associated CNVs [28].

Though no genome-wide significant hit was identified for NVC, SNPs at a suggestive significance $P < 5x10^{-7}$ map to chromosomal position 6q26, a region linked to ASD [111]. Moreover, this region has been associated with intellectual disability, delayed language development and dyspraxia in a case with an 8Mb microdeletion of the 6q26-q27 locus [213].

For RB we identified three genome-wide SNPs which mapped to 8p21.3. This region has been previously associated with restricted and repetitive behaviors in ASD [173]. Duplications of this region have been associated with ASD [214]. Among the other top three SNP peaks, 19q13.33 was also identified in RB. This region has also been shown previously to be associated with repetitive sensory-motor behavior [84].

No genome-wide significant hit was observed for RI, however, the top significant SNP hits for RI were also observed in migraine, sensorineural deafness, cognition, and ASD such as *NLRP3 (*NLR Family Pyrin Domain Containing 3) [215], *GNG2* (G Protein Subunit Gamma 2) [216] and *NSUN5* (NOP2/Sun RNA Methyltransferase 5) [217]. The top peak at 15q25.3 is spanning the neurotrophic receptor tyrosine kinase 3 gene *NTRK3* (Neurotrophic Receptor Tyrosine Kinase 3)*,* a gene previously associated with both ASD and Asperger syndrome [218] as well as obsessive-compulsive disorder [219].

Individual cohorts

In the individual AGP cohort, we identified nine genome-wide hits. Two hits were identified in SI, i.e. rs377634870 at chr1:84731827 (no nearest gene at 10kb) and rs9333127 at chr10:15658963 (*ITGA8*: Integrin Subunit Alpha 8). *ITGA8* is involved in sensory and motor neurons and the regulation of neurite outgrowth. A missense mutation in this gene has been associated with schizophrenia [220]. However, it has not been investigated with respect to ASD. Similarly, five genome-wide hits were reported for PI including rs7777015, rs6963792, rs7783341, rs9969152 at chr.7 (no nearest genes within 5kb). All these SNPs are present at 7q21.11, a region known to be involved in ASD [111]. Besides these SNPs, rs10115292 at chromosome 9 (no nearest gene within 5kb) which is significant in the merged cohort, is also genome-wide, significant in the AGP cohort. Genome-wide, significant SNPs have also been found for RB, i.e. rs441459 and rs388190 at 11p15.4 mapping to the gene *SLC22A18AS* (Solute Carrier Family 22 Member 18 Antisense). This gene was found to be upregulated in a group of ASD individuals [221].

We also identified two genome-wide significant hits in the German cohort. One in NVC, i.e. rs75158512 at chromosomal position 10p14, a region associated with ASD [222]. Similarly, one SNP was identified for JA, i.e. rs2151874 at 1q42.2. Previously, an inherited 2.07 Mb microduplication was found at this locus in two brothers with ASD and mental retardation [223].

The separate GWAS on IQ trait from the German cohort identified gene variants of *CNTN5* (rs10736578, rs1837768) and *MCF2L* (rs66884214, rs534618502, rs28459375), which have not been identified before in the context of IQ directly. The SNPs of these newly IQ-associated genes were among the top 10 SNPs with a $P< 5\text{x}10^{-7}$ and an FDR-corrected $P\leq 0.001$. *CNTN5* mediates cell surface interactions during nervous system development and plays a role in axon connections [224]. *MCF2L* encodes Rho guanine nucleotide exchange factor (GEF) and is expressed in the human brain [225].

The results of GWAS analysis in combined and individual analysis strengthened the plausibility of our findings as we not only identified novel variants and genes but also genes that were known to be associated with ASD previously. Moreover, we deduce that the disassociation of ASD phenotypic domains into specific subdomains led to an increase in statistical power as also previously proposed [206] and identification of genome-wide significant variants. Thus, this also validates the functioning of MAGNET in relation to identification of trait-associated common variants and their respective genes.

Identification of overlapping genes in ASD cohorts subdomains

As mentioned earlier, we followed a conservative approach for selecting the genes for downstream analysis to minimize the chance of false-positive findings. For this purpose, we only selected the genes from gene analysis which had a significant empirical $P< 0.05$ in AGP and the German cohort subdomains.

Based on MAGMA gene analysis, we identified 52 overlapping genes in SI, which include the genome-wide significant SNP mapped gene *PATJ* as well as the gene *FTL* (Ferritin Light Chain), which is involved in Neurodegeneration with Brain Iron Accumulation (NBIA) disorders [226] that are clinically characterized by a progressive movement disorder with symptoms varying significantly in terms of range and severity, such as cognitive deficits, personality changes with impulsivity and violent outbursts, depression, emotional lability, and obsessive-compulsive disorder [227]

For JA, 35 overlapping genes showed significant association. Among the most significantly associated genes we identified a neural stem cell-derived dendrite regulator protein-coding gene *DAGLA* (Diacylglycerol Lipase Alpha) implicated in seizures and neurodevelopmental disorders including ASD [228], and the *COBLL1* (Cordon-Bleu WH2 Repeat Protein Like 1) gene involved in epilepsy [229] and language impairment [230].

In the gene set analysis for PI, 59 overlapping genes were identified as significantly associated. Among these genes, we found a sodium voltage-gated ion channel gene *SCN5A,* which was found to be enriched in an ASD-associated protein interaction module [231]*.* Other ASD-associated, significant genes include *CECR2* (cat eye syndrome chromosome region candidate 2)*,* a 7.2kb exonic loss of which was found in an ASD female [228]. Another interesting hit in the list is *ENPP3* (Ectonucleotide Pyrophosphatase), variants of this gene (*ENPP4, ENPP5*) have been associated with seven brain regions in ASD, i.e. angular gyrus, anterior caudate, cingulate gyrus, dorsolateral prefrontal cortex, hippocampus middle, inferior temporal lobe, and substantia nigra [232].

NVC showed 47 replicated genes in both cohorts. The gene *SLC26A5* (Solute Carrier Family 26 Member 5) at 11p15.4 was among the top hits from the gene-based analysis. Mutations in this gene are potential candidates for causing neurosensory deafness[233]. This region is also linked with the development of speech[83]. Another important gene in the list is *RGS10* (Regulator Of G Protein Signaling 10) which is known to be implicated in neurodegenerative diseases [234].

Top significant genes for RI were associated with migraine, sensorineural deafness, cognition, Williams-Beuren syndrome and ASD such as *NLPR3* [215], *GNG2* [216]and *NSUN5* [217].

The top three most significant hits from IQ gene analysis were the genes *S100A3, S100A4*, and *S100A5*. Gene products of *S100A5* are known to be expressed in the cerebral cortex and hippocampus, which are important brain regions in ASD [235].

Although we selected a conservative approach for selecting the gene list, we found that several genes mapped from GWAS hits of the combined cohort were found at the gene level. This validates the findings of our study and provides grounds for focusing on these genes further with respect to these subdomains of ASD phenotypes.

Enrichment of distinctive pathways in ASD subdomains

To further identify the biological function of the enriched genes for each subdomain, we used MAGNET to perform GO-term and pathway enrichment analysis. The analysis identified "sensory perception" as one of the most significant pathways for SI. Atypicalities in sensory processing were found in families which had higher genetic liability for ASD [236]. For JA we identified that the topmost significant GO-term "chromatin modification" is enriched for ASD genes [237]. The most significant GO-term for PI is "hormone processing". Studies have shown that various hormones and hormone-like substances like neurotransmitters, e.g. serotonin and dopamine, can facilitate the regulation of different social behaviors in the developing brain [238]. The top GO-terms for NVC are related to protein ubiquitination and localization. Alterations in protein synthesis and changes in the ubiquitin-proteasome system could contribute to different symptom domains of ASD [239]. For RB we identified that the topmost significant GO-term is "skeletal muscle development". Studies have shown that a variety of biomarkers in skeletal muscle has been focused in view of bioenergetic deficiency in ASD children [240]. A study identified 72% of mitochondrial depletion in skeletal muscle of an ASD individual (Legido et al. 2013). For RI we found that the significant GO-terms include MAPKKK pathway, which is a module of MAPK and has been implicated in idiopathic ASD (pertaining to an unknown cause) [241].

Identification of specific spatio-temporal patterns in the brain for NVC, RB, and IQ

At the gene-expression network level, we found two co-regulated gene networks previously identified to be implicated in human brain development, namely Kang module 6 and 27. These modules are enriched for genes associated with SI and NVC, respectively.

The SI module 6 is active prior to birth and remains active during early childhood cortical development, as well as during prenatal and pubertal hippocampal development. This is in line with findings of early cortical maturation impairments in ASD [242]. An interesting pattern is observed specifically between ~5-13 years of age showing down-regulation of gene expression in the hippocampus, a time period associated with children adapting/learning externalizing behavior. Moreover, the hippocampus is known to play a profound role in social interaction [243].

The NVC-associated regulatory gene-set (module 27) is throughout expressed until puberty in the hippocampus, striatum and mediodorsal nucleus of the thalamus. These regions are well known for their role in language and communication [244,245]. Mild activation is observed ubiquitously already after birth in the frontal cortex. Overall, we observe a pattern that is more prominent starting from birth up to 3-4 years of age, an age range where children are developing language skills and communicate mostly in non-verbal gestures. We particularly see a higher expression in OFC (orbitofrontal cortex), DFC (dorsolateral prefrontal cortex), IPC (inferior parietal cortex), STC (superior temporal cortex) and hippocampus specifically in this age range.

The enriched modules for IQ, i.e. module 4 and 14 show specific up-regulation patterns during the developmental time period of 5.5.-13.5 years of age in all parts of the brain. Moreover, the enriched IQ genes *TYROPB* (TYRO Protein Tyrosine Kinase Binding Protein), and *CX3CR1* (C-X3-C Motif Chemokine Receptor 1) show increased expression in the pre-frontal cortex in post-mortem brain tissue of autistic individuals [246].

As ASD is categorized as an early childhood disorder, knowing the spatio-temporal pattern of associated genes that might be involved in a particular phenotypic construct can help to provide interventions at an early stage. Thus, MAGNET can assist researchers who are interested in a specific neuropsychiatric trait to have an overview of the enriched brain expressed gene modules and their spatio-temporal pattern.

Is the phenotypic variance of individual subdomains explained by common variants?

At the genetic level, we specifically looked at the common variants as they are known to play an important role in ASD liability. The SNP-based heritability h^2_{SNP} has been previously studied in large ASD samples to identify the additive heritability explained by genome-wide SNPs [76]. We found that h^2_{SNP} for all subdomains was higher than previously reported estimates in ASD (~17%) [203]. This indicates a strong role of common variation in the phenotypic expression of the ADI-R derived subdomains, and reduced genetic heterogeneity compared to the categorical diagnosis. SI showed the highest h^2_{SNP}, and the second-highest was observed for RI. We observe that the SNP-based heritability estimates from individual subdomains can play an important role in explaining the variance by common variants. Since the common variation-based heritability of RB was the lowest, we further suggest rare variants to be involved in modulating the phenotypic presentation of this subdomain. Although the studies focusing on rare genetic variants agree that an increased genetic burden for rare variants in ASD is associated with increased severity[119], a direct association with RB is lacking. Our study is the first to identify SNP-based heritability of dimensional ASD subdomains and thus highlights that characterizing ASD domains into subdomains can reduce genetic heterogeneity.

Genetic correlation between subdomains partially reflects phenotypic domains

To test whether it is equally likely that the same set of genotypic variation responsible for a particular phenotype is also contributing to the appearance of another phenotype, we performed genetic correlation analysis among the subdomains. We aimed at identifying if the two diagnostic domains of ASD are independent of each other or interconnected at the genetic level. For this purpose we determined the genetic correlation r_g of individual subdomains to identify if the subdomains related to domain A overlap with subdomains of domain B and vice versa.

The genetic correlation r_g across the subdomains identified that SI and NVC are highly correlated (0.97), which also confirms previous observations at phenotypic levels [247]. This genetic correlation reflects the fact that non-verbal skills represent important aspects of everyday social interaction, which are a prerequisite for adequate psychosocial adjustment [248,249], and thus both behavioral dimensions are modulated by the same genetic variants.

A complete genetic correlation of 1 was found for JA and PI, which shows that there is a strong overlap of common genetic variation underlying JA and PI.

The genetic correlation analysis of the two subdomains related to domain B showed only weak correlation and thus may be genetically independent with respect to common variation. Previous studies have also shown evidence of only a few overlapping linkage findings of the two subdomains of domain B derived from ADI-R algorithm, i.e. “repetitive sensory-motor behavior” (RSMB) and “insistence on sameness”.[250]. We also identified that RB did not correlate genetically with any other subdomain suggesting that the genetic mechanism behind RB is independent. There are contradictory studies suggesting that no genetic covariation was found between SI and RB scores[78] to a strong genetic overlap of the extreme values of impaired social communication and restricted behaviors derived from SCQ in a twin-based study[251]. The differential role of common and rare variation in domain A subdomains and RB in ASD individuals might be responsible for these contrasting findings since rare variation might be playing a stronger role in RB[252].

Polygenic risk of ASD

Given our finding that the genetic risk for the individual subdomains is only partially correlated, the polygenic risk score for ASD only explained small proportions of variance in subdomains. However, the highest genetic correlation of the ASD-PRS was seen for SI and RI, suggesting that the PRS captures both domains A and B related subdomains but might miss some of the genetic risk underlying other phenotypically relevant domains. Thus, we suggest that the PRS for ASD should be investigated to improve its validity at subdomains’ level.

4. Conclusion and outlook

In this work, we present an integrative bioinformatics framework designed for researchers with minimal expertise in working with computational tools and handling big data. MAGNET streamlines the methods for performing and interpreting GWAS and mapping these findings to the human developing brain by integrating brain transcriptome data. MAGNET is a combination of state-of-the-art tools, providing a detailed workflow of the QC, GWAS and post-GWAS steps with standardized thresholds for each process within one shell. Further, to deduce more insight into the trait of interest, MAGNET provides information regarding the brain regions and time where the trait-associated genes are expressed. To overcome the challenges faced by big data MAGNET is equipped with data parsing, data parallelization assuring the quality of the data. Thus, this will help researchers to spend less time and effort in the compilation of various tools and data handling processes and can assist them to gather a meaningful interpretation of a neuropsychological trait of interest.

MAGNET performs data integration from three different levels, i.e. phenotype, genotype, and transcriptome levels. It can aid in identifying genes and mechanisms in neuropsychiatric genetics and in generating new research hypotheses. Such frameworks can help to develop personalized medicine-based approaches by understanding the genetic underpinnings of disorder-related phenotypes.

This framework is designed to be applied to any neuropsychiatric disorder with a phenotypic trait of high heritability. As a proof of concept, we applied it to six subdomains/traits from two ASD cohorts, as well as on the trait IQ from the German cohort for demonstration of computational time required at each step. The framework helped to bridge the gap between the genotypic etiology and the phenotypic observations. The identified genes and gene networks revealed new genetic variants and also confirmed genetic associations already known from other studies, investigating these subdomains and neuropsychiatric disorders. Moreover, we showed the regulatory gene expression patterns of the gene-sets associated with these subdomains. This could help in a follow-on study to investigate the detailed molecular basis of the ASD subdomains classified as SI, JA, PI, NVC, RB, and RI as well as to look at the enriched brain regions and time frames.

We showed the effective time and memory usage required by each process of the framework. We outline that the time needed to assemble the results from multiple tools and to then convert the outputs into respective formats can be significantly minimized by providing one single framework, which manages the output from each tool and processes it for the next step, so the user can avoid the in-between cumbersome steps. We provide an in-depth analysis of traits of interest within a time frame of 4-5 days to foster the identification of relevant associated genes and their expression in developing human brain directly. Moreover, the modular structure of the framework makes it easily applicable, transparent and user-friendly.

Implementation of MAGNET on the quantitative ASD traits/subdomains suggested that the genetic architecture of subdomains is distinct between domain A- and B-related subdomains. Moreover, it also varies between the two subdomains (RB, RI) of domain B. We identified several new genome-wide hits and replicated previous findings, thus adding credibility to the functioning of MAGNET. Additionally, the biological pathways and gene expression patterns provided evidence that the phenotypic variability in ASD traits encompasses pathways related to neuronal development, which include brain regions such as the hippocampus, amygdala, and cortex. Further exploring the underlying genetic etiology and to answer the biological questions behind ASD subdomains, the polygenic risk score for ASD was calculated. This analysis showed that the common variants can explain relatively higher ASD risk when analysed separately in homogenous subdomains.

The results of our study have to be replicated in larger samples with different ethnic populations. In addition, a combined analysis of common and rare variants may clarify the specific role of common variants in shaping the ASD phenotype in relation to the reported subdomains. Moreover, the time and memory required to run MAGNET can still be minimized by integrating more parallel computing codes. With the upgraded versions of SNP and genome builds available, MAGNET reference files are required to be updated. We further plan to deploy MAGNET as an application with all libraries and dependencies as one package that could be used on any Linux platform irrespective of the customized settings defined by the user. This would reduce the size constraints and increase the performance of MAGNET.

5. Appendix

5.1. Genetic terminologies

Genotype: The difference among individuals based on DNA (Deoxyribonucleotide acid) sequence variation within a population defines the variation at the genetic level. The individual's genetic sequence is also defined as the genotype. These genetic variations can be modulators of a particular trait (also called phenotype). Genetic variations are thus possible risk factors contributing to complex diseases.

Penetrance: Another important term is penetrance which refers to the effect of a variant onto the expression of a phenotype[14]. The magnitude of the effect of an allele on a phenotype is termed as the effect size. Figure 1 shows these key concepts in detail.

Heritability: A fundamental concept in genetics is heritability which is the proportion of phenotypic variability that is attributable to genetic factors, large heritability estimates indicate that the genetic variability has more influence on the variability of a given trait in the population [15].

Minor allele frequency: Genetic variations can be classified by frequency in the population and or type of variation. The most frequent allele of a variant is defined as the **major allele** and the other(s) as the **minor allele**. The minor allele frequency (MAF) is the second most frequent allele.

Common and rare variants: Common variants are defined based on the MAF between 0.01–0.05 and higher. Rare variants are defined with a MAF < 0.01 [16]. Though rare variants have a small effect size but are found to increase genetic liability and clinical presentation of neurodevelopmental disorders such as ASD. Common variants contribute significantly to the genetics of ASD, although the identification of individual risk polymorphisms is still not clear due to their small effect sizes and limited sample sizes available for association studies [1]. More details about the MAF calculation are explained in 2.6.3.

Locus and allele: The position on a chromosome where a genetic marker is located is called **locus** and the different version of the same genetic variant on a chromosome is termed an **allele**. For example in Mendelian diseases like Huntington's, one rare mutation of the single gene *HTT* (Huntingtin) is responsible for the disease (high penetrance). However, associations of rare variants with small effect sizes are very hard to detect. Thus, in current GWAS common variants with modest effect sizes can be identified which, however, can not completely account for the phenotype risk. For variants with very low allele frequency, it is difficult to find enough cases and get significant associations.

SNVs and CNVs: With respect to type, variants can be classified as single nucleotide variation (SNVs) and structural copy number variations (CNVs). The umbrella term SNV considers changes of a single nucleotide, i.e. A (Adenine), T (Thymine), C (Cytosine), or G (Guanine) irrespective of their frequency in a population. A possible estimate of human genes containing at least one SNVs is between 81% [17]-93% [18]. The most prominent SNVs are single nucleotide polymorphisms (SNP). The 1000 genomes project [19] has made available 88 million variants (84.7 million single nucleotide polymorphisms (SNPs), 3.6 million short insertions/deletions (indels), and 60,000 structural variants) in their dataset with 26 different populations across Africa, Asia, Europe, and America [19].

SNPs: The most frequent type of genetic variation in the human genome and are important genetic markers identified which contribute to phenotypic diversity. In general, if at least 1% of a population harbors the same nucleotide variation, then this SNV is assigned as a SNP. There are ~15 million SNPs currently annotated in the human genome [20]. SNPs have served as genetic markers in complex genetic disorders [21], such as for ASD [22], breast cancer [23]; Crohn's disease [24], type-II diabetes mellitus [25], and SZ [26].

Heterozygosity: Carrying two different alleles of a specific SNP, the rate of heterozygosity can explain the proportion of heterozygous genotypes. Since our focus is on the common variation we considered only common SNPs for our study. CNVs describe genomic alterations with an abnormal number of copies of one or more genes, which is varying among individuals. CNVs are DNA segments with a size > 1kb (kilobase) 27 and can occur as insertions, transpositions, or deletions. Moreover, CNVs contain more nucleotides per genome than the total number of SNPs. Like SNPs, certain CNVs have been associated with disease susceptibility and are strongly implicated in, ASD [28], BD [29], SZ [30] and breast cancer [31]

5.2. Genotype file formats

Following is a detailed description of how each file appears, their respective columns and data types:

5.2.1. PLINK ped and map files

i. ped file: The pedigree file contains the individuals and the genetic data arranged in columns without headers as below. The file can be space or tab-separated, where each line corresponds to a single individual. The first 6 columns represent the phenotype information and data type for each column are also mentioned:

1. Family ID [string]: Alphanumeric identifier representing an individual’s family. This identifier is specific to all individuals in a family.
2. Individual ID [string]: Alphanumeric identifier representing individual, which should be unique in that family.
3. Paternal ID [string]: Alphanumeric identifier representing an individual’s father; 0 if “not known”.
4. Maternal ID [string]: Alphanumeric identifier representing an individual’s mother; 0 if “not known”.
5. Gender [integer]: Gender is encoded as 1 or 2, where 1 indicates a male and 2 represents a female and 0/-9 indicates not known.

6. Affection status [integer]: Affected individuals are mostly represented as 2 while unaffected as 1. 0/ -9 indicate an unknown status.
7. Columns after column number 6 represent the genotype information.
8. Genotypes: Each SNP carries two alleles which are represented in two columns, e.g. column 7 and 8 code for SNP 1, then column 9 and 10 code for SNP 2 and so on. Missing data is coded as 0.
9. Two columns represent one SNP so the total number of columns for PED file varies depending on the number of SNPs. So if the number of SNPs is ***k*** then the number of genotype columns is k*2. The total number of columns in ped files = k*2+6 (phenotype).

ii. **map file:** The file contains SNP information arranged as follows:

1. Chromosome [integer]: Chromosome number for the respective SNP.
2. Marker ID [string]: Name of the SNP, usually an rs id.
3. Genetic distance [float]: Genetic distance from previous SNP, unit is centimorgan (cM).
4. Physical position [integer]: Physical position of SNP in base pair (bp).

This file should have ***n*** lines and 4 columns, where ***n*** is the number of SNPs contained in the dataset. Each SNP must have a unique physical position. All the SNPs must be ordered by physical position.

5.2.2. PLINK bed, bim and fam files

These files contain the same information as PLINK flat files but are compressed and more efficient to work with.

i. **bed:** This file is encoded in binary format and is in a machine-readable format. The file includes information on the SNP for each individual.

ii. **bim:** This file is similar to a map file but includes allele information for each marker. The first four columns are the same, i.e. a chromosome number, marker id, genetic distance, and physical position. The four columns are followed by a column for allele 1 and one for allele 2.

iii. **fam:** This file corresponds to the first six columns of the ped file.

5.3. Statistical terms

5.3.1. Fisher's exact test

It is a test of significance which tests for two categorical variables if the proportions of one variable differ from the other. The following equation is implemented to obtain the probability of combination of frequencies:

$$p = ((a + b)!\,(c + d)!\,(a + c)!\,(b + d)!)/a!\,b!\,c!\,d!\,N!,$$

where a, b, c, and d are the individual frequencies of the 2X2 contingency table, and N is the total frequency.

5.3.2. Benjamini-Hochberg correction

Benjamini-Hochberg (BH) is a p-value adjustment method to decrease the false discovery rate (FDR) for multiple hypothesis testing. Adjusting this rate could help to reduce the possibility of chance findings. The method first orders the ***m*** hypothesis by ascending p-values, ***P_i*** is the p-value at the ***ith*** position with the associated hypothesis ***H_i*** . Assuming ***k*** is the largest *i* then $P_i \leq \frac{i}{m}q$. Benjamini Hochberg controls the FDR for all tests at a level of ***q***.

5.4. Supplementary figure

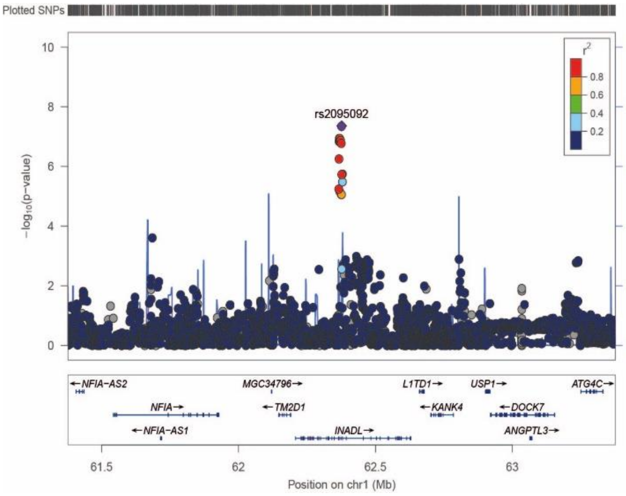

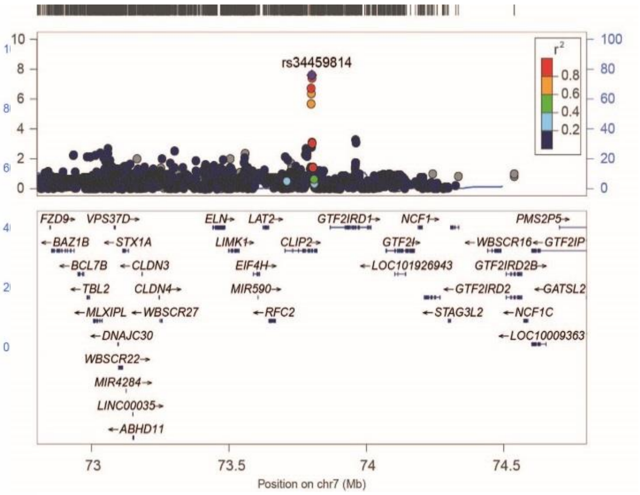

SI_Peak 1 SI_Peak 2

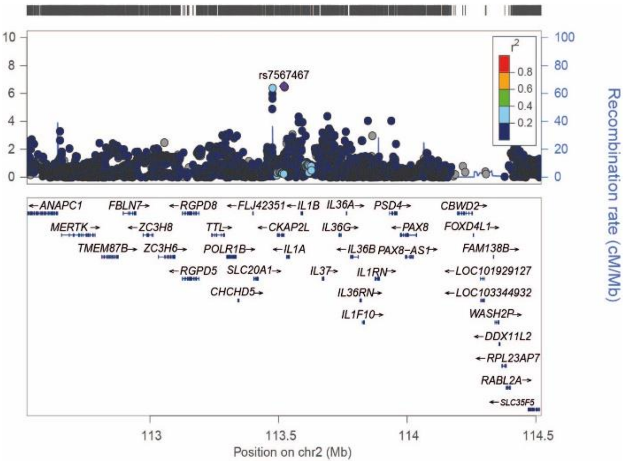

SI_Peak 3

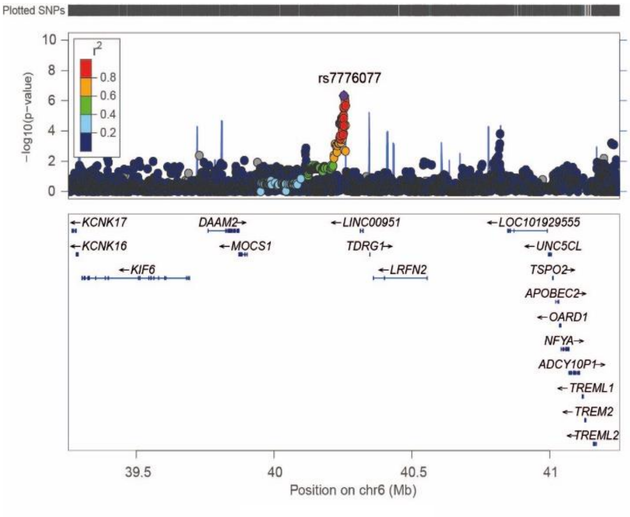

JA_Peak 1

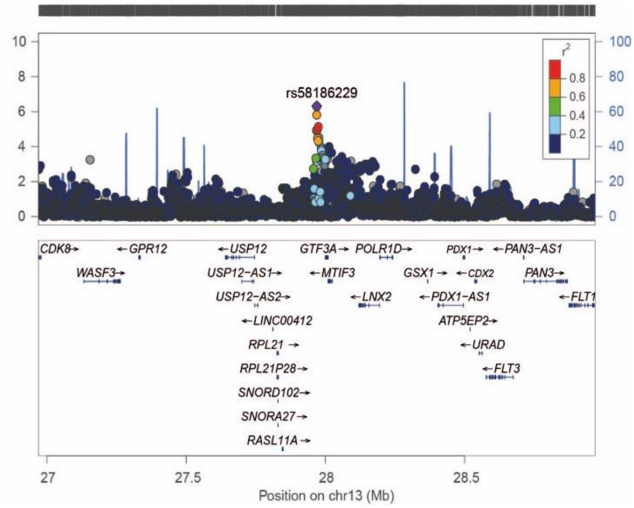

JA_Peak 2

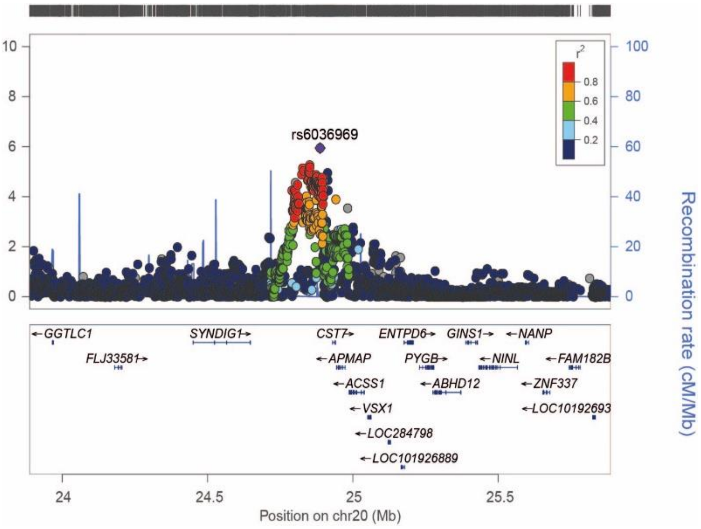

JA_Peak 3

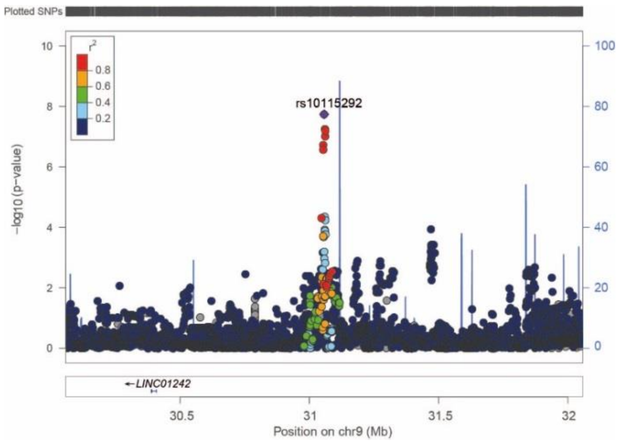

PI_Peak 1

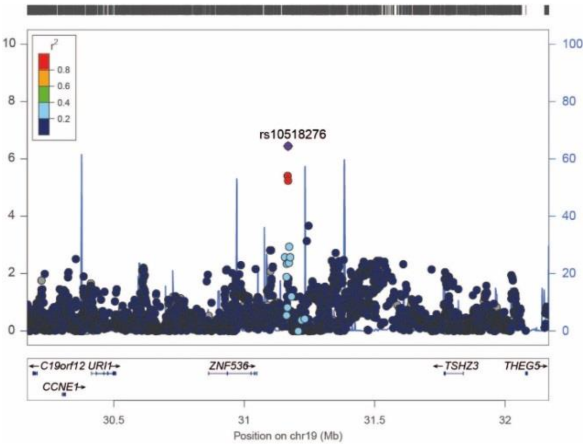

PI_Peak 2

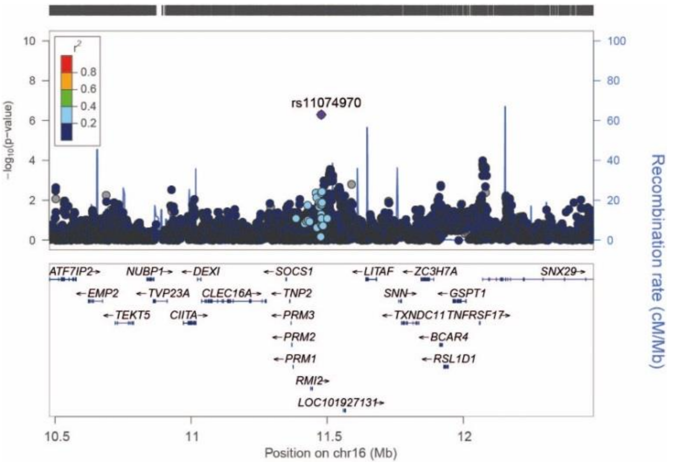

PI_Peak 3

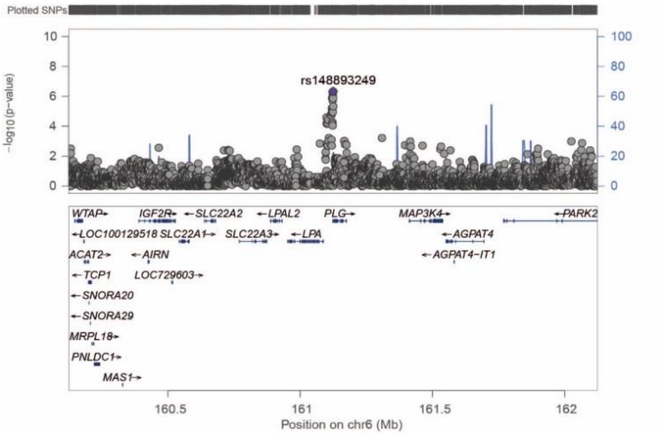

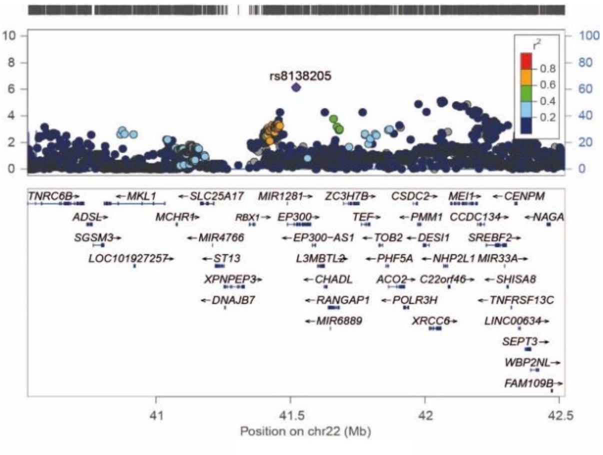

NVC_Peak **NVC_Peak**

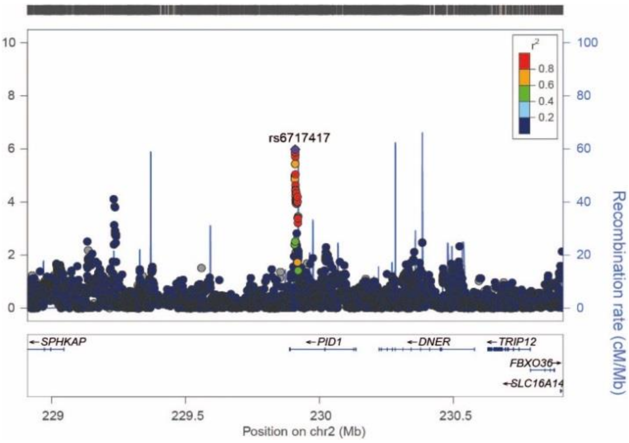

NVC_Peak

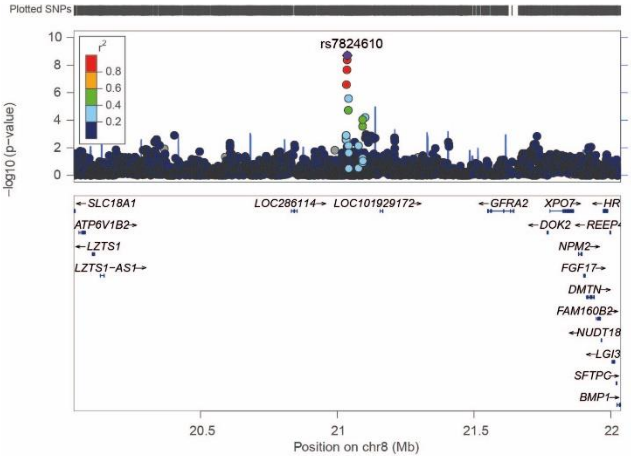

RB_Peak 1

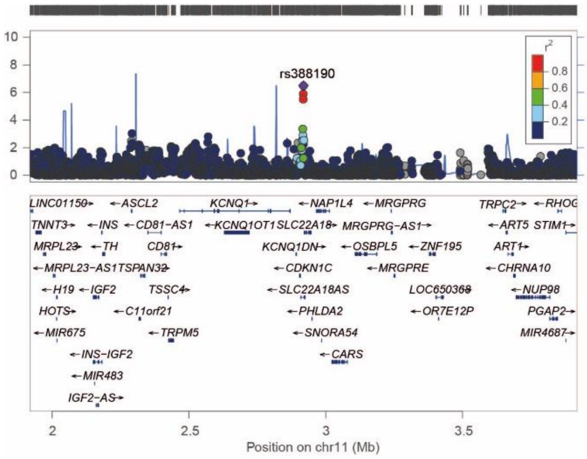

RB_Peak 2

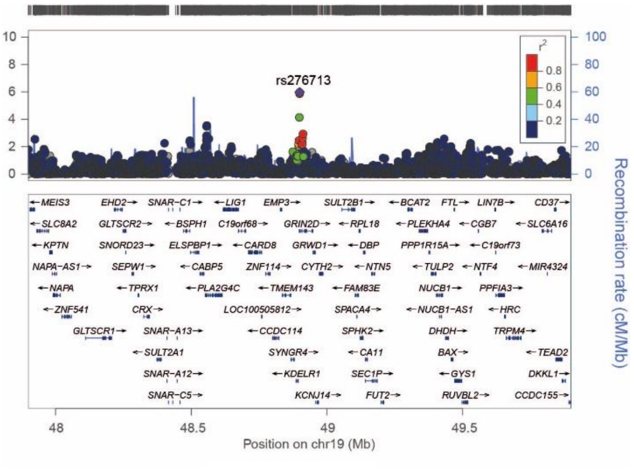

RB_Peak 3

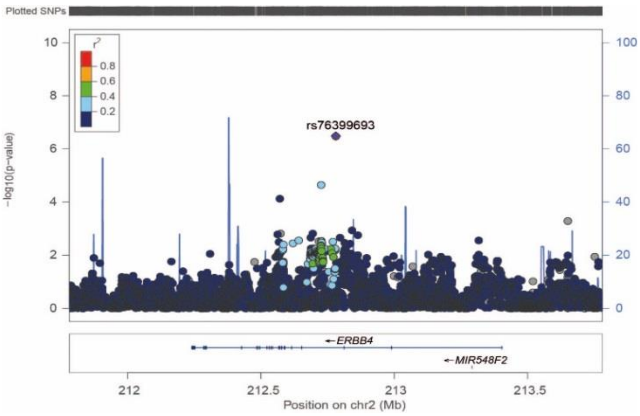

RI_Peak 1

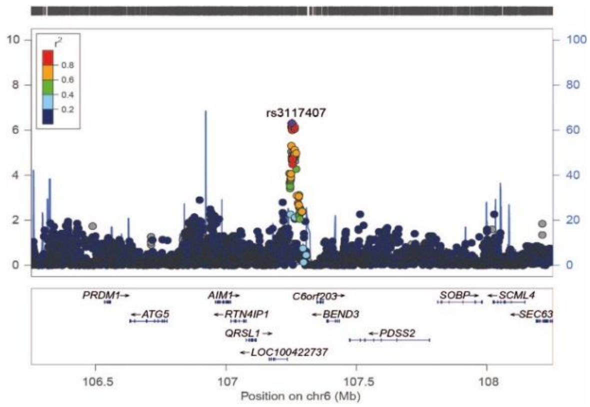

RI_Peak 2

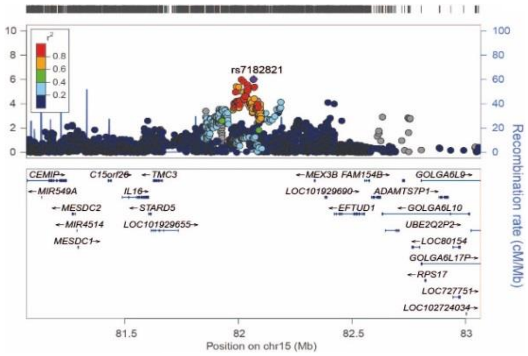

RI_Peak 3

Supplementary Figure 1: Locus plots of top three peaks for each subdomain from the combined cohort

Abbreviations: SI: Social Interaction; JA: Joint Attention; PI: Peer Interaction; NVC: Non-verbal Communication; RB: Repetitive sensory-motor Behavior; RI: Restricted Interest. The plot shows the genes in the region with there locations shown at the bottom, the SNP positions are shown at the top and the regional associations from GWAS are shown in the middle. The right axis gives the recombination rate shown as light blue line. The −log10 P values are shown for SNPs distributed in a 0.8-Mb genomic region that is centered where the most strongly associated signal is found, here shown as a purple diamond.

6. References

1 Torrico B, Chiocchetti AG, Bacchelli E, Trabetti E, Hervas A, Franke B *et al.* Lack of replication of previous autism spectrum disorder GWAS hits in European populations. *Autism Research* 2016.

2 Chiocchetti AG, Yousaf A, Bour HS, Haslinger D, Waltes R, Duketis E *et al.* Common functional variants of the glutamatergic system in Autism spectrum disorder with high and low intellectual abilities. *Journal of Neural Transmission (Vienna, Austria 1996)* 2018; **125**: 259–271.

3 Haslinger D, Waltes R, Yousaf A, Lindlar S, Schneider I, Lim CK *et al.* Loss of the Chr16p11.2 ASD candidate gene QPRT leads to aberrant neuronal differentiation in the SH-SY5Y neuronal cell model. *Molecular Autism* 2018; **9**: 56.

4 Kang HJ, Kawasawa YI, Cheng F, Zhu Y, Xu X, Li M *et al.* Spatio-temporal transcriptome of the human brain. *Nature* 2011; **478**: 483–489.

5 Barnett JH, Smoller JW. The genetics of bipolar disorder. *Neuroscience* 2009; **164**: 331–343.

6 Faraone SV, Larsson H. Genetics of attention deficit hyperactivity disorder. *Molecular Psychiatry* 2019; **24**: 562–575.

7 Hilker R, Helenius D, Fagerlund B, Skytthe A, Christensen K, Werge TM et al. Heritability of Schizophrenia and Schizophrenia Spectrum Based on the Nationwide Danish Twin Register. Biological Psychiatry 2018; 83: 492–498.

8 Sandin S, Lichtenstein P, Kuja-Halkola R, Hultman C, Larsson H, Reichenberg A. The Heritability of Autism Spectrum Disorder. JAMA 2017; 318: 1182–1184.

9 Gondro C, Porto-Neto LR, Lee SH. SNPQC—an R pipeline for quality control of Illumina SNP genotyping array data. Animal Genetics 2014; 45: 758–761.

10 Hibar DP, Stein JL, Renteria ME, Arias-Vasquez A, Desrivières S, Jahanshad N et al. Common genetic variants influence human subcortical brain structures. Nature 2015; 520: 224–229.

11 Kanterakis A, Deelen P, van Dijk F, Byelas H, Dijkstra M, Swertz MA. Molgenis-impute: Imputation pipeline in a box. BMC Research Notes 2015; 8: 359.

12 Muñiz-Fernandez F, Carreño-Torres A, Morcillo-Suarez C, Navarro A. Genome-wide association studies pipeline (GWASpi): A desktop application for genome-wide SNP analysis and management. Bioinformatics (Oxford, England) 2011; 27: 1871–1872.

13 Ripke S, Thomas B. Ricopili: Tool for visualizing regions of interest in selected GWAS data sets., 2011. https://data.broadinstitute.org/mpg/ricopili/ (accessed 8 Mar 2018).

14 Emery and Rimoin's principles and practice of medical genetics and genomics: Foundations. Academic Press is an imprint of Elsevier: London, U.K, 2019.

15 Principles and practice of sleep medicine. Elsevier: Philadelphia, PA, 2017.

16 Lee H-S, Kim Y, Park T. New Common and Rare Variants Influencing Metabolic Syndrome and Its Individual Components in a Korean Population. Scientific Reports 2018; 8: 5701.

17 Lehne B, Lewis CM, Schlitt T. From SNPs to genes: disease association at the gene level. PLoS ONE 2011; 6: e20133.

18 Chakravarti A. To a future of genetic medicine. Nature 2001; 409: 822–823.

19 Auton A, Brooks LD, Durbin RM, Garrison EP, Kang HM, Korbel JO et al. A global reference for human genetic variation. Nature 2015; 526: 68–74.

20 Botstein D, Risch N. Discovering genotypes underlying human phenotypes: past successes for mendelian disease, future approaches for complex disease. Nature Genetics 2003; 33 Suppl: 228–237.

21 Cantor CR. The use of genetic SNPs as new diagnostic markers in preventive medicine. Annals of the New York Academy of Sciences 2005; 1055: 48–57.

22 Jiao Y, Chen R, Ke X, Cheng L, Chu K, Lu Z et al. Single nucleotide polymorphisms predict symptom severity of autism spectrum disorder. Journal of Autism and Developmental Disorders 2012; 42: 971–983.

23 Yang Y, Wang W, Liu G, Yu Y, Liao M. Association of single nucleotide polymorphism rs3803662 with the risk of breast cancer. Scientific Reports 2016; 6: 29008.

24 Franke A, McGovern DPB, Barrett JC, Wang K, Radford-Smith GL, Ahmad T et al. Genome-wide meta-analysis increases to 71 the number of confirmed Crohn's disease susceptibility loci. Nature Genetics 2010; 42: 1118–1125.

25 Flannick J, Florez JC. Type 2 diabetes: genetic data sharing to advance complex disease research. Nature Reviews. Genetics 2016; 17: 535–549.

26 Purcell SM, Wray NR, Stone JL, Visscher PM, O'Donovan MC, Sullivan PF et al. Common polygenic variation contributes to risk of schizophrenia and bipolar disorder. Nature 2009; 460: 748–752.

27 Feuk L, Carson AR, Scherer SW. Structural variation in the human genome. Nature Reviews. Genetics 2006; 7: 85–97.

28 Marshall CR, Noor A, Vincent JB, Lionel AC, Feuk L, Skaug J et al. Structural variation of chromosomes in autism spectrum disorder. American Journal of Human Genetics 2008; 82: 477–488.

29 Green EK, Rees E, Walters JTR, Smith K-G, Forty L, Grozeva D et al. Copy number variation in bipolar disorder. Molecular Psychiatry 2016; 21: 89–93.

30 Marshall CR, Howrigan DP, Merico D, Thiruvahindrapuram B, Wu W, Greer DS et al. Contribution of copy number variants to schizophrenia from a genome-wide study of 41,321 subjects, 49.

31 Kumaran M, Cass CE, Graham K, Mackey JR, Hubaux R, Lam W et al. Germline copy number variations are associated with breast cancer risk and prognosis. Scientific Reports 2017; 7: 14621.

32 Constantino JN, Todd RD. Autistic traits in the general population: A twin study. Archives of General Psychiatry 2003; 60: 524–530.

33 Ronald A, Hoekstra RA. Autism spectrum disorders and autistic traits: A decade of new twin studies. American journal of medical genetics. Part B, Neuropsychiatric genetics the official publication of the International Society of Psychiatric Genetics 2011; 156: 255–274.

34 Bölte S, Poustka F. Diagnostische Beobachtungsskala für Autistische Störungen (ADOS): Erste Ergebnisse zur Zuverlässigkeit und Gültigkeit. Zeitschrift für Kinder- und Jugendpsychiatrie und Psychotherapie 2004; 32: 45–50.

35 LaFramboise T. Single nucleotide polymorphism arrays: a decade of biological, computational and technological advances. Nucleic Acids Research 2009; 37: 4181–4193.

36 Illumina Inc. SNP genotyping.

37 Gunderson KL, Steemers FJ, Lee G, Mendoza LG, Chee MS. A genome-wide scalable SNP genotyping assay using microarray technology. Nature Genetics 2005; 37: 549–554.

38 Bush WS, Moore JH. Chapter 11: Genome-wide association studies. PLoS Computational Biology 2012; 8: e1002822.

39 Kermani BG. Artificial intelligence and global normalization methods for genotyping(20060224529).

40 Teo YY, Inouye M, Small KS, Gwilliam R, Deloukas P, Kwiatkowski DP et al. A genotype calling algorithm for the Illumina BeadArray platform. Bioinformatics (Oxford, England) 2007; 23: 2741–2746.

41 Kumar S, Banks TW, Cloutier S. SNP Discovery through Next-Generation Sequencing and Its Applications. International Journal of Plant Genomics 2012; 2012: 831460.

42 Nielsen R, Paul JS, Albrechtsen A, Song YS. Genotype and SNP calling from next-generation sequencing data. Nature reviews. Genetics 2011; 12: 443–451.

43 Ritchie ME, Phipson B, Di Wu, Hu Y, Law CW, Shi W et al. limma powers differential expression analyses for RNA-sequencing and microarray studies. Nucleic Acids Research 2015; 43: e47.

44 Amin SB, Shah PK, Yan A, Adamia S, Minvielle S, Avet-Loiseau H et al. The dChip survival analysis module for microarray data. BMC Bioinformatics 2011; 12: 72.

45 Eijssen LMT, Jaillard M, Adriaens ME, Gaj S, Groot PJ de, Müller M et al. User-friendly solutions for microarray quality control and pre-processing on ArrayAnalysis.org. Nucleic Acids Research 2013; 41: W71-6.

46 Emig D, Salomonis N, Baumbach J, Lengauer T, Conklin BR, Albrecht M. AltAnalyze and DomainGraph: analyzing and visualizing exon expression data. Nucleic Acids Research 2010; 38: W755-62.

47 Xu G, Strathearn L, Liu B, Bao W. Prevalence of Autism Spectrum Disorder Among US Children and Adolescents, 2014-2016. JAMA 2018; 319: 81–82.

48 Elsabbagh M, Divan G, Koh Y-J, Kim YS, Kauchali S, Marcín C et al. Global prevalence of autism and other pervasive developmental disorders. Autism research official journal of the International Society for Autism Research 2012; 5: 160–179.

49 Lord C, Rutter M, Le Couteur A. Autism Diagnostic Interview-Revised: A revised version of a diagnostic interview for caregivers of individuals with possible pervasive developmental disorders. Journal of Autism and Developmental Disorders 1994; 24: 659–685.

50 World Health Organization. ICD-10: international statistical classification of diseases and related health problems: 10th revision: Geneva, 1992.

51 GUZE SB. Diagnostic and Statistical Manual of Mental Disorders, 4th ed. (DSM-IV), 152, 1995.

52 Kim SH, Thurm A, Shumway S, Lord C. Multisite study of new autism diagnostic interview-revised (ADI-R) algorithms for toddlers and young preschoolers. Journal of Autism and Developmental Disorders 2013; 43: 1527–1538.

53 Lord C, Rutter M, Goode S, Heemsbergen J, Jordan H, Mawhood L et al. Autism diagnostic observation schedule: a standardized observation of communicative and social behavior. Journal of Autism and Developmental Disorders 1989; 19: 185–212.

54 Bailey A, Le Couteur A, Gottesman I, Bolton P, Simonoff E, Yuzda E et al. Autism as a strongly genetic disorder: evidence from a British twin study. Psychological Medicine 1995; 25: 63–77.

55 Tick B, Bolton P, Happé F, Rutter M, Rijsdijk F. Heritability of autism spectrum disorders: A meta-analysis of twin studies. Journal of Child Psychology and Psychiatry 2016; 57: 585–595.

56 Bai D, Yip BHK, Windham GC, Sourander A, Francis R, Yoffe R et al. Association of Genetic and Environmental Factors With Autism in a 5-Country Cohort. JAMA psychiatry 2019.

57 Grove J, Ripke S, Als TD, Mattheisen M, Walters RK, Won H et al. Identification of common genetic risk variants for autism spectrum disorder. Nature Genetics 2019; 51: 431–444.

58 Leblond CS, Cliquet F, Carton C, Huguet G, Mathieu A, Kergrohen T et al. Both rare and common genetic variants contribute to autism in the Faroe Islands. NPJ Genomic Medicine 2019; 4: 1.

59 Huguet G, Bourgeron T. Genetic Causes of Autism Spectrum Disorders.

60 Bourgeron T. From the genetic architecture to synaptic plasticity in autism spectrum disorder. Nature reviews. Neuroscience 2015; 16: 551–563.

61 Sun H-Y, Ji F-Q, Fu L-Y, Wang Z-Y, Zhang H-Y. Structural and energetic analyses of SNPs in drug targets and implications for drug therapy. Journal of Chemical Information and Modeling 2013; 53: 3343–3351.

62 Gaugler T, Klei L, Sanders SJ, Bodea CA, Goldberg AP, Lee AB et al. Most genetic risk for autism resides with common variation. Nature Genetics 2014; 46: 881–885.

63 Sayad A, Noroozi R, Omrani MD, Taheri M, Ghafouri-Fard S. Retinoic acid-related orphan receptor alpha (RORA) variants are associated with autism spectrum disorder. Metabolic Brain Disease 2017; 32: 1595–1601.

64 Freitag CM, Staal W, Klauck SM, Duketis E, Waltes R. Genetics of autistic disorders: Review and clinical implications. European Child & Adolescent Psychiatry 2010; 19: 169–178.

65 Toma C, Pierce KD, Shaw AD, Heath A, Mitchell PB, Schofield PR et al. Comprehensive cross-disorder analyses of CNTNAP2 suggest it is unlikely to be a primary risk gene for psychiatric disorders. PLoS Genetics 2018; 14: e1007535.

66 Chiocchetti AG, Kopp M, Waltes R, Haslinger D, Duketis E, Jarczok TA et al. Variants of the CNTNAP2 5′ promoter as risk factors for autism spectrum disorders: a genetic and functional approach. Molecular Psychiatry 2015; 20: 839–849.

67 Noroozi R, Taheri M, Ghafouri-Fard S, Bidel Z, Omrani MD, Moghaddam AS et al. Meta-analysis of GABRB3 Gene Polymorphisms and Susceptibility to Autism Spectrum Disorder. Journal of Molecular Neuroscience MN 2018; 65: 432–437.

68 Sanders SJ, Ercan-Sencicek AG, Hus V, Luo R, Murtha MT, Moreno-De-Luca D et al. Multiple recurrent de novo CNVs, including duplications of the 7q11.23 Williams syndrome region, are strongly associated with autism. Neuron 2011; 70: 863–885.

69 Morrow EM, Yoo S-Y, Flavell SW, Kim T-K, Lin Y, Hill RS et al. Identifying autism loci and genes by tracing recent shared ancestry. Science (New York, N.Y.) 2008; 321: 218–223.

70 Xu J, Zwaigenbaum L, Szatmari P, Scherer S. Molecular Cytogenetics of Autism. CG 2004; 5: 347–364.

71 Sebat J, Lakshmi B, Malhotra D, Troge J, Lese-Martin C, Walsh T et al. Strong association of de novo copy number mutations with autism. Science (New York, N.Y.) 2007; 316: 445–449.

72 Glessner JT, Wang K, Cai G, Korvatska O, Kim CE, Wood S et al. Autism genome-wide copy number variation reveals ubiquitin and neuronal genes. Nature 2009; 459: 569–573.

73 Iossifov I, O’Roak BJ, Sanders SJ, Ronemus M, Krumm N, Levy D et al. The contribution of de novo coding mutations to autism spectrum disorder. Nature 2014; 515: 216–221.

74 Ma D, Salyakina D, Jaworski JM, Konidari I, Whitehead PL, Andersen AN et al. A genome-wide association study of autism reveals a common novel risk locus at 5p14.1. Annals of Human Genetics 2009; 73: 263–273.

75 Devlin B, Melhem N, Roeder K. Do common variants play a role in risk for autism? Evidence and theoretical musings. Brain Research 2011; 1380: 78–84.

76 The Autism Spectrum Disorders Working Group of The Psychiatric Genomics Consortium. Meta-analysis of GWAS of over 16,000 individuals with autism spectrum disorder highlights a novel locus at 10q24.32 and a significant overlap with schizophrenia. Molecular Autism 2017; 8: 21.

77 Folstein S, Rutter M. Infantile autism: a genetic study of 21 twin pairs. Journal of Child Psychology and Psychiatry 1977; 18: 297–321.

78 Ronald A, Happé F, Bolton P, Butcher LM, Price TS, Wheelwright S et al. Genetic heterogeneity between the three components of the autism spectrum: a twin study. Journal of the American Academy of Child and Adolescent Psychiatry 2006; 45: 691–699.

79 Ronald A, Happé F, Plomin R. The genetic relationship between individual differences in social and nonsocial behaviours characteristic of autism. Developmental Science 2005; 8: 444–458.

80 Rosenberg RE, Law JK, Yenokyan G, McGready J, Kaufmann WE, Law PA. Characteristics and concordance of autism spectrum disorders among 277 twin pairs. Archives of Pediatrics & Adolescent Medicine 2009; 163: 907–914.

81 Sandin S, Lichtenstein P, Kuja-Halkola R, Larsson H, Hultman CM, Reichenberg A. The familial risk of autism. JAMA 2014; 311: 1770–1777.

82 Morton NE. Logarithm of odds (lods) for linkage in complex inheritance. Proceedings of the National Academy of Sciences of the United States of America 1996; 93: 3471–3476.

83 Liu X-Q, Paterson AD, Szatmari P. Genome-wide linkage analyses of quantitative and categorical autism subphenotypes. Biological Psychiatry 2008; 64: 561–570.

84 Liu X-Q, Georgiades S, Duku E, Thompson A, Devlin B, Cook EH et al. Identification of genetic loci underlying the phenotypic constructs of autism spectrum disorders. Journal of the American Academy of Child and Adolescent Psychiatry 2011; 50: 687-696.e13.

85 Weiss LA, Arking DE, Daly MJ, Chakravarti A. A genome-wide linkage and association scan reveals novel loci for autism. Nature 2009; 461: 802–808.

86 Price AL, Spencer CCA, Donnelly P. Progress and promise in understanding the genetic basis of common diseases. Proceedings. Biological Sciences 2015; 282: 20151684.

87 McCarthy MI, Abecasis GR, Cardon LR, Goldstein DB, Little J, Ioannidis JPA et al. Genome-wide association studies for complex traits: consensus, uncertainty and challenges. Nature Reviews Genetics 2008; 9: 356–369.

88 Benjamini Y, Hochberg Y. Controlling the False Discovery Rate: A Practical and Powerful Approach to Multiple Testing. Journal of the Royal Statistical Society. Series B (Methodological) 1995; 57: 289–300.

89 NEYMAN J, PEARSON ES. ON THE USE AND INTERPRETATION OF CERTAIN TEST CRITERIA FOR PURPOSES OF STATISTICAL INFERENCE PART I. Biometrika 1928; 20A: 175–240.

90 Zhang L, Liu L, Wen Y, Ma M, Cheng S, Yang J et al. Genome-wide association study and identification of chromosomal enhancer maps in multiple brain regions related to autism spectrum disorder. Autism research official journal of the International Society for Autism Research 2019; 12: 26–32.

91 Poelmans G, Franke B, Pauls DL, Glennon JC, Buitelaar JK. AKAPs integrate genetic findings for autism spectrum disorders. Translational Psychiatry 2013; 3: e270.

92 Coon KD, Myers AJ, Craig DW, Webster JA, Pearson JV, Lince DH et al. A high-density whole-genome association study reveals that APOE is the major susceptibility gene for sporadic late-onset Alzheimer’s disease. The Journal of Clinical Psychiatry 2007; 68: 613–618.

93 Fung H-C, Scholz S, Matarin M, Simón-Sánchez J, Hernandez D, Britton A et al. Genome-wide genotyping in Parkinson’s disease and neurologically normal controls: first stage analysis and public release of data. The Lancet. Neurology 2006; 5: 911–916.

94 Matarín M, Brown WM, Scholz S, Simón-Sánchez J, Fung H-C, Hernandez D et al. A genome-wide genotyping study in patients with ischaemic stroke: initial analysis and data release. The Lancet. Neurology 2007; 6: 414–420.

95 Schizophrenia working group of the Psychiatric Genomics Consortium. Biological insights from 108 schizophrenia-associated genetic loci. Nature 2014; 511: 421–427.

96 Wang K, Zhang H, Ma D, Bucan M, Glessner JT, Abrahams BS et al. Common genetic variants on 5p14.1 associate with autism spectrum disorders. Nature 2009; 459: 528–533.

97 Anney R, Klei L, Pinto D, Regan R, Conroy J, Magalhaes TR et al. A genome-wide scan for common alleles affecting risk for autism. Human Molecular Genetics 2010; 19: 4072–4082.

98 Connolly JJ, Glessner JT, Hakonarson H. A genome-wide association study of autism incorporating autism diagnostic interview-revised, autism diagnostic observation schedule, and social responsiveness scale. Child Development 2013; 84: 17–33.

99 Cross-Disorder Group of the Psychiatric Genomics Consortium. Identification of risk loci with shared effects on five major psychiatric disorders: A genome-wide analysis. THE LANCET 2013; 381: 1371–1379.

100 Cantor RM, Navarro L, Won H, Walker RL, Lowe JK, Geschwind DH. ASD restricted and repetitive behaviors associated at 17q21.33: genes prioritized by expression in fetal brains. Molecular Psychiatry 2018; 23: 993–1000.

101 Zarrei M, Macdonald JR, Merico D, Scherer SW. A copy number variation map of the human genome. Nature reviews. Genetics 2015; 16: 172–183.

102 Pinto D, Darvishi K, Shi X, Rajan D, Rigler D, Fitzgerald T et al. Comprehensive assessment of array-based platforms and calling algorithms for detection of copy number variants. Nature biotechnology 2011; 29: 512–520.

103 Kushima I, Aleksic B, Nakatochi M, Shimamura T, Okada T, Uno Y et al. Comparative Analyses of Copy-Number Variation in Autism Spectrum Disorder and Schizophrenia Reveal Etiological Overlap and Biological Insights. Cell reports 2018; 24: 2838–2856.

104 Dajani R, Li J, Wei Z, Glessner JT, Chang X, Cardinale CJ et al. CNV Analysis Associates AKNAD1 with Type-2 Diabetes in Jordan Subpopulations. Scientific reports 2015; 5: 13391.

105 Marshall CR, Howrigan DP, Merico D, Thiruvahindrapuram B, Wu W, Greer DS et al. Contribution of copy number variants to schizophrenia from a genome-wide study of 41,321 subjects. Nature Genetics 2017; 49: 27–35.

106 Pinto D, Pagnamenta AT, Klei L, Anney R, Merico D, Regan R et al. Functional impact of global rare copy number variation in autism spectrum disorders. Nature 2010; 466: 368–372.

107 Levy D, Ronemus M, Yamrom B, Lee Y-h, Leotta A, Kendall J et al. Rare de novo and transmitted copy-number variation in autistic spectrum disorders. Neuron 2011; 70: 886–897.

108 Kim H-G, Kishikawa S, Higgins AW, Seong I-S, Donovan DJ, Shen Y et al. Disruption of neurexin 1 associated with autism spectrum disorder, 2008.

109 Roohi J, Montagna C, Tegay DH, Palmer LE, DeVincent C, Pomeroy JC et al. Disruption of contactin 4 in three subjects with autism spectrum disorder. Journal of Medical Genetics 2009; 46: 176–182.

110 Moessner R, Marshall CR, Sutcliffe JS, Skaug J, Pinto D, Vincent J et al. Contribution of SHANK3 mutations to autism spectrum disorder. American Journal of Human Genetics 2007; 81: 1289–1297.

111 Szatmari P, Paterson AD, Zwaigenbaum L, Roberts W, Brian J, Liu X-Q et al. Mapping autism risk loci using genetic linkage and chromosomal rearrangements. Nature Genetics 2007; 39: 319–328.

112 Manning MA, Cassidy SB, Clericuzio C, Cherry AM, Schwartz S, Hudgins L et al. Terminal 22q deletion syndrome: a newly recognized cause of speech and language disability in the autism spectrum. Pediatrics 2004; 114: 451–457.

113 Kumar RA, KaraMohamed S, Sudi J, Conrad DF, Brune C, Badner JA et al. Recurrent 16p11.2 microdeletions in autism. Human Molecular Genetics 2008; 17: 628–638.

114 Yin C-L, Chen H-I, Li L-H, Chien Y-L, Liao H-M, Chou MC et al. Genome-wide analysis of copy number variations identifies PARK2 as a candidate gene for autism spectrum disorder. Molecular Autism 2016; 7: 23.

115 Talkowski ME, Rosenfeld JA, Blumenthal I, Pillalamarri V, Chiang C, Heilbut A et al. Sequencing chromosomal abnormalities reveals neurodevelopmental loci that confer risk across diagnostic boundaries. Cell 2012; 149: 525–537.

116 Xu B, Roos JL, Dexheimer P, Boone B, Plummer B, Levy S et al. Exome sequencing supports a de novo mutational paradigm for schizophrenia. Nature Genetics 2011; 43: 864–868.

117 Cai N, Bigdeli T, Kretzschmar Wea. Sparse whole-genome sequencing identifies two loci for major depressive disorder. Nature 2015; 523: 588–591.

118 Sanders SJ, Murtha MT, Gupta AR, Murdoch JD, Raubeson MJ, Willsey AJ et al. De novo mutations revealed by whole-exome sequencing are strongly associated with autism. Nature 2012; 485: 237–241.

119 Rubeis S de, He X, Goldberg AP, Poultney CS, Samocha K, Cicek AE et al. Synaptic, transcriptional and chromatin genes disrupted in autism. Nature 2014; 515: 209–215.

120 Dong S, Walker MF, Carriero NJ, DiCola M, Willsey AJ, Ye AY et al. De novo insertions and deletions of predominantly paternal origin are associated with autism spectrum disorder. Cell Reports 2014; 9: 16–23.

121 Chen L, Page GP, Mehta T, Feng R, Cui X. Single nucleotide polymorphisms affect both cis- and trans-eQTLs. Genomics 2009; 93: 501–508.

122 Cookson W, Liang L, Abecasis G, Moffatt M, Lathrop M. Mapping complex disease traits with global gene expression. Nature Reviews. Genetics 2009; 10: 184–194.

123 Cheng Y, Quinn JF, Weiss LA. An eQTL mapping approach reveals that rare variants in the SEMA5A regulatory network impact autism risk. Human Molecular Genetics 2013; 22: 2960–2972.

124 O'Brien HE, Hannon E, Hill MJ, Toste CC, Robertson MJ, Morgan JE et al. Expression quantitative trait loci in the developing human brain and their enrichment in neuropsychiatric disorders. Genome Biology 2018; 19: 194.

125 Bhalala OG, Nath AP, Inouye M, Sibley CR. Identification of expression quantitative trait loci associated with schizophrenia and affective disorders in normal brain tissue. PLoS Genetics 2018; 14: e1007607.

126 Davis LK, Gamazon ER, Kistner-Griffin E, Badner JA, Liu C, Cook EH et al. Loci nominally associated with autism from genome-wide analysis show enrichment of brain expression quantitative trait loci but not lymphoblastoid cell line expression quantitative trait loci. Molecular Autism 2012; 3: 3.

127 He X, Fuller CK, Song Y, Meng Q, Zhang B, Yang X et al. Sherlock: detecting gene-disease associations by matching patterns of expression QTL and GWAS. American Journal of Human Genetics 2013; 92: 667–680.

128 Yin X, Cheng H, Lin Y, Fan X, Cui Y, Zhou F et al. Five regulatory genes detected by matching signatures of eQTL and GWAS in psoriasis. Journal of Dermatological Science 2014; 76: 139–142.

129 Yang C-P, Li X, Wu Y, Shen Q, Zeng Y, Xiong Q et al. Comprehensive integrative analyses identify GLT8D1 and CSNK2B as schizophrenia risk genes. Nature communications 2018; 9: 838.

130 Lord C, Storoschuk S, Rutter M, Pickles A. Using the ADI-R to diagnose autism in preschool children. Infant Ment. Health J. 1993; 14: 234–252.

131 Hus V, Lord C. Effects of child characteristics on the Autism Diagnostic Interview-Revised: implications for use of scores as a measure of ASD severity. Journal of Autism and Developmental Disorders 2013; 43: 371–381.

132 Akshoomoff N, Corsello C, Schmidt H. The Role of the Autism Diagnostic Observation Schedule in the Assessment of Autism Spectrum Disorders in School and Community Settings. The California School Psychologist CASP 2006; 11: 7–19.

133 Anderson CA, Pettersson FH, Clarke GM, Cardon LR, Morris AP, Zondervan KT. Data quality control in genetic case-control association studies. Nature Protocols 2010; 5: 1564–1573.

134 Illumina Inc. Improved Cluster Generation with Gentrain2.Technical Note: DNA Analysis., 2009. https://www.illumina.com/documents/products/technotes/technote_gentrain2.pdf (accessed 17 Apr 2018).

135 Band G, Marchini J. QCTOOL.

136 D’Angelo GM, Kamboh MI, Feingold E. A Likelihood-Based Approach for Missing Genotype Data. Human Heredity 2010; 69: 171–183.

137 Clayton DG, Walker NM, Smyth DJ, Pask R, Cooper JD, Maier LM et al. Population structure, differential bias and genomic control in a large-scale, case-control association study. Nature Genetics 2005; 37: 1243–1246.

138 Howie B, Fuchsberger C, Stephens M, Marchini J, Abecasis GR. Fast and accurate genotype imputation in genome-wide association studies through pre-phasing. Nature Genetics 2012; 44: 955–959.

139 Stephens M, Scheet P. Accounting for decay of linkage disequilibrium in haplotype inference and missing-data imputation. American Journal of Human Genetics 2005; 76: 449–462.

140 Scheet P, Stephens M. A fast and flexible statistical model for large-scale population genotype data: applications to inferring missing genotypes and haplotypic phase. American Journal of Human Genetics 2006; 78: 629–644.

141 Kimmel G, Shamir R. GERBIL: Genotype resolution and block identification using likelihood. Proceedings of the National Academy of Sciences of the United States of America 2005; 102: 158–162.

142 Lemieux Perreault L-P, Legault M-A, Asselin G, Dubé M-P. genipe: An automated genome-wide imputation pipeline with automatic reporting and statistical tools. Bioinformatics (Oxford, England) 2016; 32: 3661–3663.

143 Chen J, Lippold D, Frank J, Rayner W, Meyer-Lindenberg A, Schwarz E. Gimpute: An efficient genetic data imputation pipeline. Bioinformatics (Oxford, England) 2018.

144 Purcell S, Neale B, Todd-Brown K, Thomas L, Ferreira MAR, Bender D et al. PLINK: A tool set for whole-genome association and population-based linkage analyses. American Journal of Human Genetics 2007; 81: 559–575.

145 Delaneau O, Marchini J, Zagury J-F. A linear complexity phasing method for thousands of genomes. Nature Methods 2011; 9: 179–181.

146 Das S, Forer L, Schonherr S, Sidore C, Locke AE, Kwong A et al. Next-generation genotype imputation service and methods. Nature Genetics 2016; 48: 1284–1287.

147 Browning BL, Browning SR. Genotype Imputation with Millions of Reference Samples. American Journal of Human Genetics 2016; 98: 116–126.

148 Duncan LE, Ostacher M, Ballon J. How genome-wide association studies (GWAS) made traditional candidate gene studies obsolete. Neuropsychopharmacology Official Publication of the American College of Neuropsychopharmacology 2019; 44: 1518–1523.

149 Grimm DG, Roqueiro D, Salomé PA, Kleeberger S, Greshake B, Zhu W et al. easyGWAS: A Cloud-Based Platform for Comparing the Results of Genome-Wide Association Studies. The Plant Cell 2017; 29: 5–19.

150 Gogarten SM, Bhangale T, Conomos MP, Laurie CA, McHugh CP, Painter I et al. GWASTools: an R/Bioconductor package for quality control and analysis of genome-wide association studies. Bioinformatics (Oxford, England) 2012; 28: 3329–3331.

151 Wray NR, Lee SH, Mehta D, Vinkhuyzen AAE, Dudbridge F, Middeldorp CM. Research review: Polygenic methods and their application to psychiatric traits. Journal of Child Psychology and Psychiatry, and Allied Disciplines 2014; 55: 1068–1087.

152 Wang L, Jia P, Wolfinger RD, Chen X, Zhao Z. Gene set analysis of genome-wide association studies: methodological issues and perspectives. Genomics 2011; 98: 1–8.

153 Leeuw CA de, Mooij JM, Heskes T, Posthuma D. MAGMA: Generalized gene-set analysis of GWAS data. PLoS Computational Biology 2015; 11: e1004219.

154 Mishra A, Macgregor S. VEGAS2: Software for More Flexible Gene-Based Testing. Twin Research and Human Genetics the Official Journal of the International Society for Twin Studies 2015; 18: 86–91.

155 Lee PH, O'Dushlaine C, Thomas B, Purcell SM. INRICH: Interval-based enrichment analysis for genome-wide association studies. Bioinformatics (Oxford, England) 2012; 28: 1797–1799.

156 Holmans P, Green EK, Pahwa JS, Ferreira MAR, Purcell SM, Sklar P et al. Gene ontology analysis of GWA study data sets provides insights into the biology of bipolar disorder. American Journal of Human Genetics 2009; 85: 13–24.

157 Liu JZ, McRae AF, Nyholt DR, Medland SE, Wray NR, Brown KM et al. A versatile gene-based test for genome-wide association studies. American Journal of Human Genetics 2010; 87: 139–145.

158 Segrè AV, Groop L, Mootha VK, Daly MJ, Altshuler D. Common inherited variation in mitochondrial genes is not enriched for associations with type 2 diabetes or related glycemic traits. PLoS Genetics 2010; 6.

159 Huang DW, Sherman BT, Tan Q, Collins JR, Alvord WG, Roayaei J et al. The DAVID Gene Functional Classification Tool: a novel biological module-centric algorithm to functionally analyze large gene lists. Genome Biology 2007; 8: R183.

160 Song GG, Lee YH. Pathway analysis of genome-wide association studies for Parkinson's disease. Molecular Biology Reports 2013; 40: 2599–2607.

161 Mi H, Muruganujan A, Casagrande JT, Thomas PD. Large-scale gene function analysis with the PANTHER classification system. Nature Protocols 2013; 8: 1551–1566.

162 Zambon AC, Gaj S, Ho I, Hanspers K, Vranizan K, Evelo CT et al. GO-Elite: A flexible solution for pathway and ontology over-representation. Bioinformatics (Oxford, England) 2012; 28: 2209–2210.

163 Berument SK, Rutter M, Lord C, Pickles A, Bailey A. Autism screening questionnaire: diagnostic validity. The British Journal of Psychiatry the Journal of Mental Science 1999; 175: 444–451.

164 Lord C, Risi S, Lambrecht L, Cook EH, Leventhal BL, DiLavore PC et al. The autism diagnostic observation schedule-generic: A standard measure of social and communication deficits associated with the spectrum of autism. Journal of Autism and Developmental Disorders 2000; 30: 205–223.

165 Janca A, Ustün TB, Early TS, Sartorius N. The ICD-10 symptom checklist: A companion to the ICD-10 classification of mental and behavioural disorders. Social Psychiatry and Psychiatric Epidemiology 1993; 28: 239–242.

166 Poustka F, Lisch S, Rühl D, Sacher A, Schmötzer G, Werner K. The standardized diagnosis of autism, Autism Diagnostic Interview-Revised: Interrater reliability of the German form of the interview. Psychopathology 1996; 29: 145–153.

167 Rabbee N, Speed TP. A genotype calling algorithm for affymetrix SNP arrays. Bioinformatics (Oxford, England) 2006; 22: 7–12.

168 Stef van Buuren, Karin Groothuis-Oudshoorn. mice: Multivariate Imputation by Chained Equations in R 2011.

169 Azur MJ, Stuart EA, Frangakis C, Leaf PJ. Multiple imputation by chained equations: what is it and how does it work? International Journal of Methods in Psychiatric Research 2011; 20: 40–49.

170 RUBIN DB. Statistical Matching Using File Concatenation with Adjusted Weights and Multiple Imputations. Journal of Business & Economic Statistics 1986; 4: 87.

171 Horton NJ, Kleinman KP. Much ado about nothing: A comparison of missing data methods and software to fit incomplete data regression models. The American Statistician 2007; 61: 79–90.

172 Frazier TW, Youngstrom EA, Kubu CS, Sinclair L, Rezai A. Exploratory and confirmatory factor analysis of the autism diagnostic interview-revised. Journal of Autism and Developmental Disorders 2008; 38: 474–480.

173 Tao Y, Gao H, Ackerman B, Guo W, Saffen D, Shugart YY. Evidence for contribution of common genetic variants within chromosome 8p21.2-8p21.1 to restricted and repetitive behaviors in autism spectrum disorders. BMC Genomics 2016; 17: 163.

174 Bölte S, Poustka F. Die Faktorenstruktur des Autismus Diagnostischen Interviews-Revision (ADI-R): Eine Untersuchung zur dimensionalen versus kategorialen Klassifikation autistischer Störungen. Zeitschrift für Kinder- und Jugendpsychiatrie und Psychotherapie 2001; 29: 221–229.

175 Barrett PT, Kline P. The observation to variable ratio in factor analysis. Personality Study and Group Behavior.

176 Aleamoni LM. The Relation of Sample Size to the Number of Variables in Using Factor Analysis Techniques. Educational and Psychological Measurement 1976; 36: 879–883.

177 Kaiser HF. An index of factorial simplicity, 39, 1974.

178 William Revelle. psych: Procedures for Psychological, Psychometric, and Personality Research, 2017.

179 Kaiser HF. The Application of Electronic Computers to Factor Analysis. Educational and Psychological Measurement 1960; 20: 141–151.

180 Thorndike RL. Who belongs in the family? Psychometrika 1953; 18: 267–276.

181 Anderson TW, Rubin H. Statistical Inference in Factor Analysis. Neyman, J., Ed., Proceedings of the Third Berkeley Symposium on Mathematical Statistics and Probability 1956; 5: 111–150.

182 Comrey AL. Factor-analytic methods of scale development in personality and clinical psychology. Journal of Consulting and Clinical Psychology 1988; 56: 754–761.

183 Guadagnoli E, Velicer WF. Relation of sample size to the stability of component patterns. Psychological Bulletin 1988; 103: 265–275.

184 Tabachnick BG, Fidell LS. Using multivariate statistics, 6th edn. Pearson Education: Boston, 2013.

185 Faul F, Erdfelder E, Buchner A, Lang A-G. Statistical power analyses using G*Power 3.1: Tests for correlation and regression analyses. Behavior Research Methods 2009; 41: 1149–1160.

186 Lam M, Awasthi S, Watson HJ, Goldstein J, Panagiotaropoulou G, Trubetskoy V et al. RICOPILI: Rapid Imputation for COnsortias PIpeLIne. Bioinformatics (Oxford, England) 2019.

187 Turner S, Armstrong LL, Bradford Y, Carlson CS, Crawford DC, Crenshaw AT et al. Quality control procedures for genome-wide association studies. Current Protocols in Human Genetics 2011; Chapter 1: Unit1.19.

188 Kido T, Sikora-Wohlfeld W, Kawashima M, Kikuchi S, Kamatani N, Patwardhan A et al. Are minor alleles more likely to be risk alleles? BMC Medical Genomics 2018; 11: 3.

189 Marees AT, Kluiver H de, Stringer S, Vorspan F, Curis E, Marie-Claire C et al. A tutorial on conducting genome-wide association studies: Quality control and statistical analysis. International Journal of methods in Psychiatric Research 2018; 27: e1608.

190 Rédei GP (ed). Encyclopedia of genetics, genomics, proteomics, and informatics, 3rd edn. Springer reference. Springer part of Springer Science + Business Media: Dordrecht, 2008.

191 Abbott S, Fairbanks DJ. Experiments on Plant Hybrids by Gregor Mendel. Genetics 2016; 204: 407–422.

192 Lowe JK, Maller JB, Pe'er I, Neale BM, Salit J, Kenny EE et al. Genome-wide association studies in an isolated founder population from the Pacific Island of Kosrae. PLoS Genetics 2009; 5: e1000365.

193 Tyner C, Barber GP, Casper J, Clawson H, Diekhans M, Eisenhart C et al. The UCSC Genome Browser database: 2017 update. Nucleic Acids Research 2017; 45: D626-D634.

194 Verma SS, Andrade M de, Tromp G, Kuivaniemi H, Pugh E, Namjou-Khales B et al. Imputation and quality control steps for combining multiple genome-wide datasets. Front. Genet. 2014; 5.

195 Yang J, Lee SH, Goddard ME, Visscher PM. GCTA: A tool for genome-wide complex trait analysis. American Journal of Human Genetics 2011; 88: 76–82.

196 Euesden J, Lewis CM, O'Reilly PF. PRSice: Polygenic Risk Score software. Bioinformatics (Oxford, England) 2015; 31: 1466–1468.

197 Bentler PM. Comparative fit indexes in structural models. Psychological Bulletin 1990; 107: 238–246.

198 Hu L-t, Bentler PM. Cutoff criteria for fit indexes in covariance structure analysis: Conventional criteria versus new alternatives. Structural Equation Modeling: A Multidisciplinary Journal 1999; 6: 1–55.

199 Browne MW, Cudeck R. Alternative Ways of Assessing Model Fit. Sociological Methods & Research 2016; 21: 230–258.

200 MacCallum RC, Browne MW, Sugawara HM. Power analysis and determination of sample size for covariance structure modeling. Psychological Methods 1996; 1: 130–149.

201 Lin S, Chakravarti A, Cutler DJ. Haplotype and missing data inference in nuclear families. Genome Research 2004; 14: 1624–1632.

202 Sicotte H, Proddutur N. EZimputer.

203 Lee SH, Ripke S, Neale BM, Faraone SV, Purcell SM, Perlis RH et al. Genetic relationship between five psychiatric disorders estimated from genome-wide SNPs. Nature Genetics 2013; 45: 984–994.

204 Freitag CM, Jensen K, Elsuni L, Sachse M, Herpertz-Dahlmann B, Schulte-Rüther M et al. Group-based cognitive behavioural psychotherapy for children and adolescents with ASD: the randomized, multicentre, controlled SOSTA-net trial. Journal of Child Psychology and Psychiatry, and Allied Disciplines 2016; 57: 596–605.

205 Shuster J, Perry A, Bebko J, Toplak ME. Review of factor analytic studies examining symptoms of autism spectrum disorders. Journal of Autism and Developmental Disorders 2014; 44: 90–110.

206 Stranger BE, Stahl EA, Raj T. Progress and promise of genome-wide association studies for human complex trait genetics. Genetics 2011; 187: 367–383.

207 Tadevosyan-Leyfer O, Dowd M, Mankoski R, Winklosky B, Putnam S, McGrath L et al. A principal components analysis of the Autism Diagnostic Interview-Revised. Journal of the American Academy of Child and Adolescent Psychiatry 2003; 42: 864–872.

208 Anzai N, Deval E, Schaefer L, Friend V, Lazdunski M, Lingueglia E. The multivalent PDZ domain-containing protein CIPP is a partner of acid-sensing ion channel 3 in sensory neurons. The Journal of Biological Chemistry 2002; 277: 16655–16661.

209 Kenny EM, Cormican P, Furlong S, Heron E, Kenny G, Fahey C et al. Excess of rare novel loss-of-function variants in synaptic genes in schizophrenia and autism spectrum disorders. Molecular Psychiatry 2014; 19: 872–879.

210 Klein-Tasman BP, Mervis CB. Autism Spectrum Symptomatology Among Children with Duplication 7q11.23 Syndrome. Journal of Autism and Developmental Disorders 2018; 48: 1982–1994.

211 Beunders G, Voorhoeve E, Golzio C, Pardo LM, Rosenfeld JA, Talkowski ME et al. Exonic deletions in AUTS2 cause a syndromic form of intellectual disability and suggest a critical role for the C terminus. American Journal of Human Genetics 2013; 92: 210–220.

212 Gao Z, Lee P, Stafford JM, Schimmelmann M von, Schaefer A, Reinberg D. An AUTS2-Polycomb complex activates gene expression in the CNS. Nature 2014; 516: 349–354.

213 Cinque M de, Palumbo O, Mazzucco E, Simone A, Palumbo P, Ciavatta R et al. Developmental Coordination Disorder in a Patient with Mental Disability and a Mild Phenotype Carrying Terminal 6q26-qter Deletion. Front. Genet. 2017; 8: 206.

214 Fisch GS, Davis R, Youngblom J, Gregg J. Genotype-phenotype association studies of chromosome 8p inverted duplication deletion syndrome. Behavior Genetics 2011; 41: 373–380.

215 Cassel SL, Joly S, Sutterwala FS. The NLRP3 inflammasome: a sensor of immune danger signals. Seminars in Immunology 2009; 21: 194–198.

216 Melliti K, Grabner M, Seabrook GR. The familial hemiplegic migraine mutation R192Q reduces G-protein-mediated inhibition of P/Q-type (Ca(V)2.1) calcium channels expressed in human embryonic kidney cells. The Journal of Physiology 2003; 546: 337–347.

217 Merla G, Brunetti-Pierri N, Micale L, Fusco C. Copy number variants at Williams-Beuren syndrome 7q11.23 region. Human Genetics 2010; 128: 3–26.

218 Chakrabarti B, Dudbridge F, Kent L, Wheelwright S, Hill-Cawthorne G, Allison C et al. Genes related to sex steroids, neural growth, and social-emotional behavior are associated with autistic traits, empathy, and Asperger syndrome. Autism research official journal of the International Society for Autism Research 2009; 2: 157–177.

219 Muiños-Gimeno M, Guidi M, Kagerbauer B, Martín-Santos R, Navinés R, Alonso P et al. Allele variants in functional MicroRNA target sites of the neurotrophin-3 receptor gene (NTRK3) as susceptibility factors for anxiety disorders. Human Mutation 2009; 30: 1062–1071.

220 Supriyanto I, Watanabe Y, Mouri K, Shiroiwa K, Ratta-Apha W, Yoshida M et al. A missense mutation in the ITGA8 gene, a cell adhesion molecule gene, is associated with schizophrenia in Japanese female patients. Progress in Neuro-Psychopharmacology & Biological Psychiatry 2013; 40: 347–352.

221 Kuwano Y, Kamio Y, Kawai T, Katsuura S, Inada N, Takaki A et al. Autism-Associated Gene Expression in Peripheral Leucocytes Commonly Observed between Subjects with Autism and Healthy Women Having Autistic Children. PLoS One 2011; 6.

222 Girirajan S, Dennis MY, Baker C, Malig M, Coe BP, Campbell CD et al. Refinement and discovery of new hotspots of copy-number variation associated with autism spectrum disorder. American Journal of Human Genetics 2013; 92: 221–237.

223 Crepel A, Breckpot J, Fryns J-P, La Marche W de, Steyaert J, Devriendt K et al. DISC1 duplication in two brothers with autism and mild mental retardation. Clinical Genetics 2010; 77: 389–394.

224 Oguro-Ando A, Zuko A, Kleijer KTE, Burbach JPH. A current view on contactin-4, -5, and -6: Implications in neurodevelopmental disorders. Molecular and Cellular Neurosciences 2017; 81: 72–83.

225 Charalsawadi C, Maisrikhaw W, Praphanphoj V, Wirojanan J, Hansakunachai T, Roongpraiwan R et al. A case with a ring chromosome 13 in a cohort of 203 children with non-syndromic autism and review of the cytogenetic literature. Cytogenetic and Genome Research 2014; 144: 1–8.

226 Bettencourt C, Forabosco P, Wiethoff S, Heidari M, Johnstone DM, Botía JA et al. Gene co-expression networks shed light into diseases of brain iron accumulation. Neurobiology of Disease 2016; 87: 59–68.

227 Gregory A, Polster BJ, Hayflick SJ. Clinical and genetic delineation of neurodegeneration with brain iron accumulation. Journal of Medical Genetics 2009; 46: 73–80.

228 Prasad A, Merico D, Thiruvahindrapuram B, Wei J, Lionel AC, Sato D et al. A discovery resource of rare copy number variations in individuals with autism spectrum disorder. G3 (Bethesda, Md.) 2012; 2: 1665–1685.

229 Davidsson J, Collin A, Olsson ME, Lundgren J, Soller M. Deletion of the SCN gene cluster on 2q24.4 is associated with severe epilepsy: an array-based genotype-phenotype correlation and a comprehensive review of previously published cases. Epilepsy Research 2008; 81: 69–79.

230 Chen C-P, Lin S-P, Chern S-R, Chen Y-J, Tsai F-J, Wu P-C et al. Array-CGH detection of a de novo 2.8 Mb deletion in 2q24.2--q24.3 in a girl with autistic features and developmental delay. European Journal of Medical Genetics 2010; 53: 217–220.

231 Li J, Shi M, Ma Z, Zhao S, Euskirchen G, Ziskin J et al. Integrated systems analysis reveals a molecular network underlying autism spectrum disorders. Molecular Systems Biology 2014; 10: 774.

232 Zhang L, Liu L, Wen Y, Ma M, Cheng S, Yang J et al. Genome-wide association study and identification of chromosomal enhancer maps in multiple brain regions related to autism spectrum disorder. Autism Research Official Journal of the International Society for Autism Research 2019; 12: 26–32.

233 Liu XZ, Ouyang XM, Xia XJ, Zheng J, Pandya A, Li F et al. Prestin, a cochlear motor protein, is defective in non-syndromic hearing loss. Human Molecular Genetics 2003; 12: 1155–1162.

234 Lee J-K, McCoy MK, Harms AS, Ruhn KA, Gold SJ, Tansey MG. Regulator of G-protein signaling 10 promotes dopaminergic neuron survival via regulation of the microglial inflammatory response. The Journal of Neuroscience: The Official Journal of the Society for Neuroscience 2008; 28: 8517–8528.

235 Guerra DJ. The molecular genetics of autism spectrum disorders: Genomic mechanisms, neuroimmunopathology, and clinical implications. Autism Research and Treatment 2011; 2011: 398636.

236 Robertson CE, Baron-Cohen S. Sensory perception in autism. Nature Reviews. Neuroscience 2017; 18: 671–684.

237 Lasalle JM. Autism genes keep turning up chromatin. OA Autism 2013; 1: 14.

238 Tareen RS, Kamboj MK. Role of endocrine factors in autistic spectrum disorders. Pediatric Clinics of North America 2012; 59: 75-88, x.

239 Louros SR, Osterweil EK. Perturbed proteostasis in autism spectrum disorders. Journal of Neurochemistry 2016; 139: 1081–1092.

240 Griffiths KK, Levy RJ. Evidence of Mitochondrial Dysfunction in Autism: Biochemical Links, Genetic-Based Associations, and Non-Energy-Related Mechanisms. Oxidative Medicine and Cellular Longevity 2017; 2017: 4314025.

241 Vithayathil J, Pucilowska J, Landreth GE. ERK/MAPK signaling and autism spectrum disorders. Progress in Brain Research 2018; 241: 63–112.

242 Yang DY-J, Beam D, Pelphrey KA, Abdullahi S, Jou RJ. Cortical morphological markers in children with autism: a structural magnetic resonance imaging study of thickness, area, volume, and gyrification. Molecular Autism 2016; 7: 11.

243 Rubin RD, Watson PD, Duff MC, Cohen NJ. The role of the hippocampus in flexible cognition and social behavior. Frontiers in Human Neuroscience 2014; 8: 742.

244 Duff MC, Brown-Schmidt S. The hippocampus and the flexible use and processing of language. Frontiers in Human Neuroscience 2012; 6: 69.

245 Chan S-H, Ryan L, Bever TG. Role of the striatum in language: Syntactic and conceptual sequencing. Brain and Language 2013; 125: 283–294.

246 Edmonson C, Ziats MN, Rennert OM. Altered glial marker expression in autistic post-mortem prefrontal cortex and cerebellum. Molecular Autism 2014; 5: 3.

247 Robinson EB, St Pourcain B, Anttila V, Kosmicki JA, Bulik-Sullivan B, Grove J et al. Genetic risk for autism spectrum disorders and neuropsychiatric variation in the general population. Nature Genetics 2016; 48: 552–555.

248 Phillips EL. The social skills basis of psychopathology: Alternatives to abnormal psychology and psychiatry. Current issues in behavioral psychology. Grune & Stratton: New York, 1978.

249 Trower P, Bryant B, Argyle M. Social skills and mental health. Routledge: London, 1988.

250 Cannon DS, Miller JS, Robison RJ, Villalobos ME, Wahmhoff NK, Allen-Brady K et al. Genome-wide linkage analyses of two repetitive behavior phenotypes in Utah pedigrees with autism spectrum disorders. Molecular Autism 2010; 1: 3.

251 Frazier TW, Thompson L, Youngstrom EA, Law P, Hardan AY, Eng C et al. A twin study of heritable and shared environmental contributions to autism. Journal of Autism and Developmental Disorders 2014; 44: 2013–2025.

252 Turner TN, Coe BP, Dickel DE, Hoekzema K, Nelson BJ, Zody MC et al. Genomic Patterns of De Novo Mutation in Simplex Autism. Cell 2017; 171: 710-722.e12.

253 Yang, Jian; Benyamin, Beben; McEvoy, Brian P.; Gordon, Scott; Henders, Anjali K.; Nyholt, Dale R. et al. (2010): Common SNPs explain a large proportion of the heritability for human height. In: Nature Genetics 42 (7), S. 565–569. DOI: 10.1038/ng.608

254 Legido, Agustín; Jethva, Reena; Goldenthal, Michael J. (2013): Mitochondrial dysfunction in autism. In: Seminars in Pediatric Neurology 20 (3), S. 163–175. DOI: 10.1016/j.spen.2013.10.008.